FHWA-NJ-2002-012

# Evaluation of Seismic Pavement Analyzer for Pavement Condition Monitoring

FINAL REPORT
May 2002

Submitted by

Dr. Nenad Gucunski
Associate Professor

Dr. Ali Maher
Professor and Chairman

Department of Civil & Environmental Engineering
Center for Advanced Infrastructure & Transportation (CAIT)
Rutgers, The State University
Piscataway, NJ 08854-8014



NJDOT Research Project Manager
Mr. Nicholas Vitillo

In cooperation with

New Jersey
Department of Transportation
Division of Research and Technology
and
U.S. Department of Transportation
Federal Highway Administration

# Disclaimer Statement

"The contents of this report reflect the views of the author(s) who is (are) responsible for the facts and the accuracy of the data presented herein. The contents do not necessarily reflect the official views or policies of the New Jersey Department of Transportation or the Federal Highway Administration. This report does not constitute a standard, specification, or regulation."

The contents of this report reflect the views of the authors, who are responsible for the facts and the accuracy of the information presented herein. This document is disseminated under the sponsorship of the Department of Transportation, University Transportation Centers Program, in the interest of information exchange. The U.S. Government assumes no liability for the contents or use thereof.

TECHNICAL REPORT STANDARD TITLE PAGE

| 1. Report No. | 2. Government Accession No. | 3. Recipient's Catalog No. |
|---|---|---|
| FHWA-NJ-2002-012 | | |

| 4. Title and Subtitle | 5. Report Date |
|---|---|
| Evaluation of Seismic Pavement Analyzer for Pavement Condition Monitoring | May 2002 |
| | 6. Performing Organization Code: CAIT/Rutgers |
| 7. Author(s): Dr. Nenad Gucunski and Dr. Ali Maher | 8. Performing Organization Report No.: FHWA-NJ-2002-012 |
| 9. Performing Organization Name and Address: New Jersey Department of Transportation, PO 600, Trenton, NJ 08625 | 10. Work Unit No. |
| | 11. Contract or Grant No. |
| | 13. Type of Report and Period Covered: Final Report, 3/6/1996 - 3/31/1999 |
| 12. Sponsoring Agency Name and Address: Federal Highway Administration, U.S. Department of Transportation, Washington. D.C. | 14. Sponsoring Agency Code |

15. Supplementary Notes

16. Abstract

Seismic Pavement Analyzer (SPA) is a device for nondestructive evaluation of pavements developed under the Strategic Highway Research Program (SHRP). One of the main objectives in the development of the SPA was to create a device that will allow measurement of onset of deterioration at early stages, and thus contribute to a more economic pavement management. Primary applications of the SPA include pavement profiling in terms of elastic moduli and layer thicknesses, detection of voids or loss of support under rigid pavements, delamination in rigid pavements and bridge decks, and subgrade evaluation. The SPA incorporates five seismic techniques for those purposes: Ultrasonic Body-Wave (UBW), Ultrasonic Surface-Wave (USW), Impact Echo (IE), Impulse Response (IR) and Spectral Analysis of Surface Waves (SASW). The SPA was evaluated for possible implementation in evaluation and condition monitoring of pavements in New Jersey. Specifically, the objectives of the study were to examine the applicability of the SPA in pavement structural evaluation, detection of defects and distresses, and other uses relevant for pavement evaluation and condition monitoring. With respect to the equipment itself, the objectives were to examine the robustness and consistency of the SPA hardware and software, and the soundness of the seismic methods implemented in the device. To achieve the objectives of the study, a number of flexible and rigid pavements in New Jersey were tested. Specific attention was given to pavement profiling and detection of voids or loss of support under rigid pavements. Use of the SPA in evaluation of joint load transfer in rigid pavements was examined too. The overall conclusion of the study is that the SPA is a well designed automated data collection and analysis system for seismic testing of pavements. The five seismic techniques implemented in the SPA utilize sound physical phenomena of wave propagation in layered elastic systems. However, several data interpretation procedures, in particular those related to SASW and IR, have significant space for improvement. The strongest capability of the SPA is in evaluation of the properties of the paving layer, since those are being directly measured. The SPA hardware performed very well throughout the study, with minumum failures and simple and inexpensive regular maintenance. However, transition from DOS to Windows platform is necessary to improve capabilities, versatility and user-friendliness of the SPA software. Benefits of the SPA can be significantly improved through both continued fundamental research and a number of short analytical and experimental studies. The most of the effort should be directed towards the improvement of the analytical procedures, in particular of the SASW and IR methods. Minor improvements on the hardware side should lead to significant enhancement of ultrasonic techniques. Other potential applications of the SPA still need to be examined or verified, like: the use of SPA in detection and characterization of delaminations in rigid and composite pavements, evaluation of temperature induced modulus variations in asphalt concrete, or monitoring of curing of concrete.

| 17. Key Words | 18. Distribution Statement |
|---|---|
| Pavements, Nondestructive Testing, Seismic Methods, Ultrasonic Methods, Condition Monitoring, Seismic Pavement Analyzer, Elastic Properties, Defects, Distresses | |

| 19. Security Classif (of this report) | 20. Security Classif. (of this page) | 21. No of Pages | 22. Price |
|---|---|---|---|
| Unclassified | Unclassified | 117 | |

Form DOT F 1700.7 (8-69)

## Acknowledgments

The authors gratefully acknowledge the support provided by the New Jersey Department of Transportation (NJDOT) and Federal Highway Administration (FHWA). Special thanks go to Mr. Nicholas Vitillo, the research project manager, for valuable comments, directions in the scope of work and the overall assistance in the field testing program. A number of current and former Rutgers graduate students: Dr. Vedrana Krstic, Hudson Jackson and Dr. Vahid Ganji, participated in the field data collection. Their contribution is greatly appreciated. Finally, the most sincere thanks to Dr. Soheil Nazarian from University of Texas at El Paso, for sharing experience from the development and implementation of the SPA.

## LIST OF CONTENTS

## LIST OF FIGURES

## LIST OF TABLES

## ABSTRACT

Seismic Pavement Analyzer (SPA) is a device for nondestructive evaluation of pavements developed under the Strategic Highway Research Program (SHRP). One of the main objectives in the development of the SPA was to create a device that will allow measurement of onset of deterioration at early stages, and thus contribute to a more economic pavement management. Primary applications of the SPA include pavement profiling in terms of elastic moduli and layer thicknesses, detection of voids or loss of support under rigid pavements, delamination in rigid pavements and bridge decks, and subgrade evaluation. The SPA incorporates five seismic techniques for those purposes: Ultrasonic Body-Wave (UBW), Ultrasonic Surface-Wave (USW), Impact Echo (IE), Impulse Response (IR) and Spectral Analysis of Surface Waves (SASW).

The SPA was evaluated for possible implementation in evaluation and condition monitoring of pavements in New Jersey. Specifically, the objectives of the study were to examine the applicability of the SPA in pavement structural evaluation, detection of defects and distresses, and other uses relevant for pavement evaluation and condition monitoring. With respect to the equipment itself, the objectives were to examine the robustness and consistency of the SPA hardware and software, and the soundness of the seismic methods implemented in the device. To achieve the objectives of the study, a number of flexible and rigid pavements in New Jersey were tested. Specific attention was given to pavement profiling and detection of voids or loss of support under rigid pavements. Use of the SPA in evaluation of joint load transfer in rigid pavements was examined too.

The overall conclusion of the study is that the SPA is a well designed automated data collection and analysis system for seismic testing of pavements. The five seismic techniques implemented in the SPA utilize sound physical phenomena of wave propagation in layered elastic systems. However, several data interpretation procedures, in particular those related to SASW and IR, have significant space for improvement. The strongest capability of the SPA is in evaluation of the properties of the paving layer, since those are being directly measured. The SPA hardware performed very well throughout the study, with minumum failures and simple and inexpensive regular maintenance. However, transition from DOS to Windows platform is necessary to improve capabilities, versatility and user-friendliness of the SPA software.

Benefits of the SPA can be significantly improved through both continued fundamental research and a number of short analytical and experimental studies. The most of the effort should be directed towards the improvement of the analytical procedures, in particular of the SASW and IR methods. Minor improvements on the hardware side should lead to significant enhancement of ultrasonic techniques. Other potential applications of the SPA still need to be examined or verified, like: the use of SPA in detection and characterization of delaminations in rigid and composite pavements, evaluation of temperature induced modulus variations in asphalt concrete, or monitoring of curing of concrete pavements.

# INTRODUCTION

The need for accurate, fast, cost-effective and nondestructive evaluation of civil infrastructure systems is becoming ever more important. In the case of pavement and bridge structures, the evaluation is being done to assess the pavement structure for QA/QC purposes, but more importantly to detect symptoms of deterioration at early stages to optimize economic management.

There are nearly four million miles of public highways and roads in the United States, of which about one half are either flexible or rigid pavements.[1] In the past twenty years, transportation agencies in the United States have shifted their focus from construction of new roads and bridges towards maintenance and rehabilitation of existing ones. To manage the huge investment in paved highways and bridges of the Interstate system, there was a clear need for methodologies that use a systematic, objective approach to provide assistance to agencies in selecting projects and identifying treatments. To respond to this challenge, the agencies used their current decision making and operational experience and started developing management systems in a more systematic fashion in late seventies and early eighties.[2] As a result of this process, numerous benefits are coming: from a longer service life and overall functional satisfaction, to a greater number of served users.

The core of any management system is a database of information collected, stored and available for use about systems managed. In the case of pavements and bridges, an essential part of the database is data describing the current condition. These may include data about the pavement profile (longitudinal and transverse), pavement condition (distress, and structural capacity and, roughness, friction, etc.), previous maintenance activities and their cost. A whole new group of methods, called seismic methods, can be successfully used for the purpose of evaluation of structural capacity, system identification and detection of defects and distresses in pavements and bridge decks. A special value of seismic techniques comes from their ability to evaluate and monitor changes in elastic pavement properties (Young's, shear, resilient moduli), the core parameters in the mechanistic pavement design. The advantages of the seismic techniques stem from the fact that, when incorporated into integrated devices, they can provide fast, accurate, nondestructive and economic evaluation of transportation systems. One of such devices, Seismic Pavement Analyzer (SPA) developed through the Strategic Highway Research Program (SHRP), is the scope of this study.[3]

## Objectives

The first SPA prototype was developed in 1993 at the University of Texas at El Paso. Since that time there have been a number of improvements implemented in the SPA. Because there was only a limited experience in the use, capabilities and applications of the SPA in the pavement structural evaluation and condition monitoring, the New Jersey Department of Transportation (NJDOT) has requested from the Center for Advanced Infrastructure and Transportation (CAIT) evaluation of the SPA device for possible implementation. Specifically, this study will try to answer questions about:

- applicability of the SPA in structural evaluation of pavement systems,
- applicability of the SPA in detection of defects and distresses in pavements,

- soundness of the seismic methods implemented in the SPA with respect to pavement evaluation and diagnostics,
- robustness and consistency of the SPA hardware and software, and
- other potential applications of the SPA.

In addition, the objective of the study was to gain and summarize experience in the use, operation (both on the hardware and software sides) and data interpretation, for future assistance.

**Report Organization**

The report is organized in six main sections. The first part of the report (Seismic Methods for Pavement Evaluation) discusses the fundamentals of seismic methods implemented in the SPA. Specifically, the section includes a description and examples of implementation of the methods in evaluation of properties and detection of defects and distresses in pavements. The Seismic Pavement Analyzer section discusses in detail the SPA hardware and software. The section includes also a detailed description of operation of the SPA, data analysis and data interpretation. A number of field tests conducted for the purpose of pavement modulus profiling are summarized in the section on Evaluation of the SPA in Pavement Profiling. Other applications, like detection of voids under rigid pavements, verification of rehabilitation procedures and evaluation of joint transfer for rigid pavements is presented in the section on Other Applications of SPA. Finally, the gained experience in the use, capabilities, limitations, and potential applications and benefits of the SPA are discussed in the section Status of Seismic Methods Implemented in the SPA.

## SEISMIC METHODS FOR PAVEMENT EVALUATION

Seismic methods can be described as methods for evaluation of material properties and defects in structures that are based on generation of elastic waves and measurement of their velocity of propagation and various wave propagation phenomena like reflections, refractions and dispersions. Generally, seismic methods can be divided into two groups: borehole and surface methods. Surface techniques are almost exclusively used in transportation applications, because they do not require boreholes and thus are nondestructive, testing is much faster because it is performed from the surface, and thus far less expensive. While in most cases individual techniques can be used to determine certain properties or defects, a more comprehensive and accurate evaluation is achieved using a complementary approach.

Application of seismic techniques in NDT of pavements can be divided into three main categories:

- pavement evaluation,
- pavement diagnostics, and
- quality control/quality assurance.

In terms of the frequency range of operation, the techniques can be divided into high frequency techniques (used in surface layer evaluation and diagnostics), low frequency techniques (used in subgrade evaluation), and broad range frequency techniques (used in pavement modulus profiling). The following paragraphs discuss the fundamentals of wave propagation in elastic layered half-space, factors affecting elastic moduli of pavement materials, and background and application of five seismic techniques used in evaluation of pavement systems and implemented in the SPA.

### Fundamentals of Wave Propagation in Layered Systems

Pavements systems in most instances can be represented by a layered half-space or a layered stratum. Understanding of wave propagation phenomena in layered media is essential for development, application and interpretation of results of seismic methods in evaluation of *in situ* elastic moduli and detection of defects and anomalies. This section reviews three-dimensional wave propagation in layered systems, types of waves existing in layered systems, relationships between velocity of propagation of elastic waves and elastic moduli, and factors influencing elastic moduli of pavement materials and soil.

Elastic waves in a layered half-space can be divided into body and surface waves. Body waves in a three-dimensional space can be described by a disturbance propagating in a form of an expanding sphere. Two types of body waves exist in a layered half-space: a compression or P-wave, and shear or S-wave. Deformations produced by the body waves are illustrated in Figure1. A compression wave is a wave for which the direction of wave propagation and the displacement vector (particle motion) coincide, generating a push-pull type motion. A shear wave is a wave for which the particle motion is perpendicular to the wave propagation direction. Shear waves are typically described by their components in vertical and horizontal planes, SV- and SH-waves, respectively. Since the velocity of the

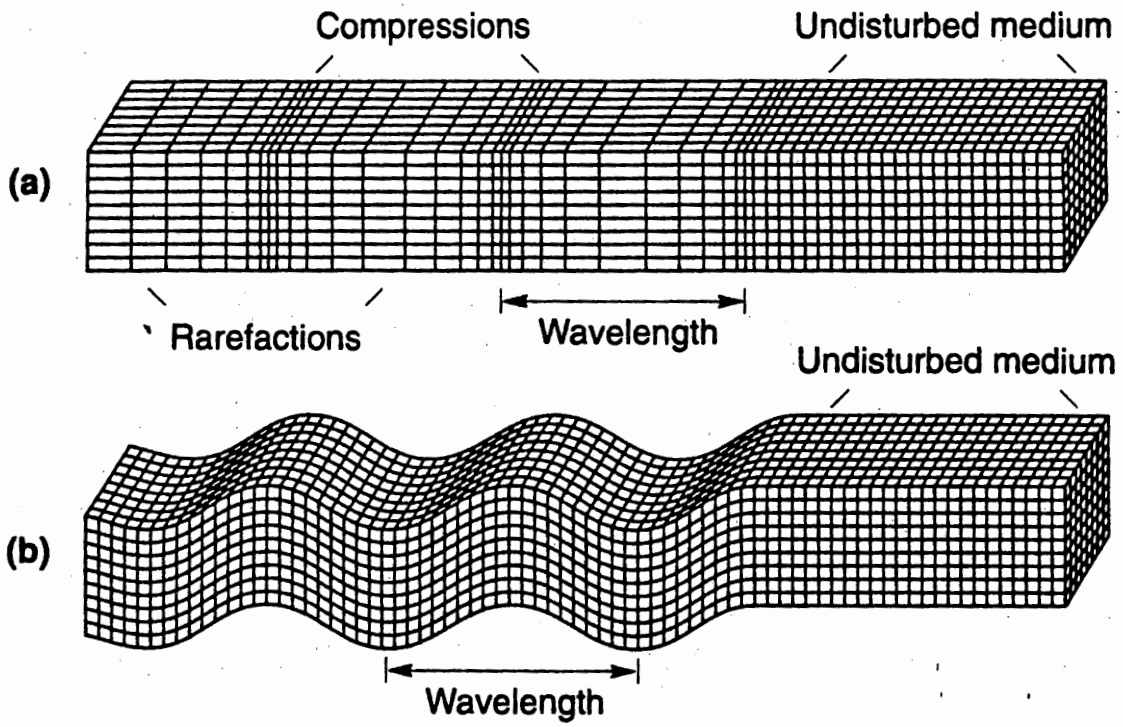


Figure 1. Deformations produced by compression (a) and shear (b) waves.[4]

compression wave, $V_p$, is higher than the shear wave velocity, $V_s$, the compression wave arrives first. It is therefore called a primary wave, while the shear wave is a secondary wave. In layered systems propagation of body waves is affected by reflections and refractions every time a body wave encounters an interface of two layers of different rigidities.

Surface waves include Rayleigh or R-waves and Love or L-waves (Figure 2). Both waves can be described as a disturbance propagating along the surface in a form of an expanding cylinder. Rayleigh wave is a two-component wave, having a horizontal component resembling a compression wave, and a vertical component resembling a shear wave. However, the velocity of a Rayleigh wave, $V_R$, is lower than of both compression and shear waves. The resulting particle motion of a Rayleigh wave is elliptic, due to a phase difference between vertical and horizontal components, as illustrated in Figure 2 by a combined volumetric and distortional deformation of a body. Displacement distributions for horizontal and vertical components of a Rayleigh wave in a half-space are shown in Figure 3. An important observation can be made that the main part of the body of the wave extends to the depth of approximately one wavelength. This feature is utilized in evaluation of elastic properties of the surface pavement layer, as discussed later in the section on the Ultrasonic Surface Wave (USW) method. Another important fact about surface waves is that attenuation with distances, due to geometry of propagation, is proportional to the square root of the distance. On the other hand, attenuation of body waves along the surface is proportional to the distance squared. Much stronger attenuation of body than surface waves leads to a fact that after a certain distance from a source, surface waves

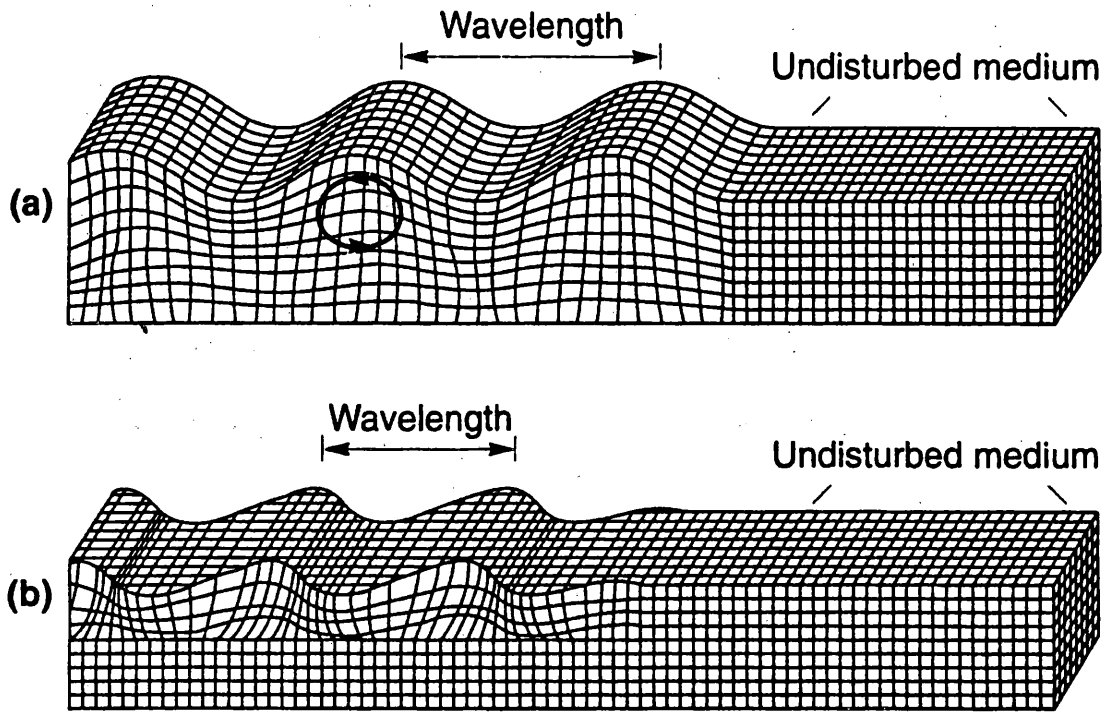


Figure 2. Deformations produced by Rayleigh (a) and Love (b) waves.[4]

dominate the wave field at the surface.

In an elastic half-space the velocity of the Rayleigh wave is dependent on the Poisson's ratio and ranges from 0.86 and 0.95 $V_S$. However, it is often approximated as about 0.9 of the shear wave velocity. Velocities of compression, shear and Rayleigh waves in an elastic half-space are related through the Poisson's ratio, as illustrated in Figure 4 . However, in a layered half-space Rayleigh waves are dispersive, i.e. the velocity of propagation becomes frequency dependent. Rayleigh wave dispersion in a layered half-space is illustrated in Figure 5 for a two-layer over a half-space system. Various lines represent different modes of Rayleigh wave propagation. In soils systems the fundamental mode, the lowest velocity one, typically dominates the wave field. However, in systems of irregular stratification, like pavements, higher and multiple modes may dominate the field.[5] The dispersion phenomenon of wave dispersion is utilized in one of the seismic technique discussed later, the Spectral Analysis of Surface Waves (SASW). Love waves are horizontally polarized shear waves, similar to SH-waves, that exist in layered systems only. Similar to Rayleigh waves, Love waves are dispersive. Because Love waves are not being used, at the moment, in pavement evaluation, they are not discussed in more details. Detailed discussions on elastic waves and wave propagation in layered media can be found in a number of references.[6,7,8,9]

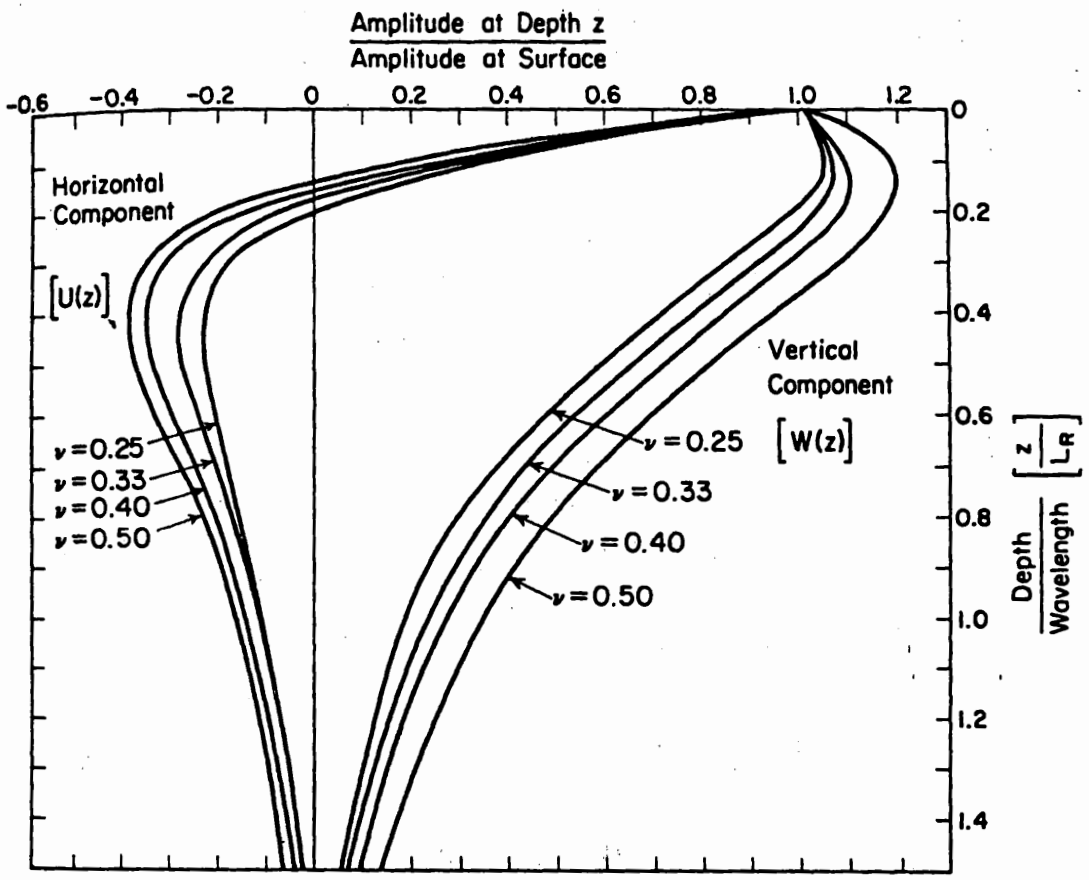


Figure 3. Amplitude ratio vs. dimensionless depth for Rayleigh wave.[7]

## Basic Relationships Between Wave Velocities and Elastic Moduli

The main advantage of seismic methods, in comparison to other geophysical methods, in evaluation of elastic properties is a result of a direct and simple relationship between wave velocities and elastic moduli. This in fact means that seismic methods are essentially capable of direct measurement of elastic properties. Very well known relationships from mathematical physics relate Young's modulus E and shear modulus G to compression and shear wave velocities for wave propagation in prismatic rods

$$V_P = \sqrt{\frac{E}{\rho}} \tag{1}$$

$$V_S = \sqrt{\frac{G}{\rho}} \tag{2}$$

where ρ is the mass density of the rod. For a three dimensional wave propagation the relationship between the shear modulus and shear wave velocity remains the same.

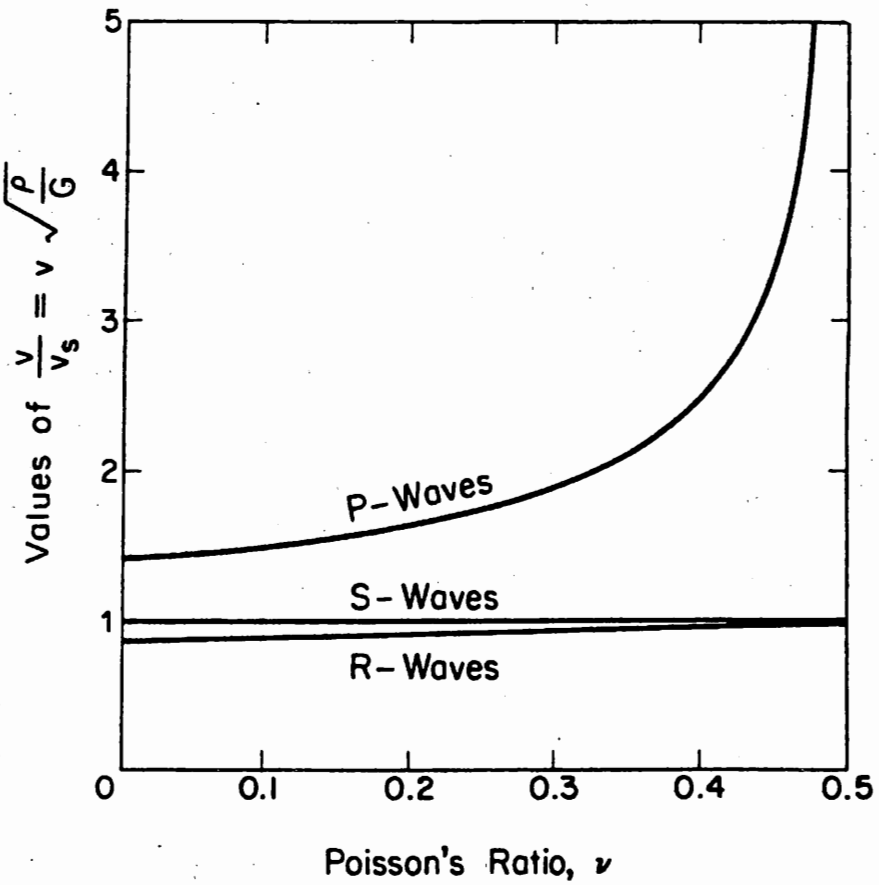


Figure 4. Relationships between Poisson's ratio, compression, shear and Rayleigh wave velocities.[7]

However, the compression wave velocity becomes related to a constrained modulus M

$$V_P = \sqrt{\frac{M}{\rho}} \tag{3}$$

The constrained modulus is related to the Young's modulus through the Poisson's ratio ν

$$M = \frac{E(1-\nu)}{(1+\nu)(1-2\nu)} \tag{4}$$

As mentioned earlier, Rayleigh wave velocity in a half-space is related to the shear wave velocity through the Poisson's ratio, and often can approximated as 0.9 $V_S$. Thus, it is related to the shear modulus. In a layered half-space, velocity of a surface wave is frequency dependent and is termed the phase velocity. It is again related to shear moduli of individual layers, however, the relationship is fairly complex, as discussed in the section on the SASW method. Finally, the Poisson's ratio can be obtained from compression and shear wave velocities

$$\nu = \frac{0.5(V_P / V_S)^2 - 1}{(V_P / V_S)^2 - 1} \tag{5}$$

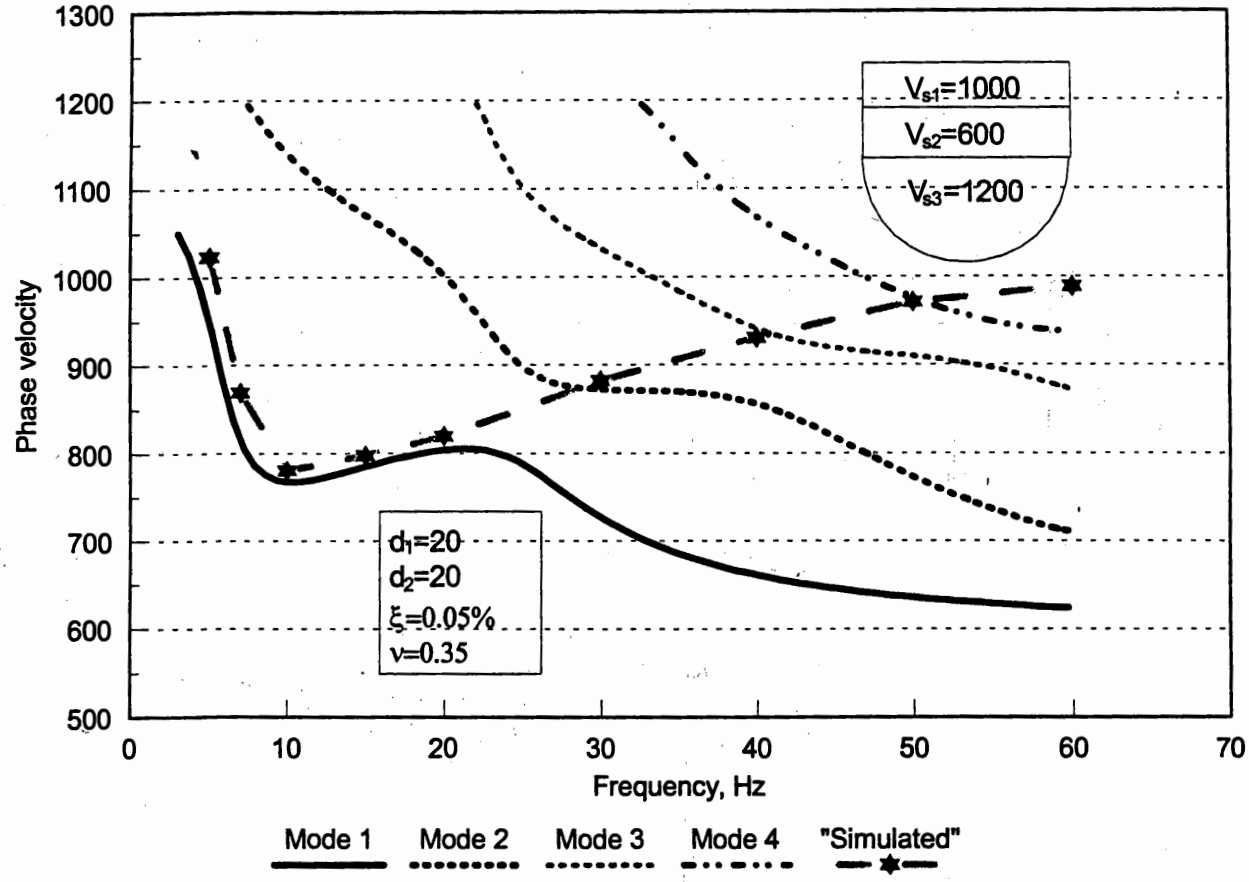


Figure 5. Rayleigh modes and the "simulated" dispersion curve for a layered half-space.

From all the elastic properties, the parameter effecting the dynamic response of pavements or soil systems is the shear modulus. Since the modulus is frequency dependent, it is often called dynamic shear modulus. The primary cause of frequency dependence is damping, whether the damping is of a hysteretic or viscous type. Testing of surface pavement layers by seismic methods is typically done in a high frequency range, anywhere from 2 to 30 kHz. As illustrated in Figure 6, the shear modulus of Hot Mix Asphalt (HMA) measured by the SASW technique may be as much as four times higher than the same modulus measured by devices like Falling Weight Deflectometer (FWD) that measures in a frequency range of 30 to 50 Hz.

The resilient modulus $M_R$ is of special importance in evaluation of long term performance of pavement materials under repeated traffic loading. It is an elastic modulus based on a recoverable strain under repeated loads

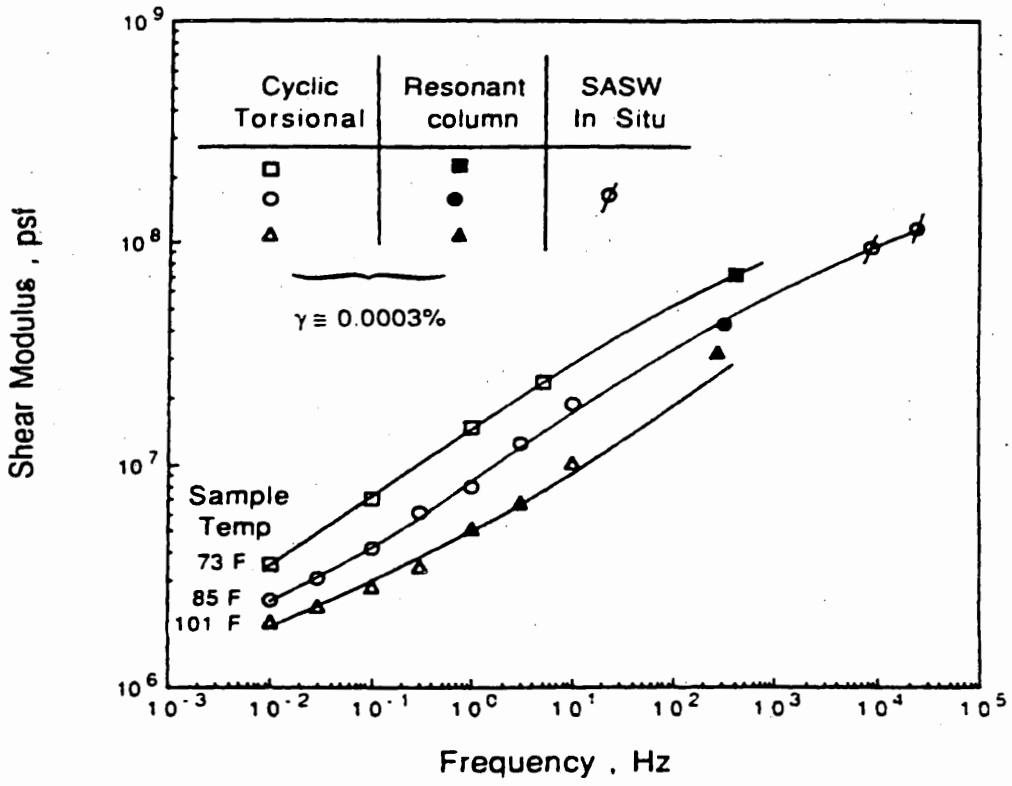


Figure 6. Influence of frequency and temperature on the small-strain shear modulus of asphalt concrete.[10]

$$M_R = \frac{\sigma_d}{\varepsilon_r} \tag{6}$$

where $\sigma_d=\sigma_1-\sigma_3$ is the applied deviatoric stress and $\varepsilon_r$ is the recoverable strain. A number of models were developed to predict the resilient modulus.[11,12,13] While the resilient modulus represents essentially a secant modulus, all the models incorporate in their formulation the initial tangent (low strain) modulus, the state of stress and the strain level. For example, the AASHTO and Pezo[13] models define resilient modulus

$$M_R = k_1\theta^{k_2} \tag{7}$$

$$M_R = k_1\sigma_d^{k_2}\sigma_c^{k_3} \tag{8}$$

where $q=\sigma_1+\sigma_2+\sigma_3=\sigma_1+2\sigma_3$ is the bulk stress, $\sigma_c=\sigma_3$ is the confining pressure and $k_i$ material parameters. Since parameter $k_i$ is related to the maximum, low strain, modulus, it is difficult to measure it accurately by triaxial testing. On the other hand, disturbances during seismic testing are at very low strain levels, and thus seismic methods are far more advantageous for evaluation of the low strain modulus. Laboratory methods should be than used to obtain the shape of the backbone (modulus versus strain) curve.

## Factors Affecting Elastic Properties of Pavement Materials

A number of factors are affecting elastic properties of pavement materials. However, since different factors are affecting soils more strongly than AC or portland cement concrete (PCC), these factors are discussed separately.

### Soil Base and Subbase Materials

Hardin and Black[14] have summarized parameters affecting the shear modulus of soils with the following functional relationship

$$G = f(\sigma_0', e, C, A, H, t, S, \tau_0, f, \xi, T) \tag{9}$$

where

- $\sigma_0$ ' = effective octatahedral normal stress,
- e = void ratio,
- C = grain characteristics, grain size and shape, grading, minearology,
- A = amplitude of strain,
- H = ambient stress history and vibration history,
- t = secondary time effects,
- S = degree of saturation,
- $\tau_0$ = octahedral shear stress,
- f = frequency of vibration,
- ξ = soil structure, and
- T = temperature.

However, the two most important factors affecting the low strain modulus of dry (0 moisture content) soil are the void ratio and the effective octahedral normal stress, as described e.g. by Hardin and Richart[15] equations

$$G = \frac{2630(2.17 - e)^2}{1 + e}\sqrt{\sigma_0'} \tag{10}$$

for round-grained sands, and

$$G = \frac{1230(2.97 - e)^2}{1 + e}\sqrt{\sigma_0'} \tag{11}$$

for angular-grained sands. In both equations G and $s_0$ 'are in lbf/in$^2$. Hardin and Drnevich [16] included effects of overconsolidation and soil plasticity by modifying Equation (11) to

$$G = \frac{1230(2.97 - e)^2}{1 + e}(OCR)^a\sqrt{\sigma_0'} \tag{12}$$

where OCR is overconsolidation ratio and a is a factor dependent on soil plasticity. A number of other relationships have been summarized in other references.[7,17,18] However, the confining pressure and soil density, whether described in terms of void ratio, relative density or else, remain the principal factors affecting the dynamic modulus of dry soil.

Other two important parameters affecting the elastic moduli of soil are strain, number of cycles of loading and moisture content. In most cases, strain causes a reduction in elastic moduli (Figure 7) , while a number of cycles of loading may cause both a reduction and

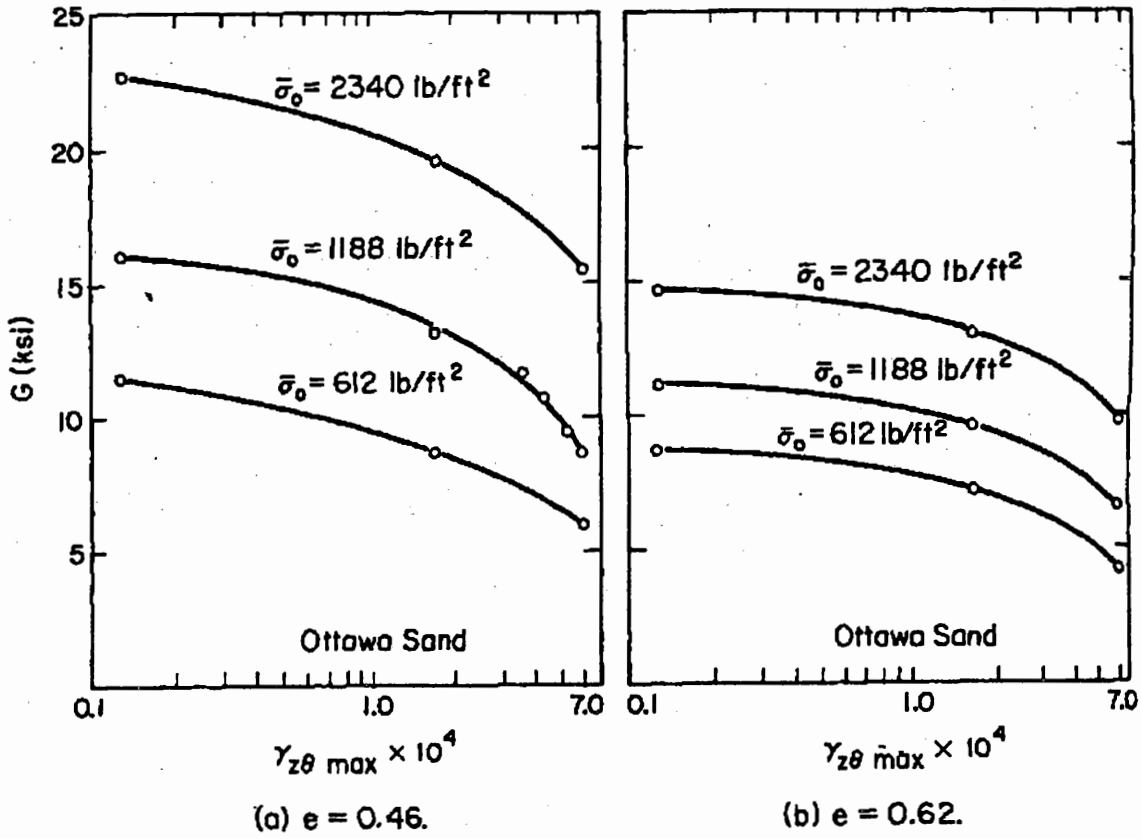


Figure 7. Dynamic shear modulus variation with maximum shear strain amplitude and confining pressure for hollow specimens.[20]

increase (Figure 8). The effect of moisture content on cohesionless soils was theoretically studied by Biot[19], where he demonstrated that it affects the Young's modulus, but has a negligible effect on the shear modulus. The effect becomes more pronounced in presence of fines, as illustrated in Figure 9 for a base material from El Paso County.

**Asphalt Concrete and Portland Cement Concrete**

Two elastic properties are often used in the description elastic moduli of asphalt concrete. The first one is resilient modulus, the second dynamic complex modulus. As for granular base and subbase materials the resilient modulus is the resilient modulus based on the recoverable strain under repeated loads. The resilient modulus uses as loading an arbitrary waveform with a given rest period to simulate traffic loading. The dynamic complex modulus is a complex number, describing the viscoelastic nature of HMA, consisting of a real part representing the elastic stiffness and an imaginary part representing the internal damping. Unlike the resilient modulus test, the dynamic complex modulus is evaluated by applying repeated sinusoidal or haversine loading with no rest. From a number of parameters affecting the elastic moduli of HMA, four parameters have the highest influence: temperature, frequency, strain level and the state of stress. An increase in temperature may significantly decrease the modulus, as illustrated in Figure 6 and in Figure

10 for two void in total mixture (VTM) ratios and two regimes of increasing and decreasing temperature. Effect of frequency was discussed in the previous section (Figure 6). Similar results, but in a low frequency range, were reported by Huang.[21] Nazarian *et al.* have demonstrated that a strong correlation between the elastic moduli measured by *in situ* seismic testing and traditional static testing on cores can be established, as illustrated in Figure11.[22] They have also demonstrated that the dispersion of results conducted by *in situ* seismic testing is far less than by static testing on cores.

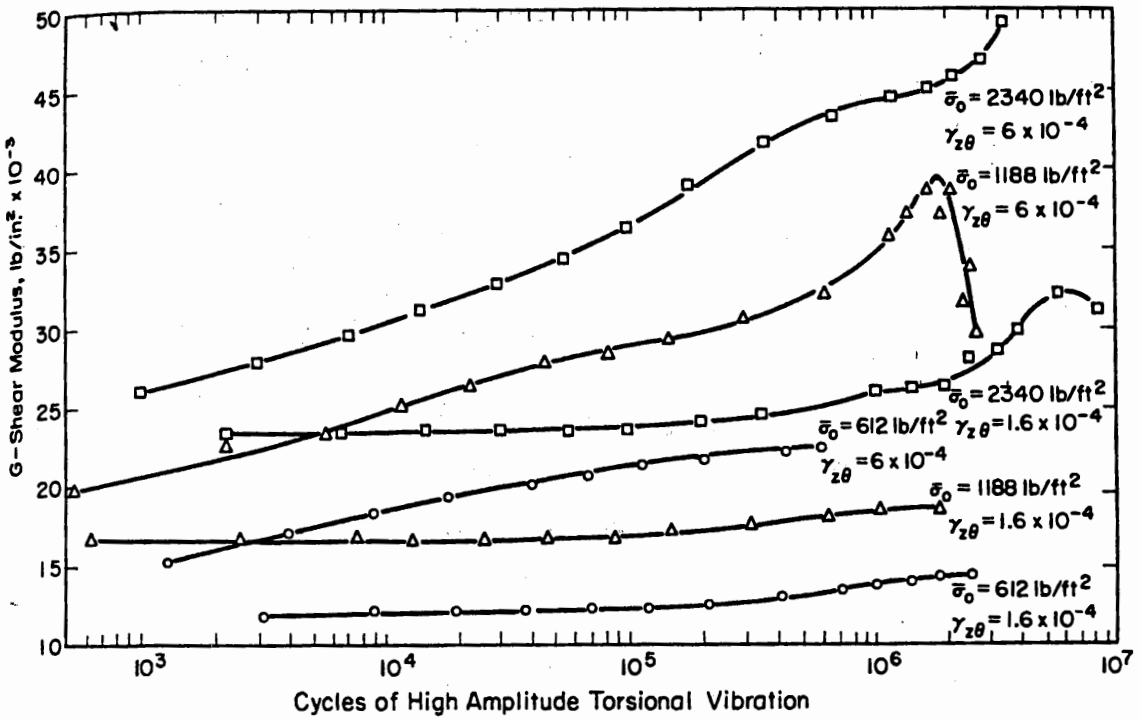


Figure 8. Effect of a number of cycles of high-amplitude vibration on the shear modulus at low amplitude (Ottawa sand, e=0.46, hollow sample).[20]

Modulus of elasticity of concrete is, according to the American Concrete Institute (ACI) code, evaluated as the secant modulus from the compressive strength cylinder strength.[24] While the modulus is primarily affected by the strength, other factors like: loads, moisture in concrete, age and temperature also have an effect.[25]

**Seismic Methods Used in Pavement Evaluation**

This section concentrates on the background of five seismic techniques that are implemented in the SPA, and so far have shown the highest potential in pavement evaluation. Application of a number of other seismic techniques used in geotechnical, geological and structural applications needs to be examines yet. The five techniques include:

1) Spectral Analysis of Surface Waves (SASW),
2) Impulse Response (IR),

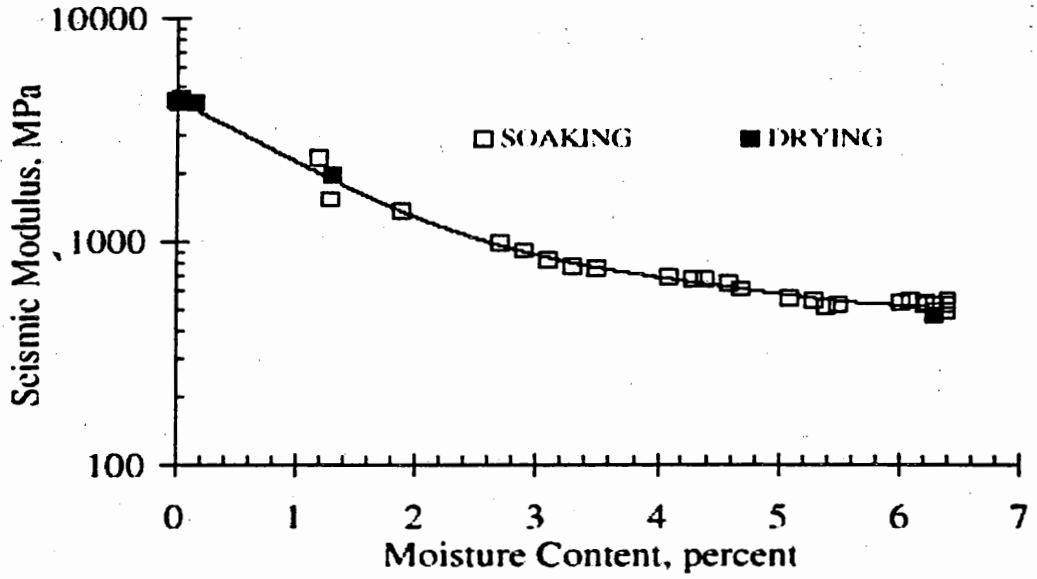


Figure 9. Variation in modulus with moisture during soaking.[23]

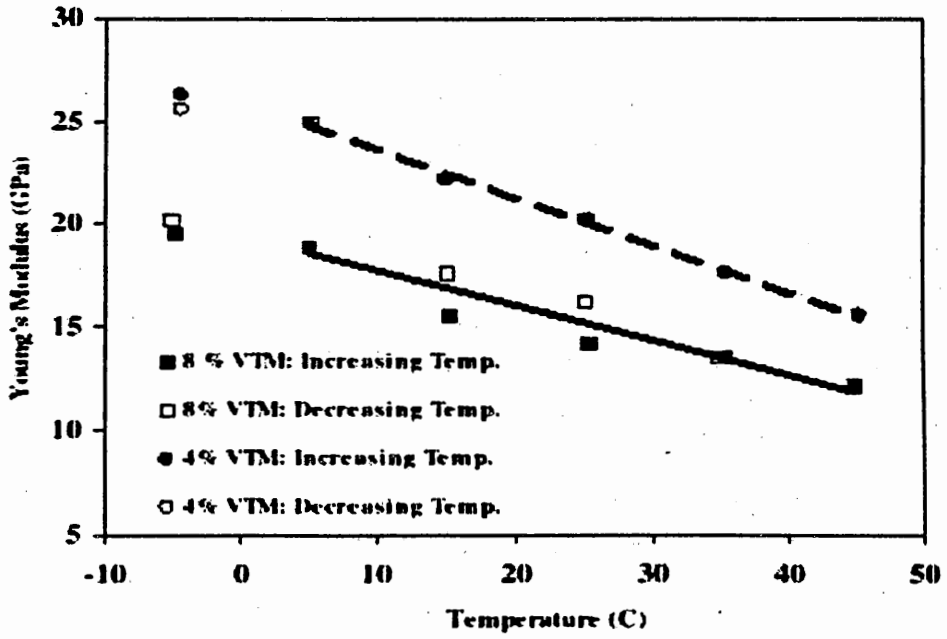


Figure 10. Variation in modulus of AC briquettes with temperature.[23]

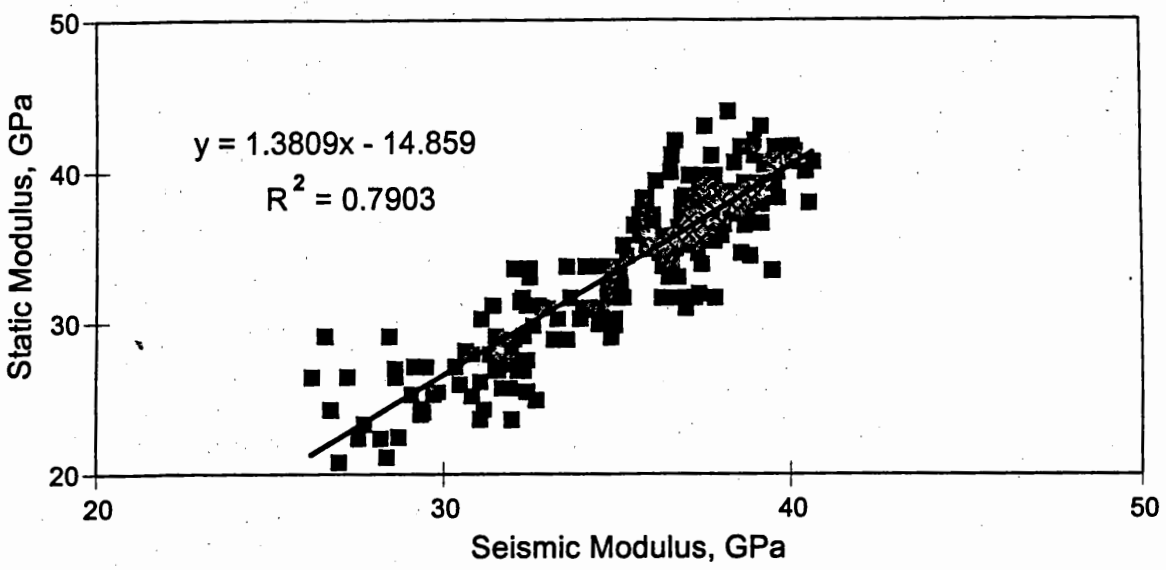


Figure 11. Static vs. seismic modulus.[26]

3) Ultrasonic Body Wave (UBW),
4) Ultrasonic Surface Wave (USW), and
5) Impact Echo (IE).

The SASW technique is a broad range frequency technique, in pavement evaluation typically covering a range from a few tens of Hz to several kHz. It is used in elastic modulus profiling of pavement systems. The IR technique is a low frequency technique, typically covering a range of a few hundreds of Hz, used in subgrade modulus evaluation and problems associated with changes in foundation layers. UBW, USW and IE are high frequency techniques, used in characterization and distress diagnostics of the surface pavement layer. Ultrasonic name is used to indicate that their frequency range extends beyond the audible range. In the SPA, the techniques cover a range of approximately few kHz to about 30 kHz. Primary applications of the five techniques are summarized in Table 1.

**Spectral Analysis of Surface Waves (SASW)**

The SASW test is a nondestructive technique for in situ evaluation of elastic moduli and layer thicknesses of layered systems like soils and pavements.[27,28] The method is based on the phenomenon of Rayleigh wave dispersion in layered systems, i.e. the phenomenon that the velocity of propagation is frequency dependent. The objective of the test is to determine the velocity-frequency relationship described by the dispersion curve, and then, through the process of inversion or backcalculation, to obtain the shear wave velocity profile. Elastic moduli profiles can then be easily obtained using simple relationships with the velocity of propagation and measured or approximated values for mass density and Poisson's ratio.

**Table 1. Application of Seismic Techniques in Pavement Evaluation and Diagnostics**

| Seismic Technique | Applications |
|---|---|
| Spectral Analysis of Surface Waves (SASW) | Elastic modulus profiling (modulus and thickness of each layer) |
| Impulse Response (IR) | Modulus of subgrade/foundation layers<br>Detection of voids or loss of support |
| Ultrasonic Body Wave (UBW) | Modulus of the top paving layer |
| Ultrasonic Surface Layer (USW) | Average or variation of modulus in the top paving layer |
| Impact Echo (IE) | Thickness of the top paving layer<br>Detection of delaminations |

A schematic of the SASW test is shown in Figure12. Elastic waves are generated (by means of impacts, vibration generators or other sources), detected by a pair or an array of receivers and recorded by a transient recorder. Recorded signals are transformed from the time to the frequency domain by the means of Fast Fourier Transform and spectral functions applied to obtain information about the velocity as a function of frequency, the phase velocity. Two functions are of special importance, the cross power spectrum and coherence (Figure 13). As described in Figure 12, the phase velocity for a particular frequency f can be obtained from the phase difference β between two receiver locations according to the relationship

$$V_{ph} = \frac{360^0 Xf}{\beta} \qquad (13)$$

where X is the receiver spacing and β is in degrees. Phase β is obtained from the phase of the cross power spectrum. The coherence function operates on averaged signals and is used to evaluate the quality of a signal at every particular frequency. For a high quality signal, high signal to noise ratio, coherence is close to one. Portions, frequency ranges, of a signal of coherence less than about 0.8 to 0.9 are usually rejected in further evaluation. Phase velocities for a range of frequencies form a dispersion curve. In an actual process the dispersion curves are evaluated for a series of receiver spacings and averaged to obtain an average dispersion curve.

The last step in the SASW test is inversion of the dispersion curve, or backcalculation, to obtain the modulus profile. In this process thicknesses and moduli (shear wave velocities) of all the layers are evaluated. This is a complex, nonlinear problem that has been solved in a number of different ways.[27,29,30,31] A typical dispersion curve for a pavement, and the backcalculated shear wave velocity profile are shown in Figure 14.

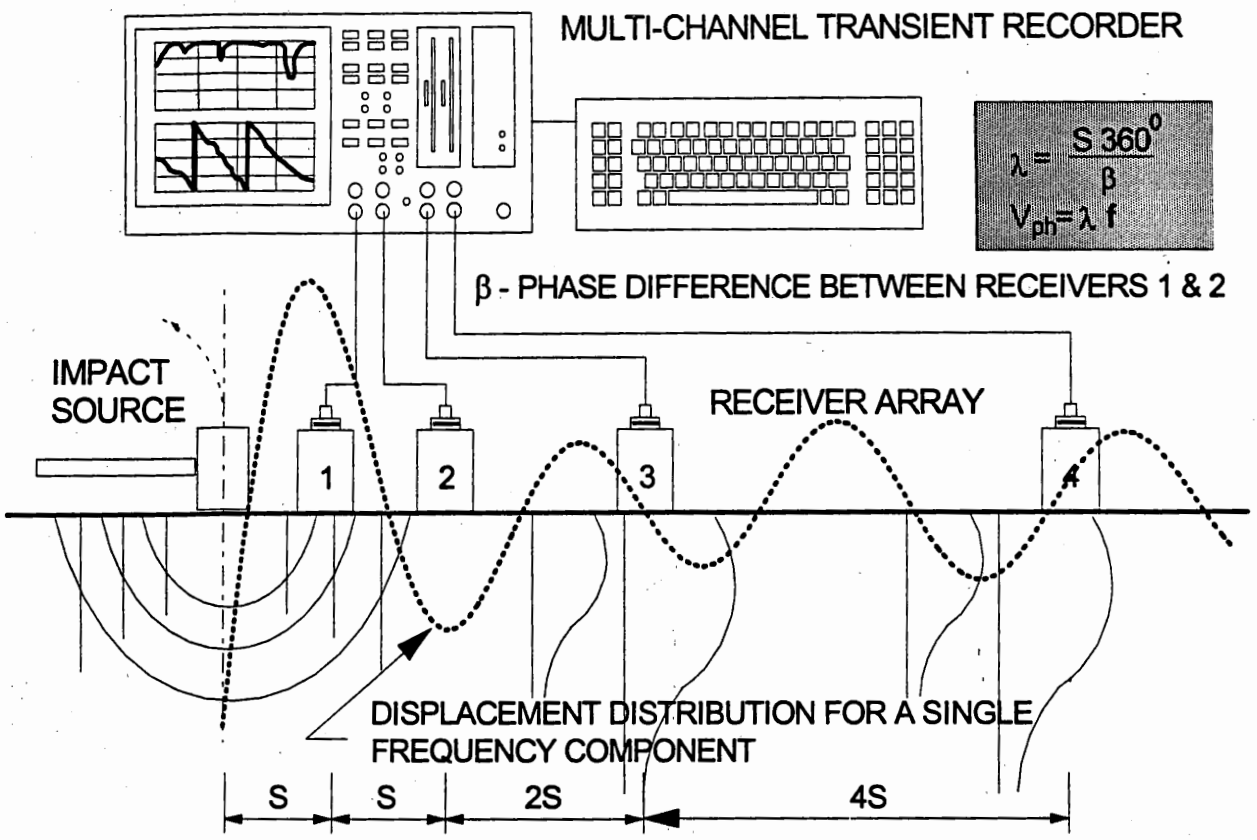


Figure 12. Schematic of the SASW test.

**Impulse Response (IR)**

The impulse response technique is used mostly for two purposes in evaluation of shear modulus of the pavements. The first purpose is to determine the modulus of subgrade reaction or the shear modulus of the subgrade for rigid pavements, or the modulus of the overall system for flexible pavements. The second purpose of IR testing is to detect the presence of voids or loss of support beneath rigid pavements. The IR method is based on the application of an impact and evaluation of the response of the pavement detected at a closely placed receiver. Use of IR in evaluation of the modulus of subgrade reaction is illustrated in Figure 15. Signals from the impact hammer, the forcing function, and the response at the nearby geophone (velocity transducer) are transformed into the frequency domain to obtain the corresponding spectra. The ratio of the displacement and impact spectra represent a flexibility spectrum, while the inverse ratio is termed a mechanical impedance (dynamic stiffness spectrum). The flexibility spectrum is matched by a flexibility spectrum (response spectrum) for an assumed single-degree-of-freedom (SDOF) system. Once the two spectra are matched, the modal properties of the SDOF system provide information about the shear modulus of the subgrade, or the modulus of subgrade reaction, and damping of the system. Matching of the two spectra, in this case impedances, is illustrated in Figure16. The underlying assumption of this process is that pavement's response can be approximated by the response of a SDOF system, A theoretical and field studies shows that the modulus in the case of rigid pavements corresponds to the

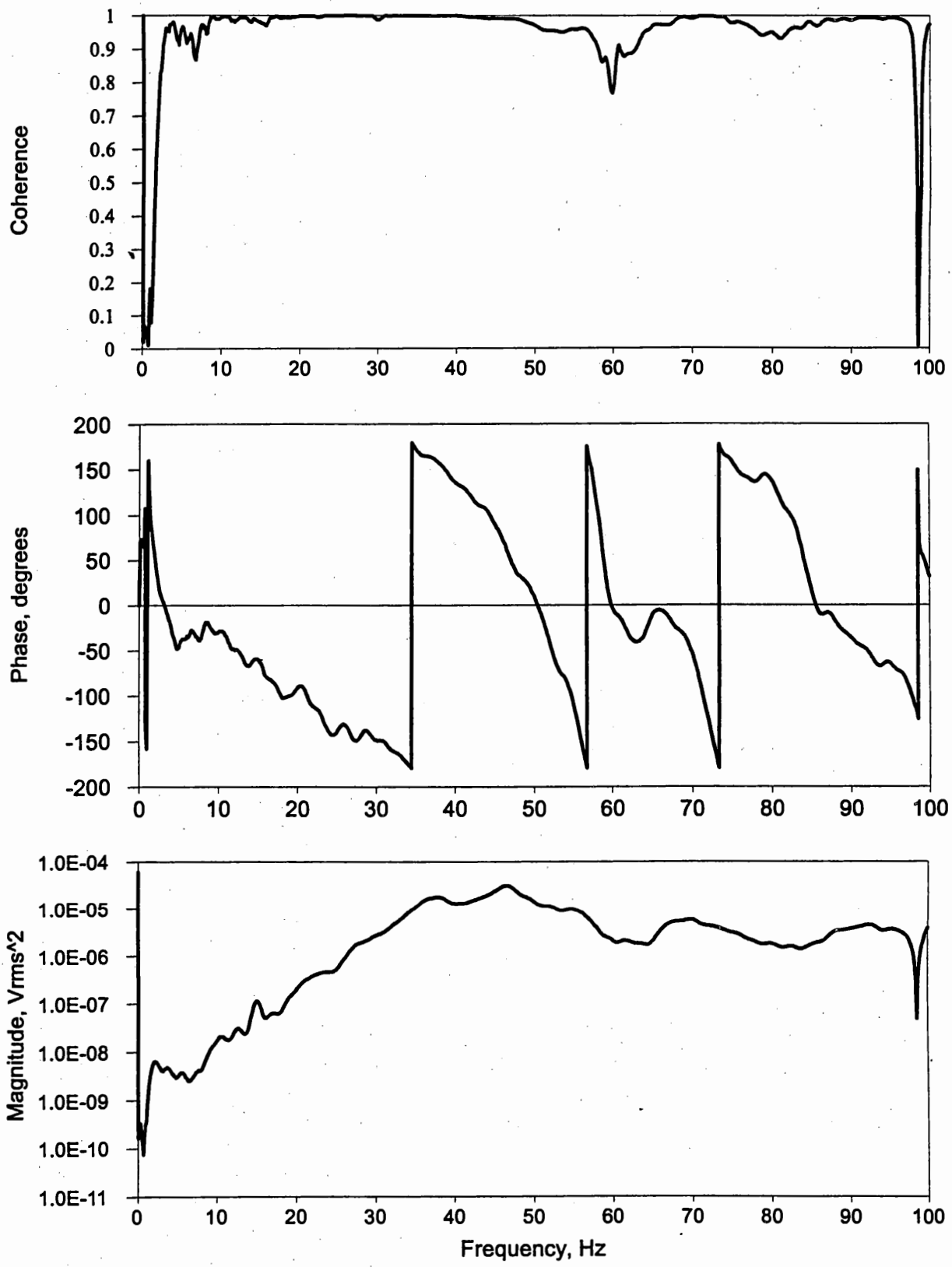


Figure 13. Coherence (top), phase of the cross power spectrum (middle) and magnitude of the cross power spectrum (bottom).

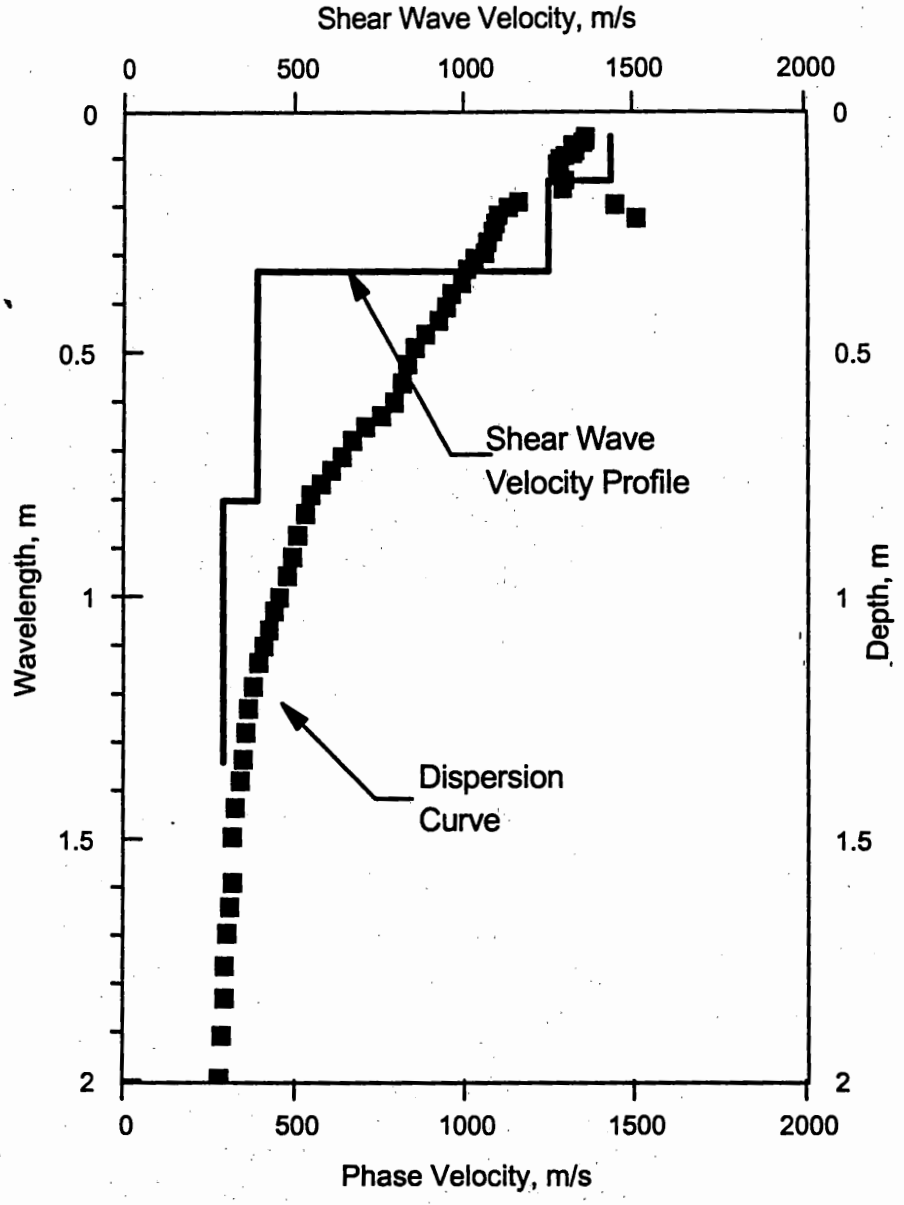


Figure 14. A dispersion curve for a pavement and the backcalculated shear wave velocity profile.

subgrade modulus, while in the case of flexible pavement should be considered as an overall modulus.[32] The SPA software utilizes for calculation of the shear modulus of the subgrade formula by Dobry and Gazetas[33]

$$G = \frac{1-\nu}{2LA_0 I_s S_z} \tag{14}$$

where L is the length of the slab, $A_0$ is the static flexibility of the slab, and $S_z$ is the shape factor, equal to 0.8 for a long flexible pavement. $I_s$ is a parameter introduced by Reddy that considers the shape of the slab and position of application of loading.[32] Low modulus is an indication of a poor support.

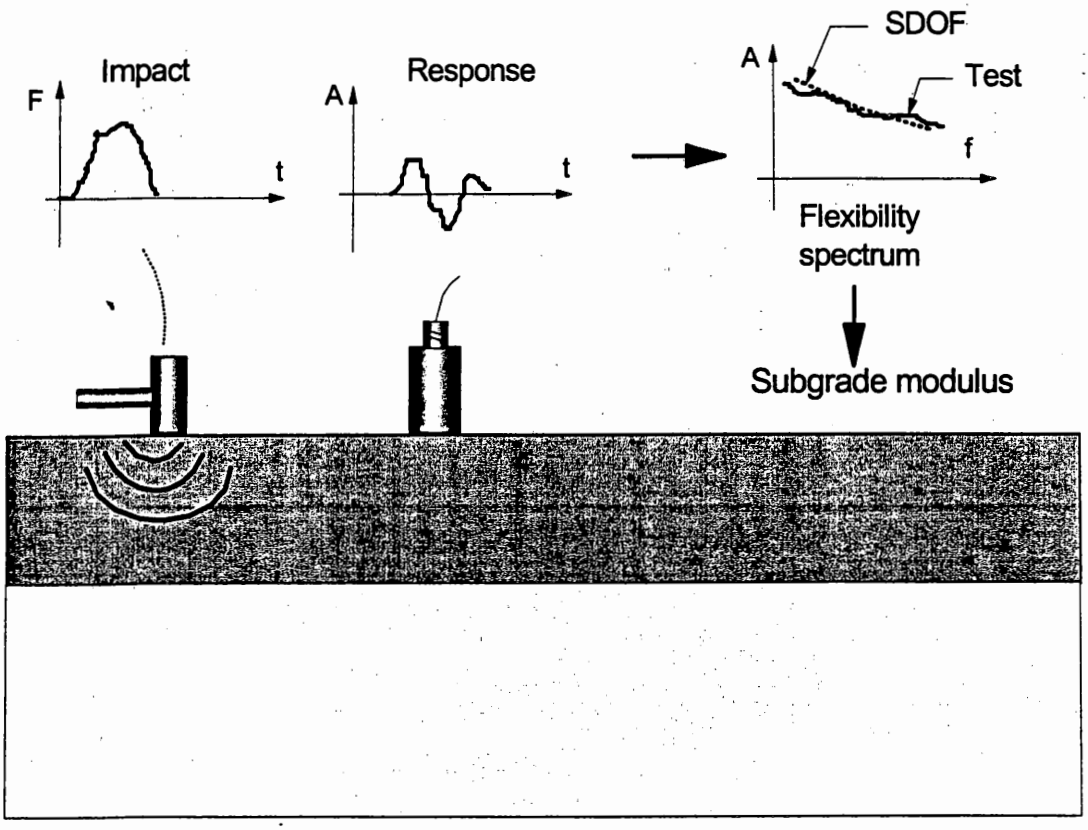


Figure 15. Evaluation of subgrade modulus by the IR technique.

The IR method is also used in detection of loss of support or presence of voids beneath rigid pavements. It is detected by a reduced subgrade modulus and low damping. This is illustrated in Figure17 for a rigid pavement with a void beneath the joint of a concrete slab. If an impact is applied at a point of sound contact and good support, or a water saturated void, energy generated by the impact will radiate towards the interior of the medium, leading to a response that can be described as a highly damped response. On the other hand, if a void is present, the energy generated by an impact will in great part be trapped within the slab, leading to a response that can be described as a lightly damped response, leading to a low damping ratio and high response. Two time histories for a slab with a void and the same slab having the void injected with polyurethane grout are shown in Figure 18. Nazarian et al.[3] define damping ratio ratios for various degrees of the slab contact. A slab in a good contact with the subgrade or with a water satured void exhibits damping ratio above 70%. A slab with an edge void exhibits damping ratio 10-40%, while the one with a void in the middle of the slab 30-60%.

## Ultrasonic Body Wave (UBW) and Utrasonic Surface Wave (USW)

The two ultrasonic techniques utilize high frequency/ultrasonic body (compression) and surface waves to measure elastic and shear moduli, respectively, of thin homogeneus structures like bridge decks, or of a near surface region in composite structures like pavements. To evaluate the elastic modulus, the compression wave (P-wave) velocity is

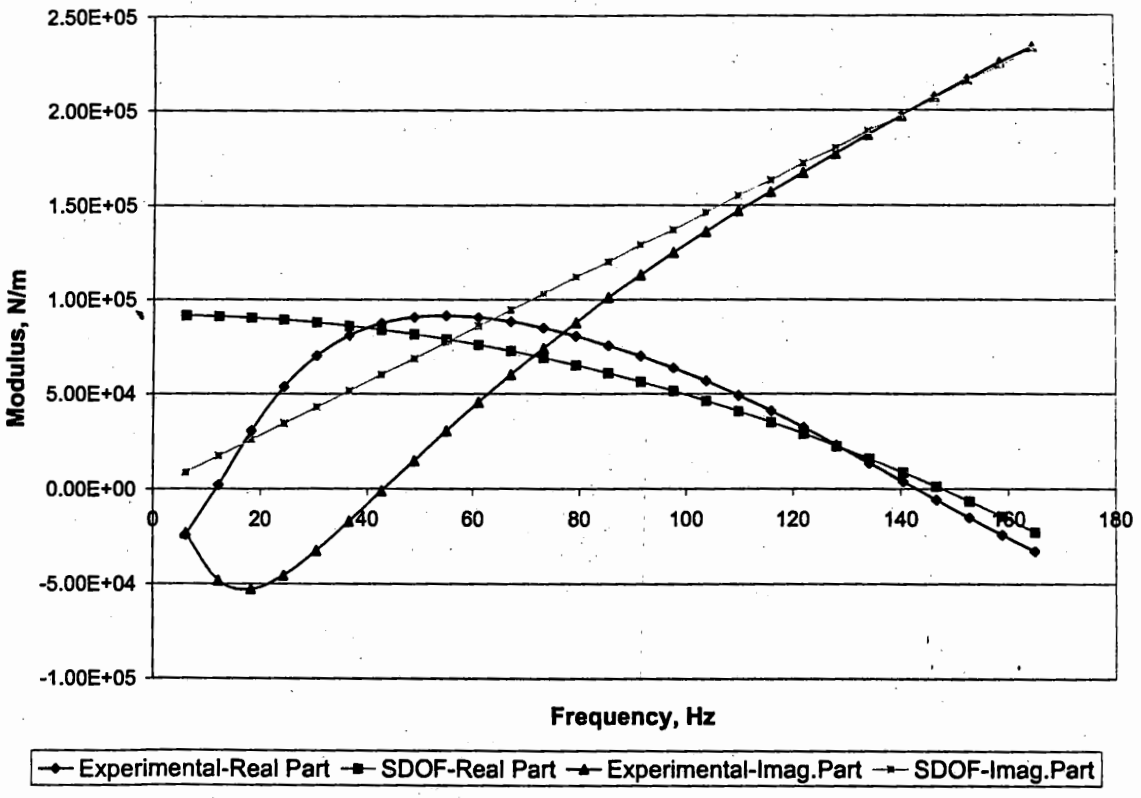


Figure 16. Matching of experimental and SDOF impedance functions.

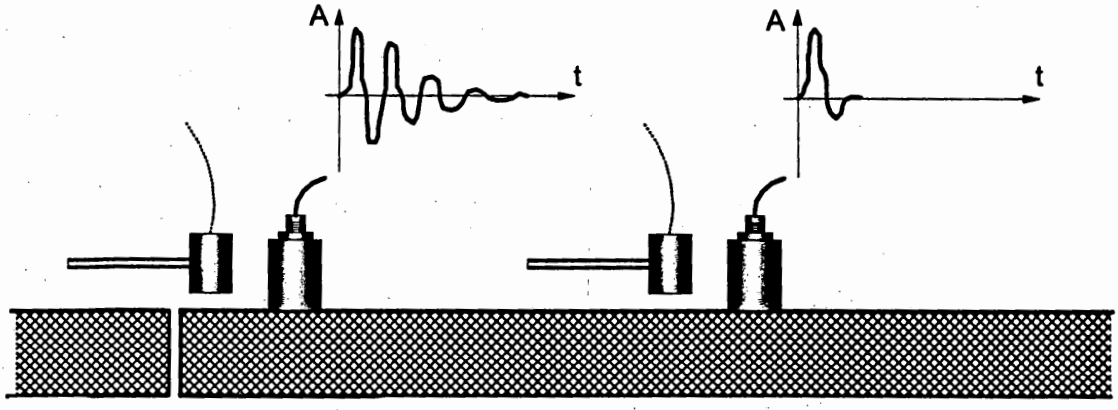


Figure 17. Detection of voids below rigid pavements by the IR technique.

measured directly from the travel time of a P-wave between two receivers, as depicted in Figure19. The elastic modulus is then calculated from a simple relationship between modulus and the P-wave velocity, Poisson's ratio and mass density. Typical time histories from UBW testing, with P-wave arrivals, that are the first arrivals, marked are shown in Figure 20.

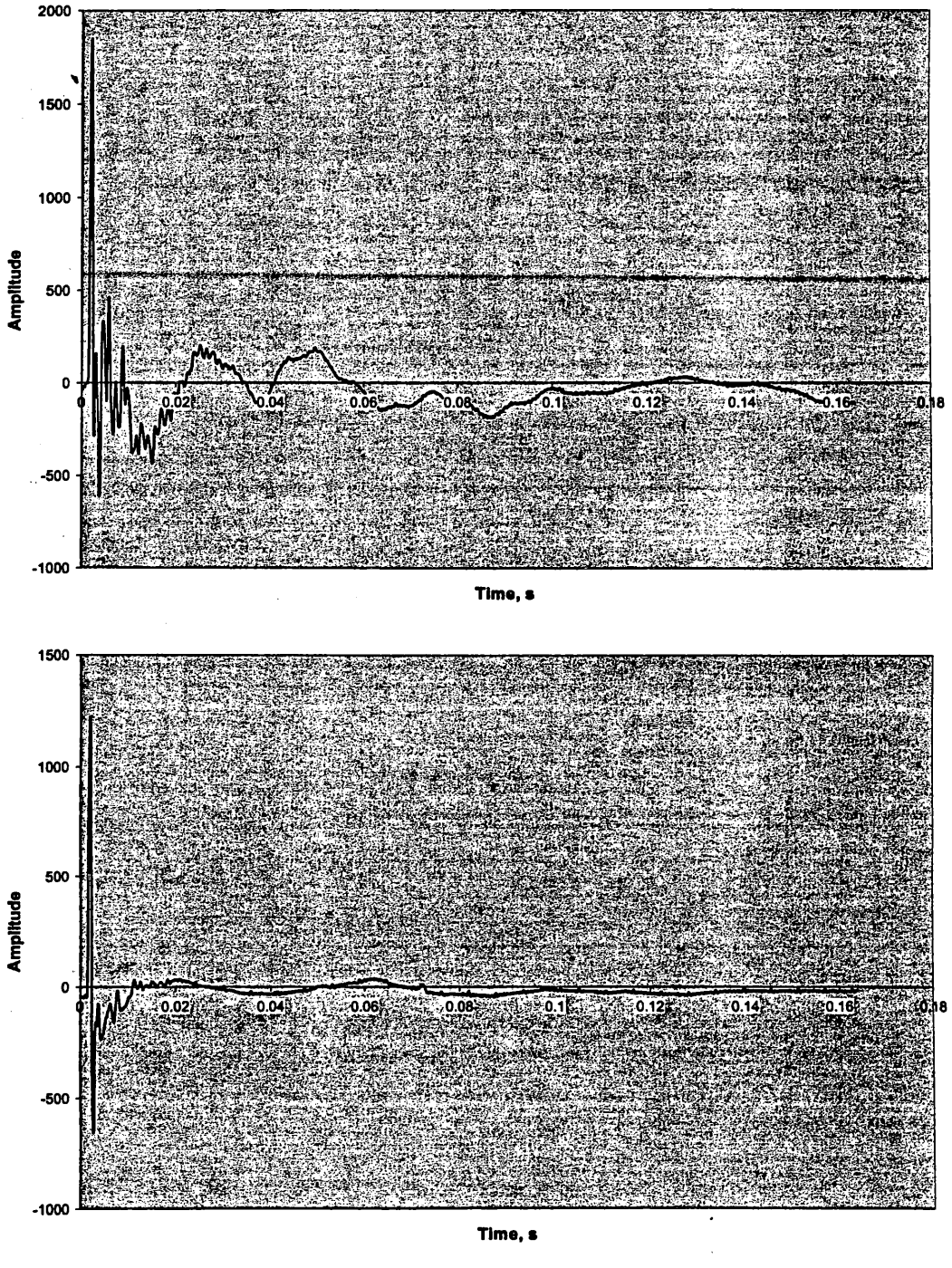


Figure 18. Time histories for a joint with void (top) and with a good support (bottom).

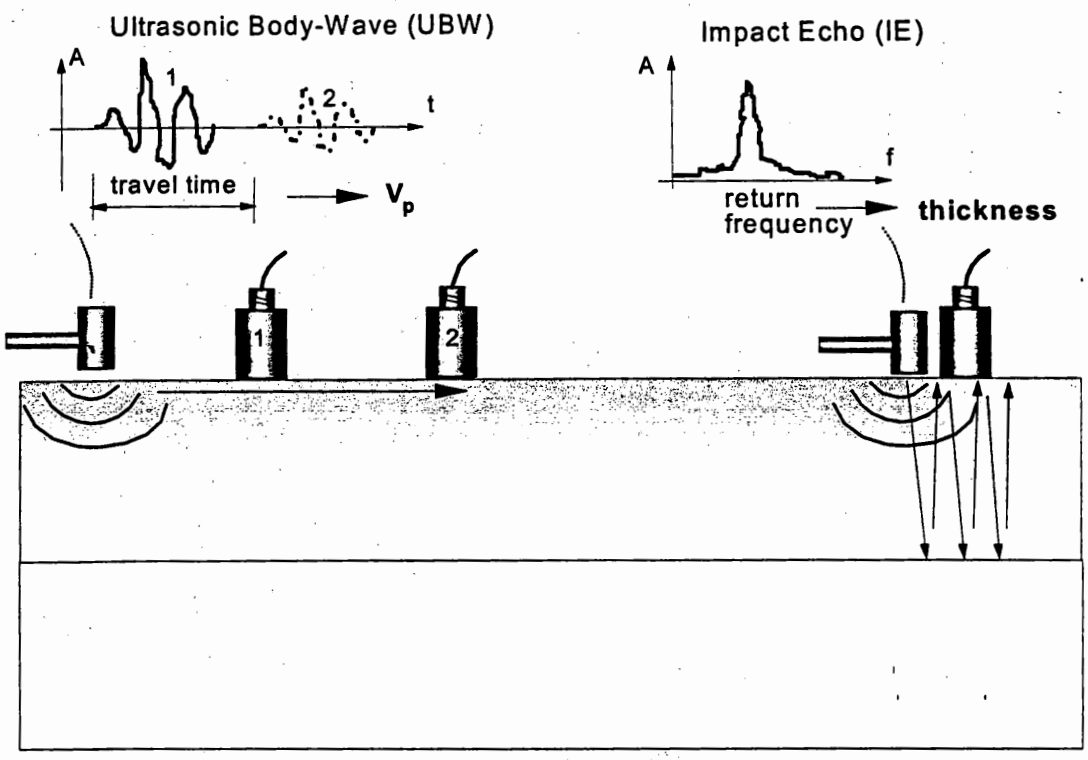


Figure 19. Evaluation of the modulus of elasticity and the thickness of the overlay by UBW and IE methods.

To evaluate the shear modulus, ultrasonic surface waves are used in the USW technique to determine the shear wave (S-wave) velocity, according to the same scheme as in the UBW technique. The only difference is that the S-wave velocity is determined from an average phase velocity of the surface wave in a high frequency and ultrasonic frequency ranges, similar to how it is being done in the SASW test. A dispersion curve and an average phase velocity are shown in Figure 21. The USW technique is a more robust technique than the UBW for evaluation of moduli of the top paving layer. One of the strong sides of the USW technique is that it is capable of measuring variations of moduli within the top paving layer. This might be of special importance of studies of effects of daily temperature changes in asphalt pavements, or uneven curing in concrete pavements. Finally, the obtained P- and S-wave velocities can be used in evaluation of the Poisson's ratio.

**Impact Echo (IE)**

Impact echo is used in conjunction with the UBW test to determine the thickness of the surface layer, or in a case of delamination of the surface layer to detect the position of the delamination. The test is based on a simple principle that whenever there is a significant change in the stiffness of a medium, a significant or complete reflection of P-waves occurs. The objective of the IE test is to determine the resonant or "return" frequency of the P-wave reflected from either the bottom of the surface layer or the delamination. It is evaluated from a linear spectrum of a signal recorded at a receiver placed close to the impact source,

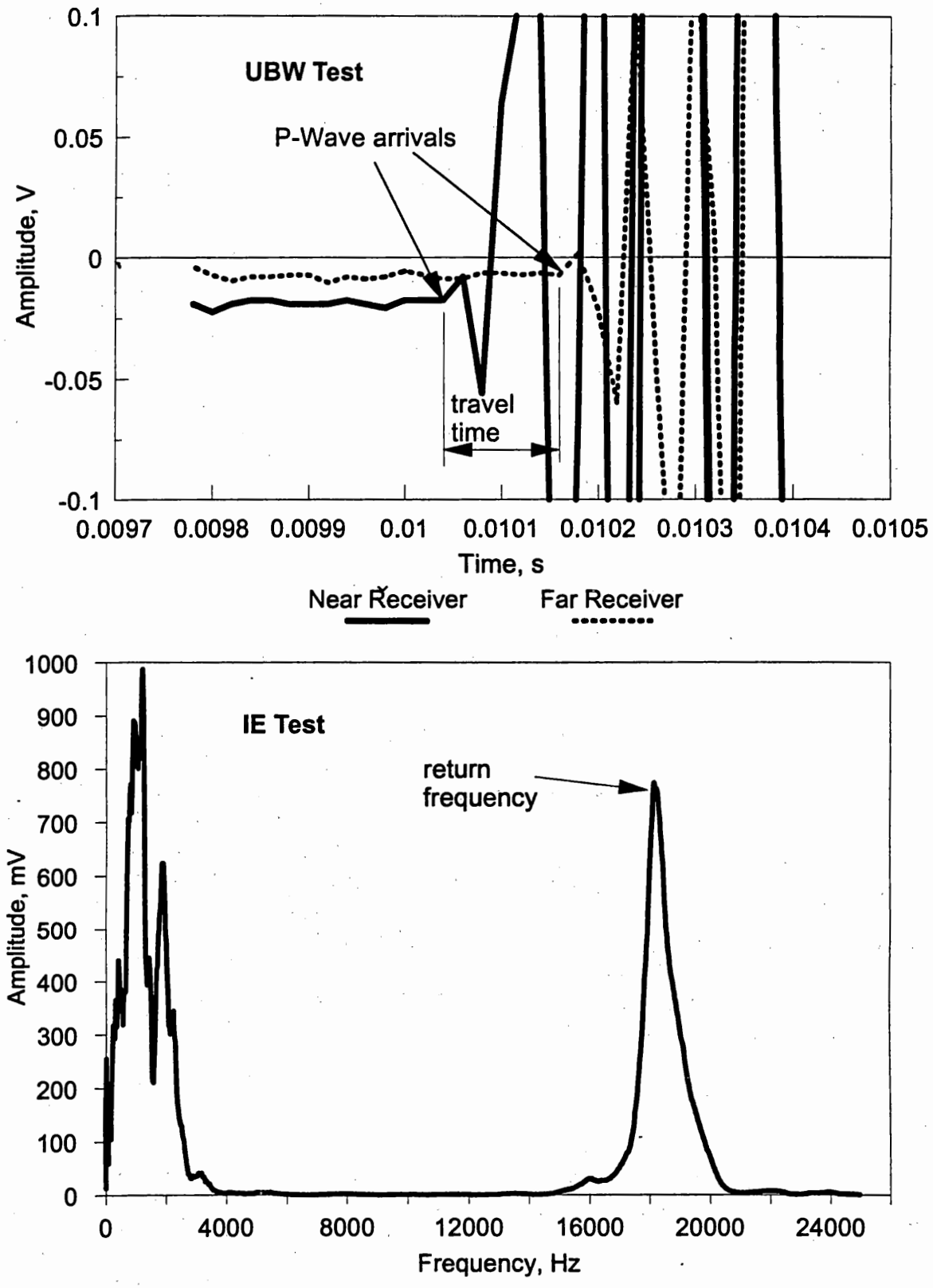


Figure 20. Time histories from UBW test and spectrum from IE test.

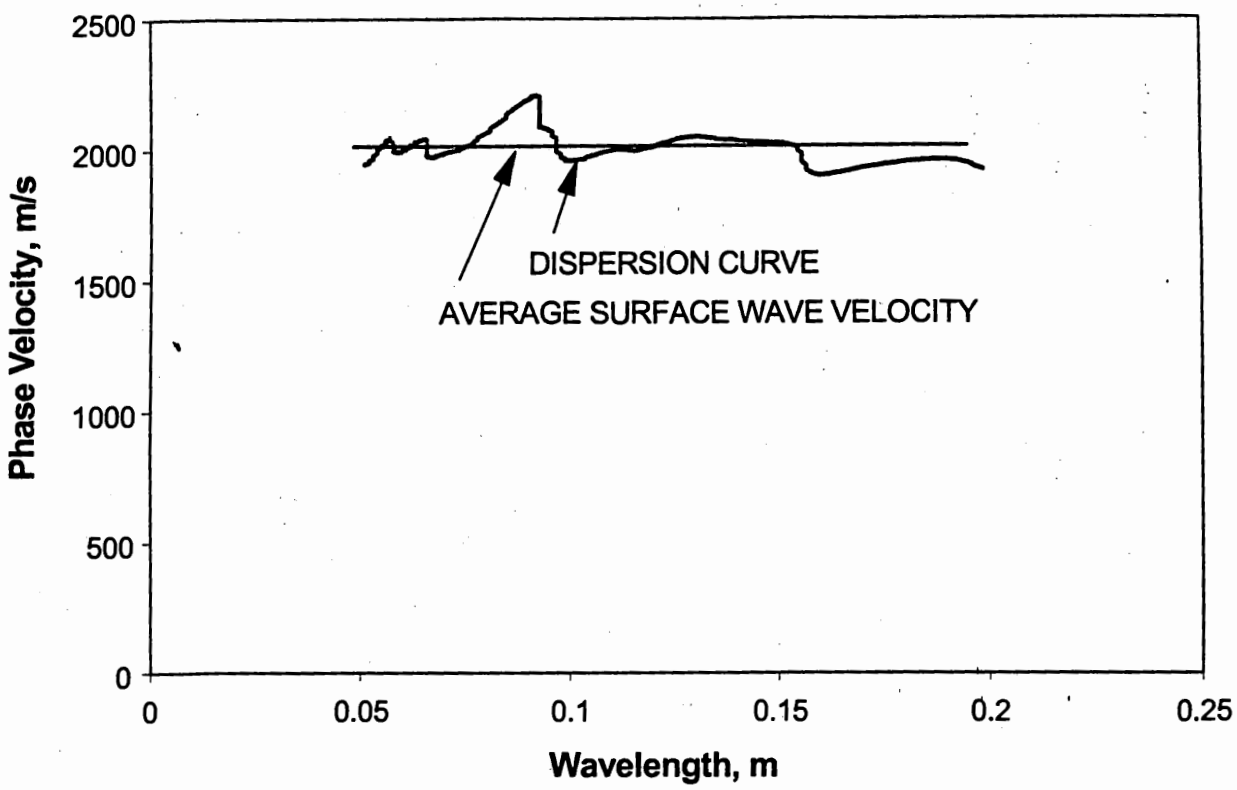


Figure 21. Dispersion curve and average surface wave velocity from USW test.

as shown in Figure 19. Once both the P-wave velocity and "return" frequency are known, the thickness of the surface layer can be calculated as a ratio of the P-wave velocity and the double "return" frequency

$$t = \frac{V_P}{2f_r} \tag{15}$$

IE test can be very successfully used in condition evaluation of concrete bridge decks with respect to corrosion induced delaminations.[34,35] Typical spectra for a sound and a delaminated deck are shown in Figure 22. The top pair are frequency spectra, where a shift of the return frequency towards higher frequencies exists. The bottom pair are thickness spectra, where the frequency axis was replaced by the thickness calculated according to Equation (15) divided by the design thickness of the deck. For an assumption that the compression wave velocity is constant, a double return frequency for a delaminated deck indicates that a delamination is present at about the half of the deck thickness.

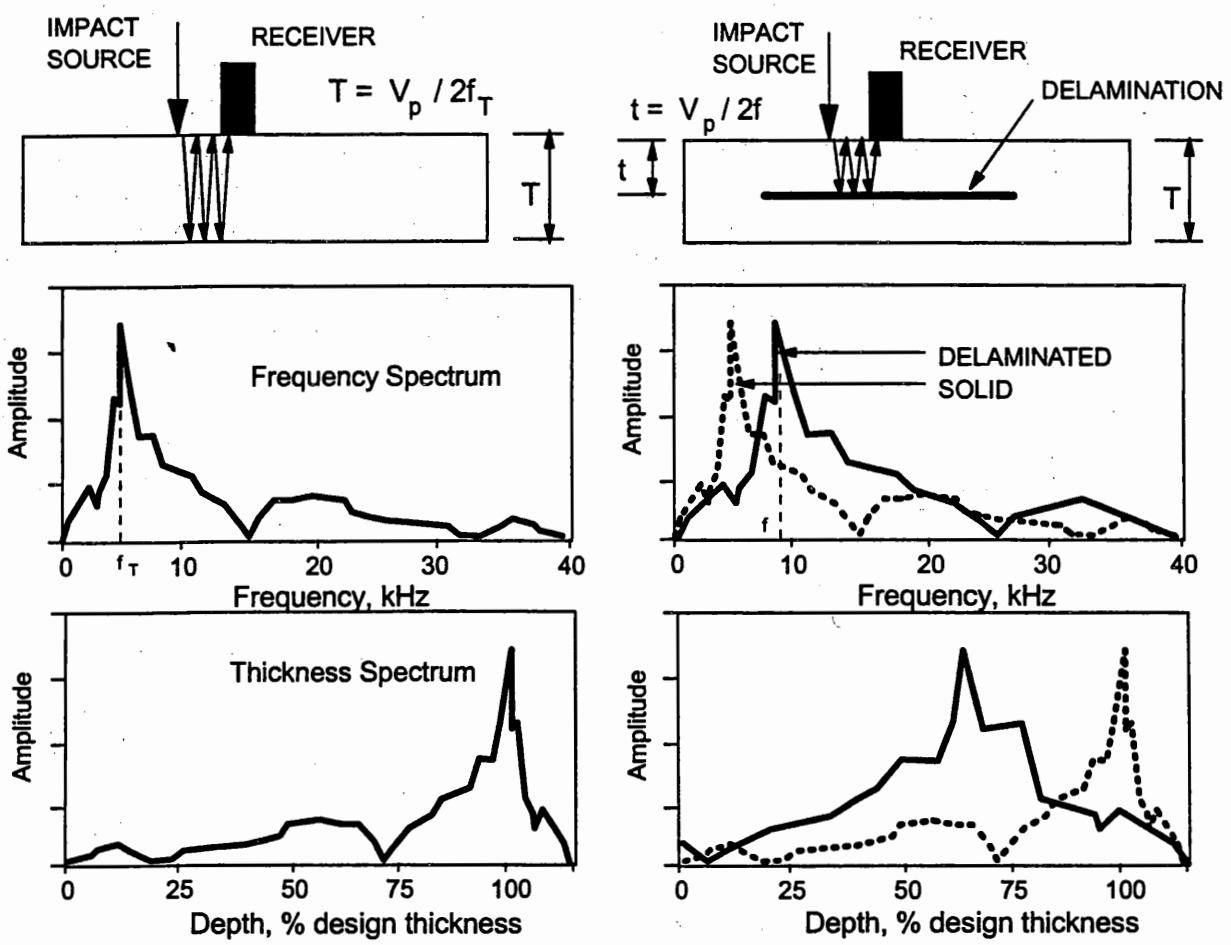


Figure 22. Frequency and thickness spectra for sound (left) and delaminated decks (right).

## SEISMIC PAVEMENT ANALYZER

The Seismic Pavement Analyzer (SPA) was developed through the Strategic Highway Research Program (SHRP) at the University of Texas at El Paso.[3] The SPA is manufactured by Geomedia Research and Development, Inc., in El Paso, Texas. The trailer mounted device (Figure 23) in a great part resembles the Falling Weight Deflectomer (FWD), a device that has been in pavement evaluation since early seventies. While the FWD can be described as a deflection measurement based device, the SPA can be described as a wave propagation measurement based device.

The SPA was developed with an objective of having a device that will in an inexpensive and precise manner meet project-level study needs of a transportation agency with respect to pavement maintenance.[3] Of special importance was to develop a device that would enable detection of distresses at their early stages, so that problems can be resolved or stabilized through preventive maintenance. As such, four major features were determined to be necessary for effective maintenance measurements:

Figure 23. Seismic Pavement Analyzer (SPA).

1) sufficient sensitivity with respect to the measurability of a factor affecting pavement performance,
2) sufficient accuracy in identification of a layer contributing to a potential distress,
3) sufficient precision in evaluation of effectiveness of preventive maintenance procedures, and
4) sufficient sophistication in differentiation between a rehabilitation activity and a maintenance activity.

Since the time of the development of the first prototype, the SPA device was improved and evaluated, and new potential applications of the device presented. Accordingly, as the capabilities of the device with respect to the stated objectives were evaluated, the description of the role of the SPA in the pavement evaluation changed.[22] The objective of this study was to evaluate the SPA with respect to the reliability of its hardware (electrical and mechanical) components, with respect to accuracy, consistency and robustness of its software, and to explore capabilities of the SPA related to pavement monitoring, maintenance and rehabilitation.

The following sections discuss:
1) the SPA hardware, with respect to the hardware components, their maintenance and experienced problems,
2) operation of the SPA in the field,
3) the SPA software, with respect to its accuracy, robustness and consistency.

These sections will also serve as a brief guideline through testing, since the manufacturer provides information about operation and analysis through help files only. Applications of the SPA in pavement evaluation for monitoring and quality assurance purposes are presented and discussed in the sections on evaluation of the SPA in pavement profiling and other applications of the SPA.

**SPA Hardware**

The SPA is a trailer mounted device consisting of two hardware subsystems. The first subsystem consisting of mechanical components, transducers and hammers. The second system consists of electrical components, including signal conditioning, data acquisition and controls. The hardware was configured to meet the needs of the seismic techniques implemented in the SPA with respect to the number, type and spacing of transducers. The five seismic techniques implemented in the SPA include:
- Spectral Analysis of Surface Waves (SASW),
- Impulse Response (IR),
- Ultrasonic Body Wave (UBW),
- Ultrasonic Surface Wave (USW), and
- Impact Echo (IE).

The SPA system consists of a trailer with transducers, hammers, pneumatic controls and conditioners, and a data acquisition and control system in the van. A schematic of the SPA trailer is given in Figure 24, while a closer look of the transducer-hammer assembly in testing is provided in Figure 25. The system has 8 transducers, 5 accelerometers marked

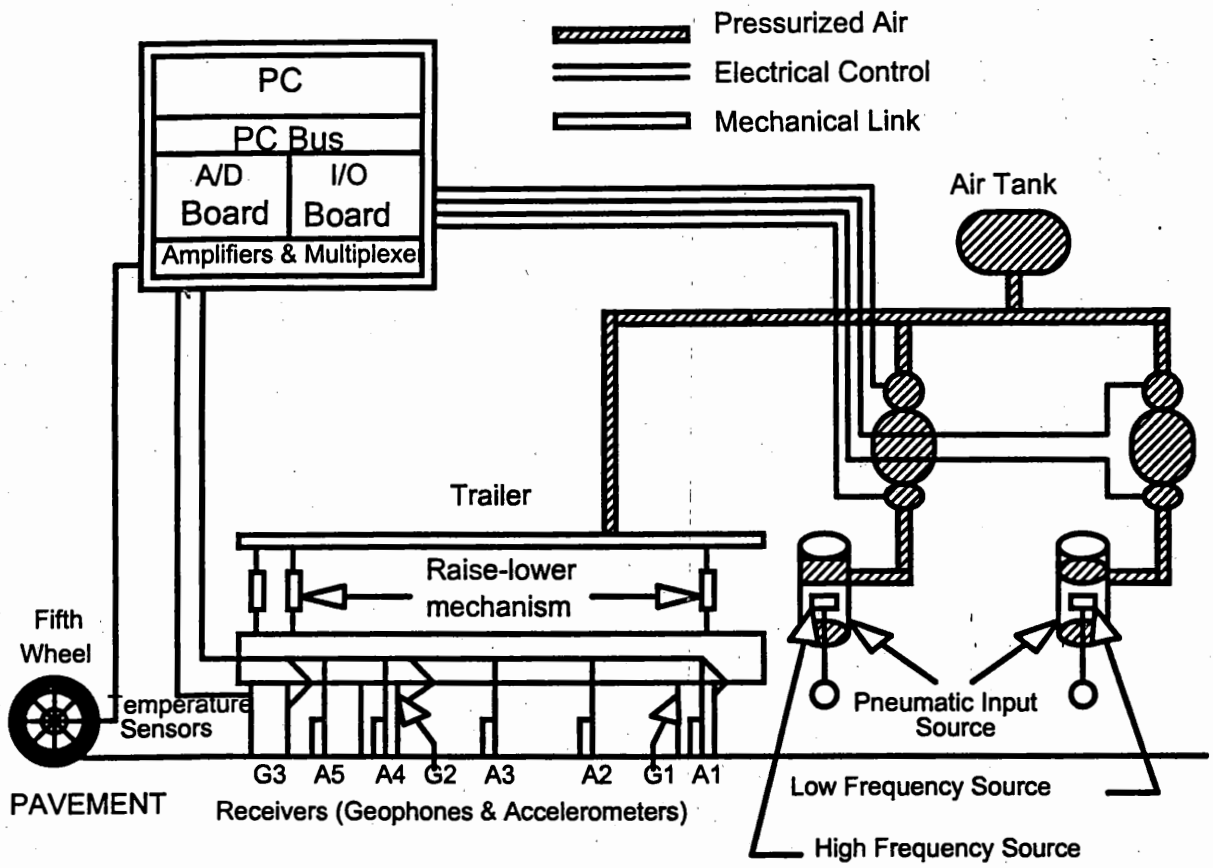


Figure 24. Schematic of the SPA.[3]

by A and 3 geophones marked by G. Accelerometers are PCB-352A78 accelerometers with the calibration factor of about 100 mV/g. Geophones are Mark products L-28 geophones with a calibration factor of about 0.2 V/in/s. The spacing between the transducers and the distance from the hammers is given in Figure 26. Calibration of SPA accelerometers and geophones is described by Tendon and Nazarian.[36] The transducer spacing reflects needs of implemented seismic methods to obtain results in the desired frequency range and to enable sufficiently deep testing for typical pavement designs. The transducers are mounted on the trailer with a double purpose pneumatic springs. The first one is to ensure good coupling with the pavement, even under conditions of high pavement roughness. The second one is to isolate the transducers from the trailer frame vibrations. Finally, the transducers have a special shell made of a PVC pipe that reduces potential resonance of steel mounting and prevents corrosion at the steel-aluminum contact. In addition to the geophones and accelerometers, there are two temperature probes close to the impact sources for measurement of air and pavement surface temperature.

The SPA has two pneumatic type impact sources: a high frequency and a low frequency source (hammer). The high frequency hammer is utilized in ultrasonic, impact echo and SASW testing. The hammer consists of an accumulator with a computer controlled solenoid valve, with a ball-peen type head (Figure 27). The impulse generated by the high frequency hammer is a half-sine impulse of an approximate duration of about 0.2 ms. The


Figure 25. SPA transducers and hammers in position for testing.

low frequency hammer is used in SASW and IR testing. It has a hard rubber head of approximately 700 mm diameter (Figure 27) and it generates half-sine impulses of an approximate duration of 2 ms. The transducers and hammers are lowered and raised pneumatically. The pneumatic system consists of a compressor, a manifold and air cylinders. A manifold has three pressure regulators: hammer firing, hammer and transducer assembly lowering and raising, and for holding down the transducers. For the SPA tested, air pressure settings were about 50 lbf/in$^2$ for the hammer firing and hammer lowering, and about 20 lbf/in$^2$ for raising and lowering of hammer and transducer assembly and for holding down the transducers (Figure 28).

The electronic system encompasses signal conditioners, multiplexers, gain control circuits and analog-to-digital (A/D) board. Signal conditioning circuits include geophone, accelerometer, load-cell, and temperature corrections. From altogether 12 input signals, the multiplexer routes only four signals at the time to the A/D board (capacity of the board). Since the signal strength varies with pavement conditions different gains are given to the signal.

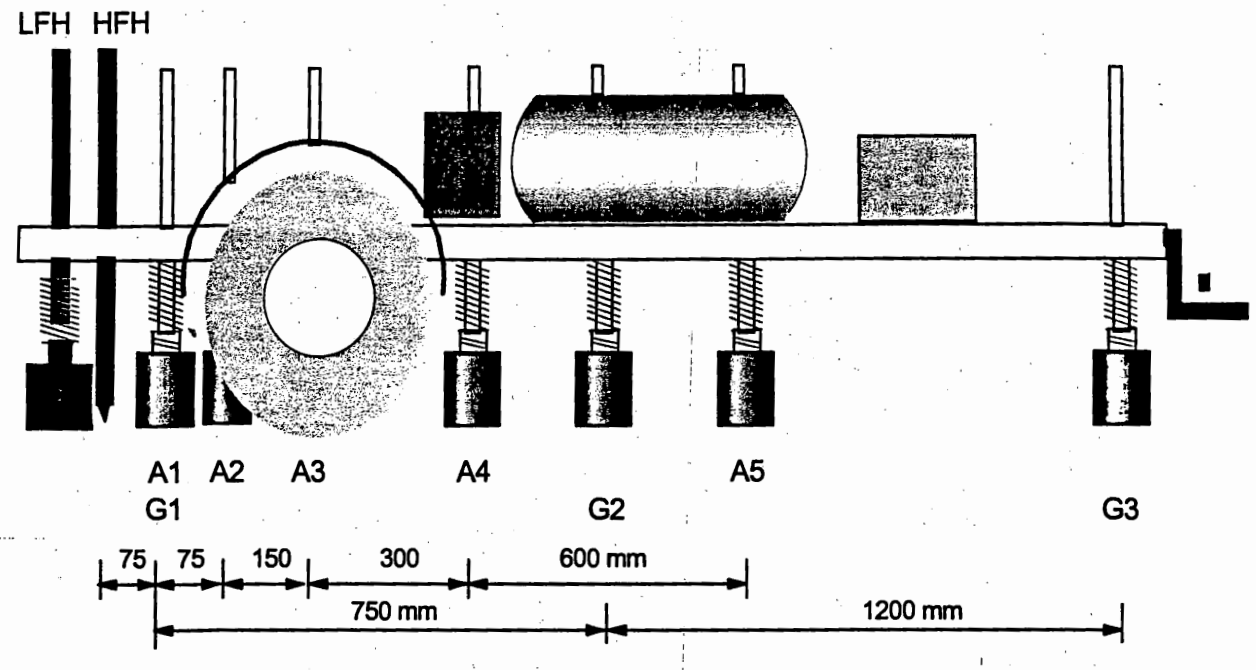


Figure 26. Transducer and hammer spacing.

**Operation of the SPA in the Field**

Testing in the field is conducted with a spacing that fits the needs of the project and anticipated variation in pavement properties. Nazarian *et al.* suggest that the spacing between test points in open highway conditions be not larger than about 30 m.[3] In the case of a rigid pavement, the test spacing should be controlled by the joint spacing. Typically, each slab should be tested at both joints and at the middle. Prior to testing, the SPA menu is initiated, and the project setup prepared. The menu of the software used in this study differs from the one described in the SHRP final report.[37] As illustrated in Figures 29 and 30, the main menu contains five main submenus:

- Acquisition - controls data collection, data viewing, results and status review and electronic testing (done at the beginning and periodically during testing),
- Reanalysis - selects old data and reanalyzes with newly selected parameters,
- Setup - defines input parameters for testing, messages and data storage,
- Help, and
- Calibration - calibration of high frequency hammer and temperature sensors.

The first step prior to testing is a project setup, that includes selection of a project directory for data storage and definition of the pavement structure. The SPA software defines the pavement as a three-layer system. For each of the layers the anticipated range of elastic properties (shear modulus and Young's modulus) and the layer thickness, and the type of the material (PCC or AC) should be given. A sample input dialog box for the paving layer is given in Figure 31. For testing on rigid pavements, slab width and length and default test location should be defined. The description of the pavement facilitates faster and more accurate data analysis in the field.

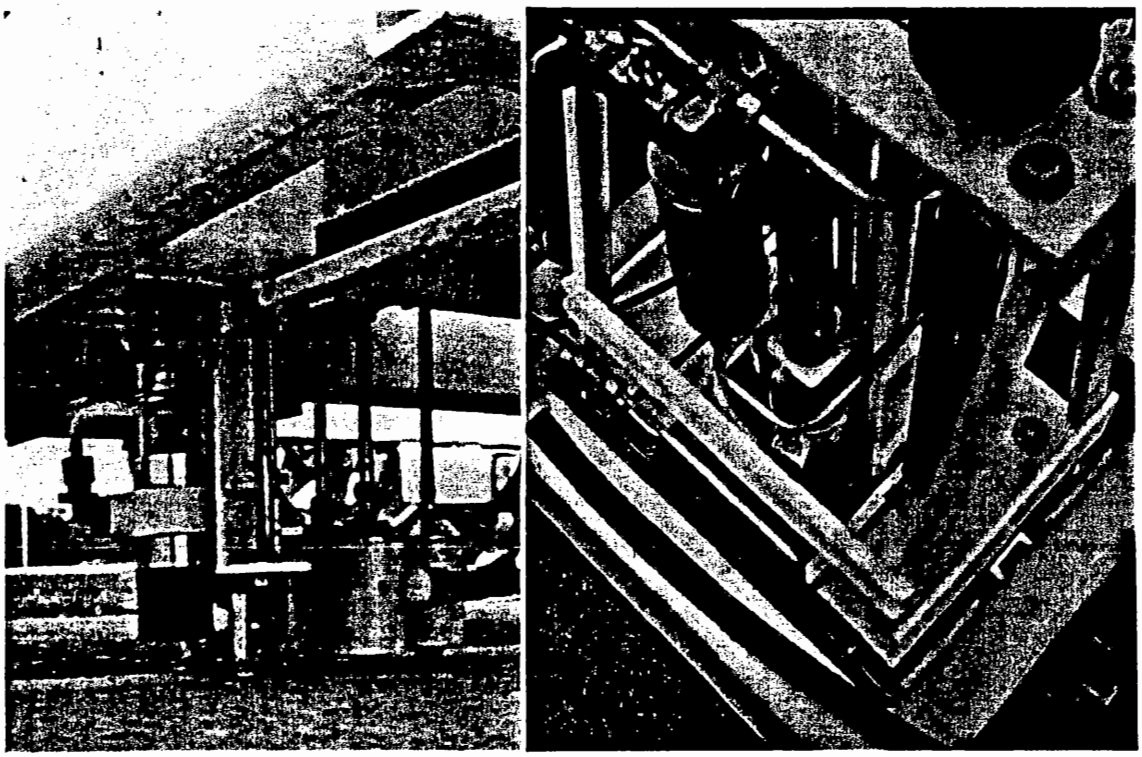

Figure 27. Low and high frequency sources (left) and air accumulators (right.)

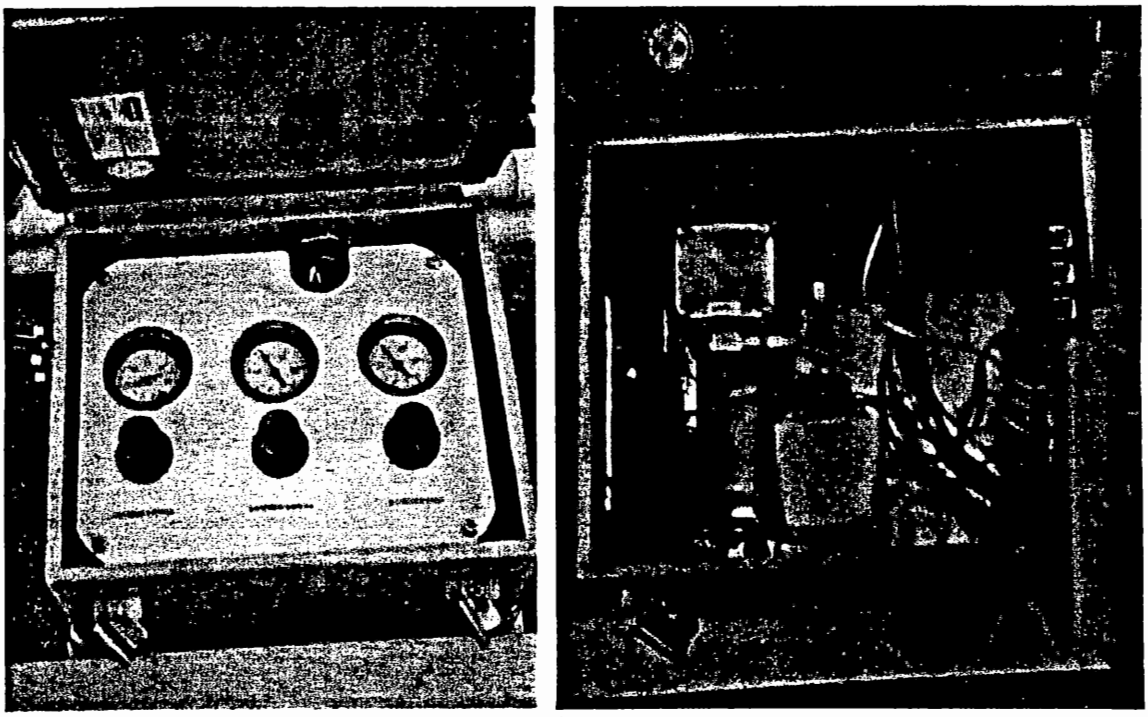

Figure 28. Manifold box with pressure regulators (left) and the compressor box (right).

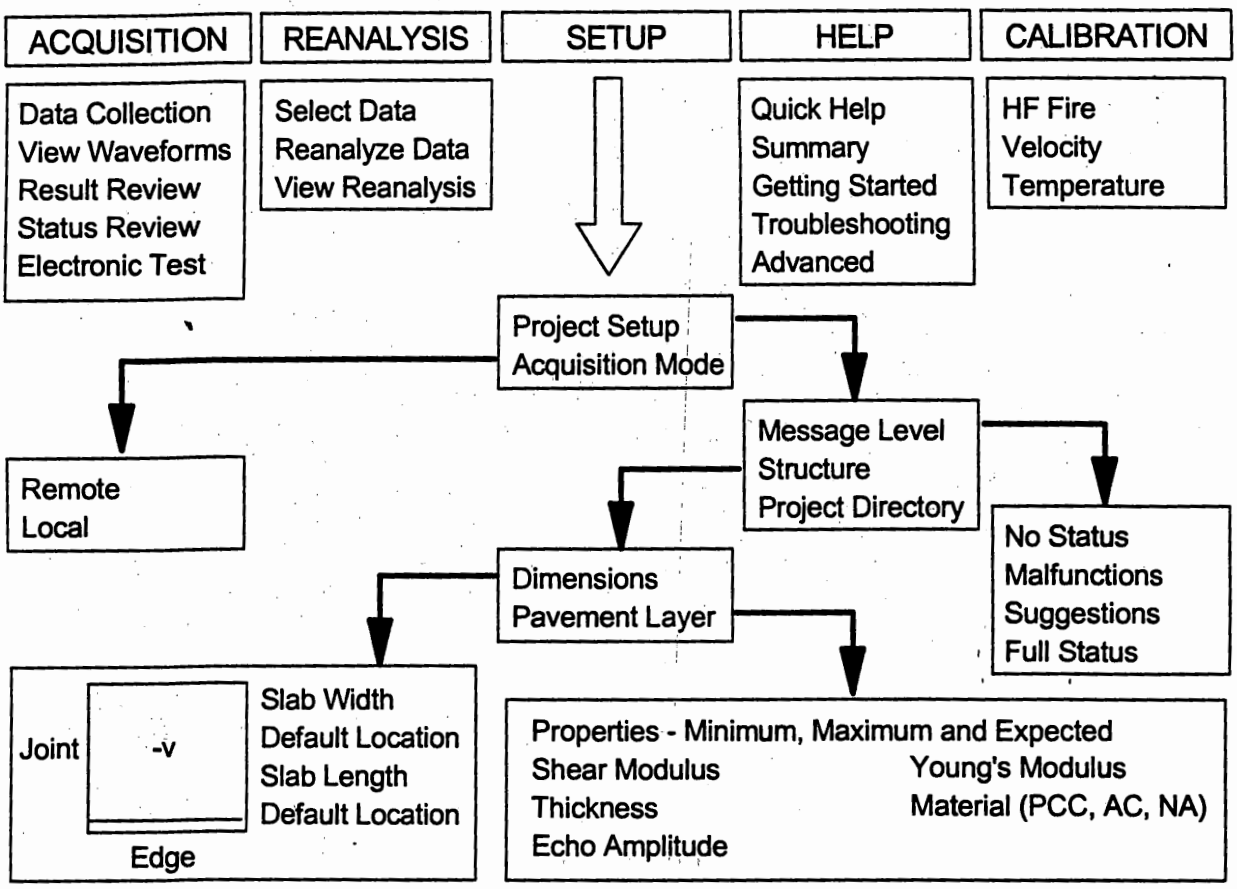


Figure 29. SPA software menus.

Once the SPA is positioned at a test point, the testing sequence is initiated through the computer by selecting the Data Collection option in the Acquisition submenu. At that moment the transducer and hammer assembly is lowered pneumatically on the pavement and hammer impacts are applied. Altogether 20-30 impacts of high (HF) and low frequency (LF) hammers are applied and data stored in five banks. It takes about 45 seconds per test, including the time for lowering and raising of transducer and hammer assembly.

In the first series of impacts, about 5 to 7 impacts of HF hammer are applied and the last three records of accelerometers A1, A2 and A3 and the load cell saved in BANK 0. The second series of HF hammer impacts are stored together with A3, A4 and A5 signals in Bank 1. The first two series are repeated and data stored in Banks 2 and 3. Finally, a series of impacts of LF hammer and signals from the three geophones are stored in Bank 4. The last bank, Bank 5, contains records of air and pavement surface temperature. The content of all of the data banks are summarized in Table 2. The order in each of the banks follows the order of colors in the data presentation viewer: blue, red, light blue and green.

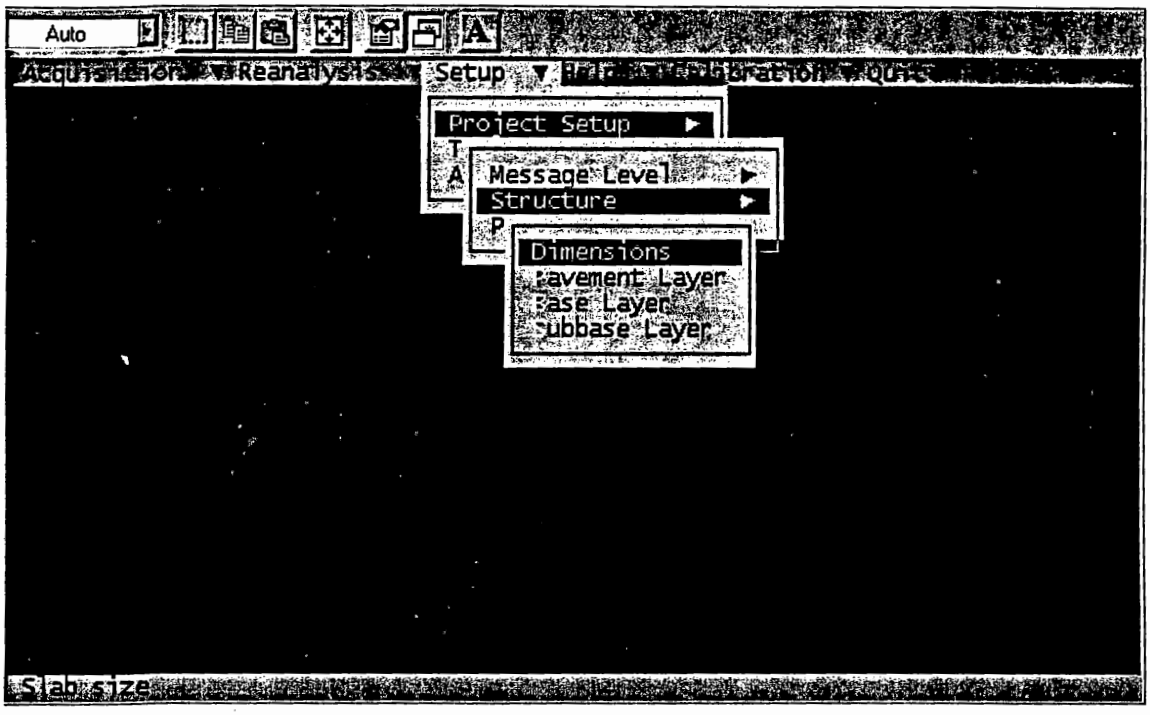


Figure 30. SPA main menu.

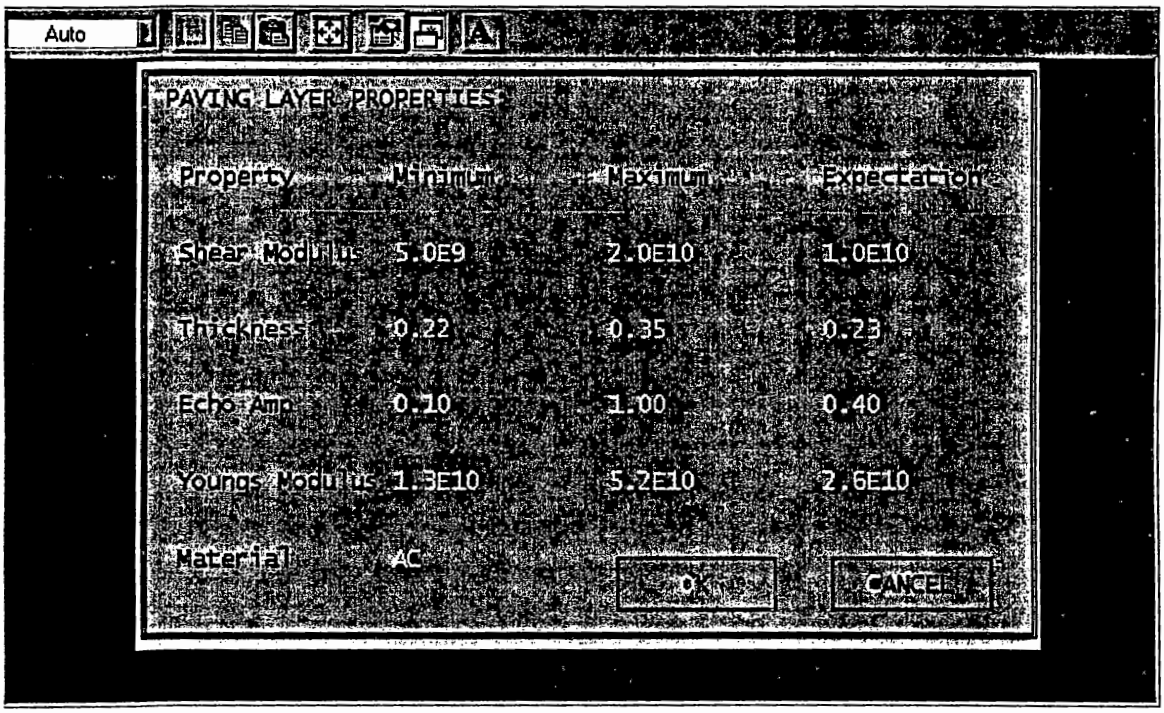


Figure 31. Dialog box for description of paving layer properties.

**Table 2. SPA Data Banks**

| Bank | Measurement Description | Hammers and Transducers | | | | Seismic Technique |
|---|---|---|---|---|---|---|
| | | Blue | Red | Light blue | Green | |
| 0 | A1KDG | L1N | A3N | A2N | A1N | USW,SASW,IE |
| 1 | B1KDG | L1F | A3F | A4F | A5F | SASW |
| 2 | A4KDN | L1PN | A3PN | A2PN | A1PN | P |
| 3 | A4KDN | L1PF | A3PF | A4PF | A5PF | P |
| 4 | C1KDG | L2F | G1F | G2F | G3F | IR(MI),SASW |
| 5 | A00NN | GT | AT | N | N | |

The following is the meaning of letters in the measurement description column:

- first letter - sample rate - A=4μs, B=20μs, C=80μs
- second letter - gain - 0-1, 1-2, 2-4, 3-10, 4-20, 5-40, 6-100, 7-200
- third letter - analog trigger level (A to Z)
- fourth letter - use of digital trigger signal (D-digital, A-analog, N-no)
- fifth letter - use multiple hits to set gains for optimal S/N ratio (G-yes, N-no)

The following are descriptions for hammers, transducers and temperature probes:

- first two letters - accelerometer and geophone number, L1-high frequency hammer, L2-low frequency hammer, GT-ground temperature, AT-air temperature
- other letters - N-near mode, F-far mode

Signals for the six banks are illustrated in Figure 32. The signals are invoked by View Waveforms from Acquistion submenu. Each of the banks can be viewed in details by double clicking on any of the bank windows. This is illustrated for Bank 0 in Figure 33. At the end of the data collection, the SPA software provides estimates of a number of pavement parameters, as described in Table 3.

**Table 3. Pavement Properties Estimated by the SPA**

| Pavement layer | Parameter Estimated and Method Used | | | | |
|---|---|---|---|---|---|
| | Young's modulus | Shear modulus | Thickness | Damping | Temperature |
| Paving | yes - UBW | yes - USW | yes - IE | no | yes |
| Base | yes - IR | yes - SASW | yes - SASW | no | no |
| Subgrade | no | yes - SASW, IR | yes - SASW | yes | no |

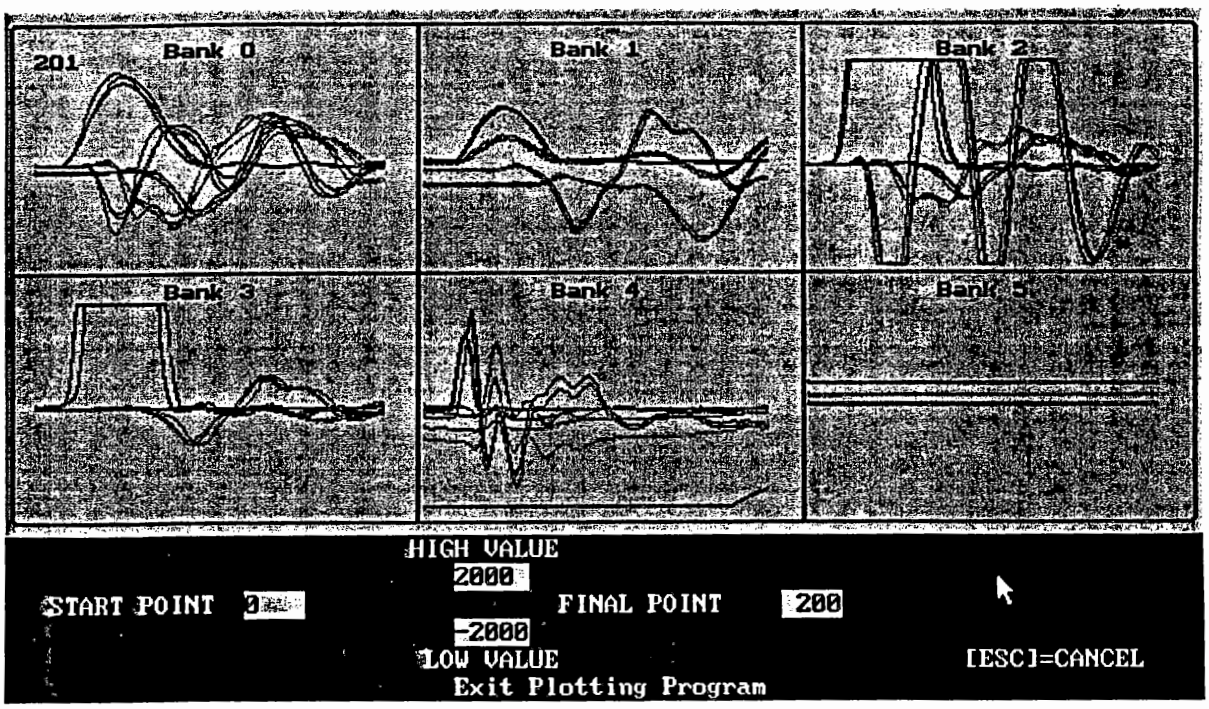


Figure 32. Waveforms for all banks - View Waveform Option.

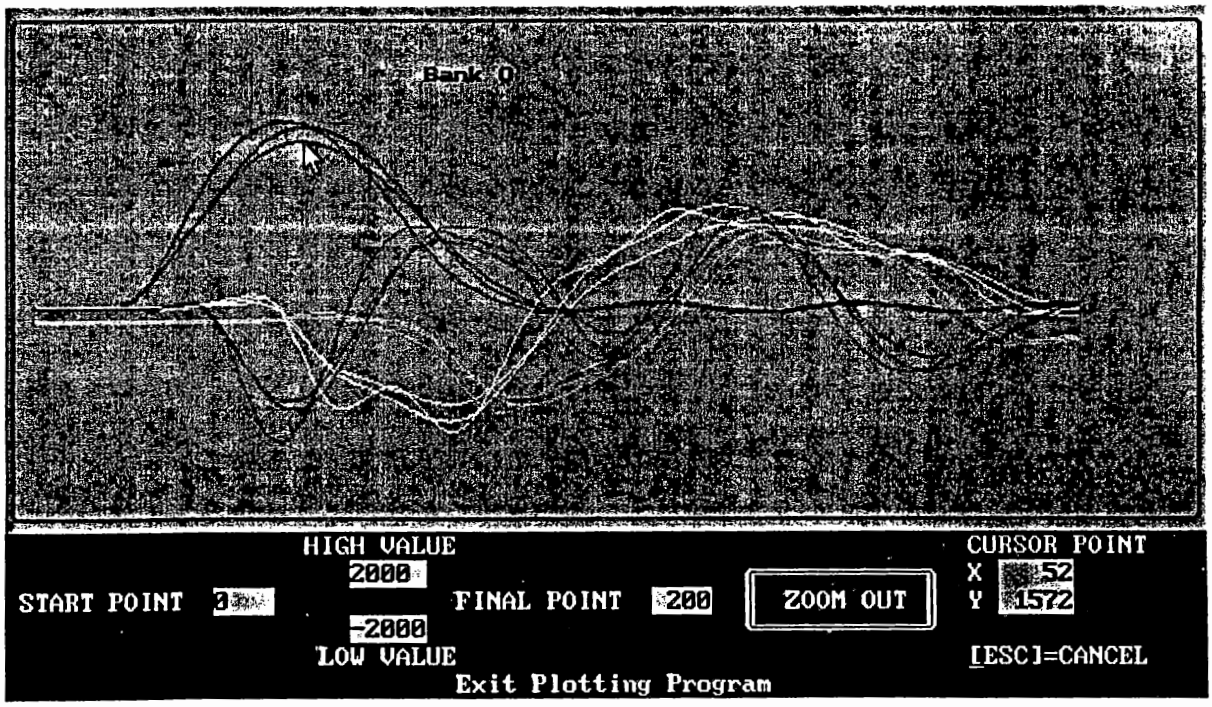


Figure 33. Bank 0 waveforms.

## Data Storage - File Structure

All the data are stored in the project directory defined during the project setup. The basic structure of the SPA directory is given in Figure 34. The main directory has five subdirectories. Bin subdirectory contains all the executable programs for test control, data acquisition and reanalysis. Tables directory contains tables describing the equipment and test setup. Files are being copied to a project directory for future reference. Rawdata directory contains data from all SPA tests. Data are in a compressed (Test_number.zip) format. Finally, test data from all projects are stored in Projects directory. Each project subdirectory contains information about the test setup, results of testing for each pavement layer, results of IR, UBW, USW and IE tests, error messages and comments. With respect to the results of measurements files Pavmod.txt, Basemod.txt and Sbmod.txt summarize results for the paving, base and subbase/subgrade layer, respectively. The following information is provided in Pavmod.txt file: Young's and shear moduli, layer thickness, echo amplitude, ground and air temperatures. Basemod.txt file contains the shear modulus, thickness and damping ratio. Sbmod.txt contains information about the shear modulus and thickness (constant).

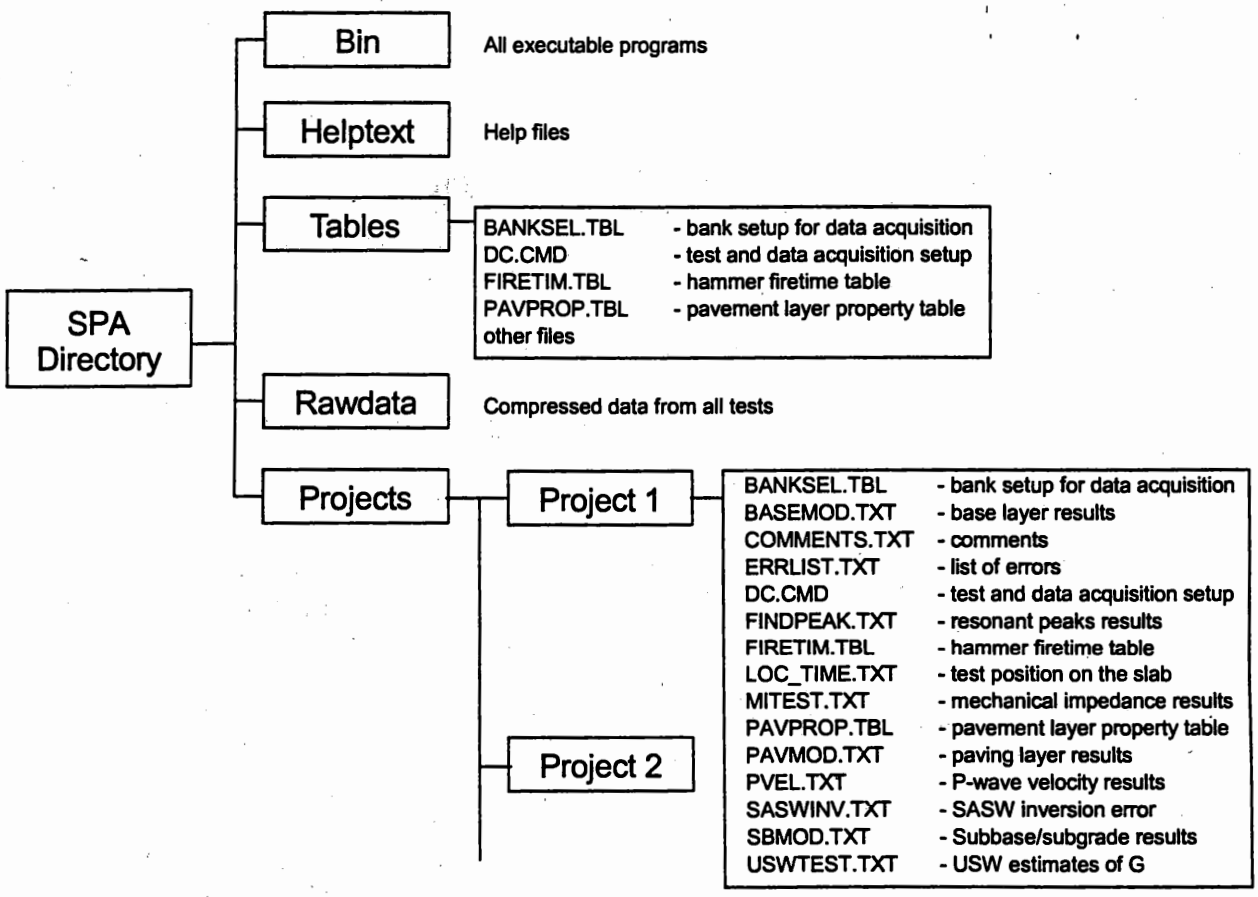


Figure 34. SPA directory structure.

## SPA Software Reanalysis

Some of the results obtained by the SPA are at the same time final results and can not be improved. However, improvements can be achieved for some tests, SASW in particular, by selecting different starting parameters in the reanalysis option. The first step in the reanalysis is to select data from a chosen project directory. Once the data are selected and reanalysis requested, results for the five seismic tests can be viewed (Figure 35). Examples of reanalyzed data are given in Figures 36 to 39. For example, Figure 36 contains the phase of the cross power spectrum (white) and coherence (black) for the USW test invoked by the USW option. Similarly, the phase of the cross power spectrum (white) and coherence (black) for the A3 and A4 transducers invoked by the SASW test option are given in Figure 37. As described earlier, the phase of the cross power spectrum is used in the development of the dispersion curve (phase velocity vs. frequency). Dispersion curves for all receiver spacings are averaged. The SASW summary window provides dispersion curves for all five receiver spacings for examination. If there is a major discrepancy between dispersion curves for various receiver spacings, as illustrated in Figure 38, the problem can be corrected by the intervention of the operator. Another example of the use of the SPA reanalysis option is given in Figure 39 for the spectrum amplitude plot of the Impact Echo test.

## SASW and IR Postprocessing

Accuracy of SASW, USW and IR results can be improved by doing in-house postprocessing.[38] The following sections describe operation of the Reinterp routine for elastic modulus profiling using the SASW and USW data, and IR routine for calculation of the modulus of subgrade reaction and damping ratio of the system from the IR data.

### USW and SASW Analysis by Reinterp

While many of the routines present in the Reinterp match those in the SPA reanalysis program, the main two differences of Reinterp are:

1. Control in generation of dispersion curves for all receiver spacings, and
2. An improved inversion routine.

The control in generation of the dispersion curves from the USW test is illustrated in Figure 40. The phase of the cross-power spectrum from the recorded data (dashed line) is being approximated by a "smoothed" phase (full line). There are three parameters that control the smoothing process. They that take into consideration the coherence function (g), the slope of the curve (h), and the closeness of the approximation (i). The coherence function parameter assigns a weighing factor relative to the coherence. By changing this parameter the weight to a section of the curve with a high coherence can be increased or decreased. A typical value is 0.70 to 0.75. The slope parameter forces the slope of the phase curve to follow an anticipated slope of paving materials. For concrete pavements it should be about 0.0004, and for AC about 0.0007. Finally, the closeness parameter i defines how close the approximated curve should be to the raw curve. The lower the factor the closer the two curves. Typically, i should be set to about 50 for the USW test, and should decrease as the receiver spacing increases. The proper selection of the three parameters requires a moderately experienced operator.

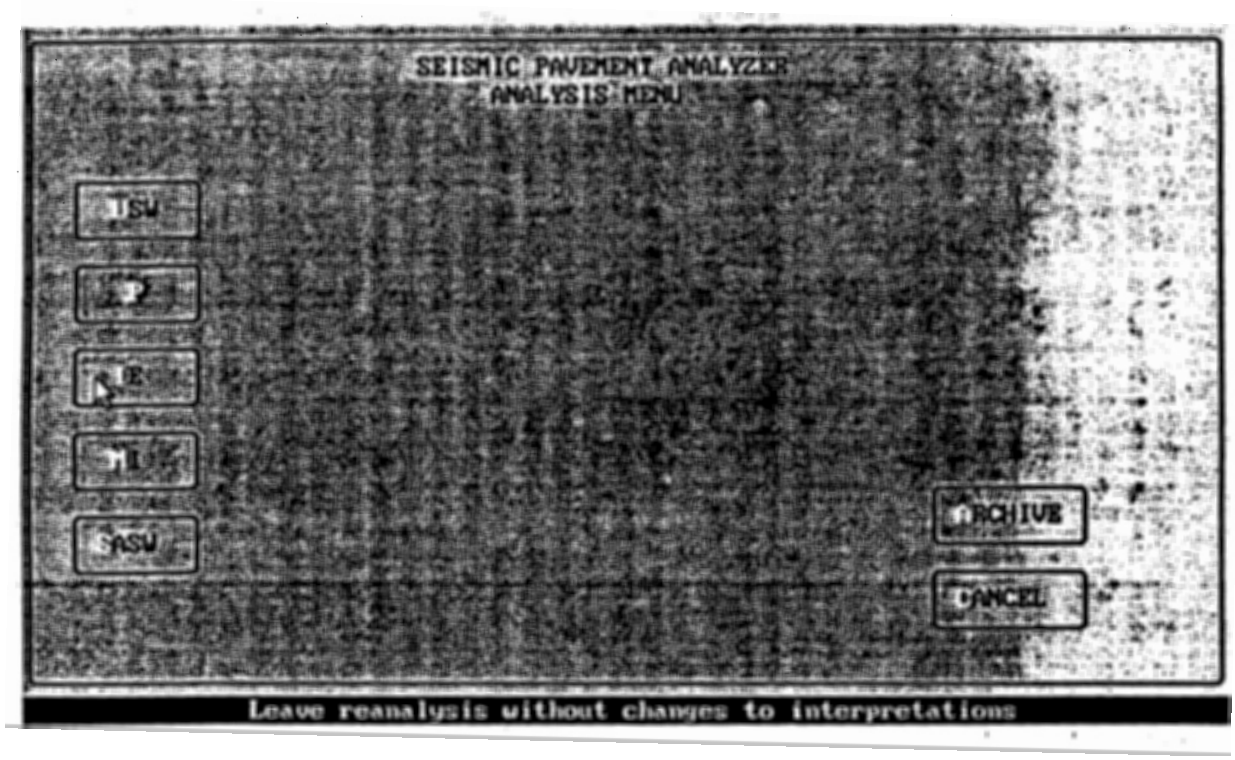


Figure 35. View Reanalysis dialog box.

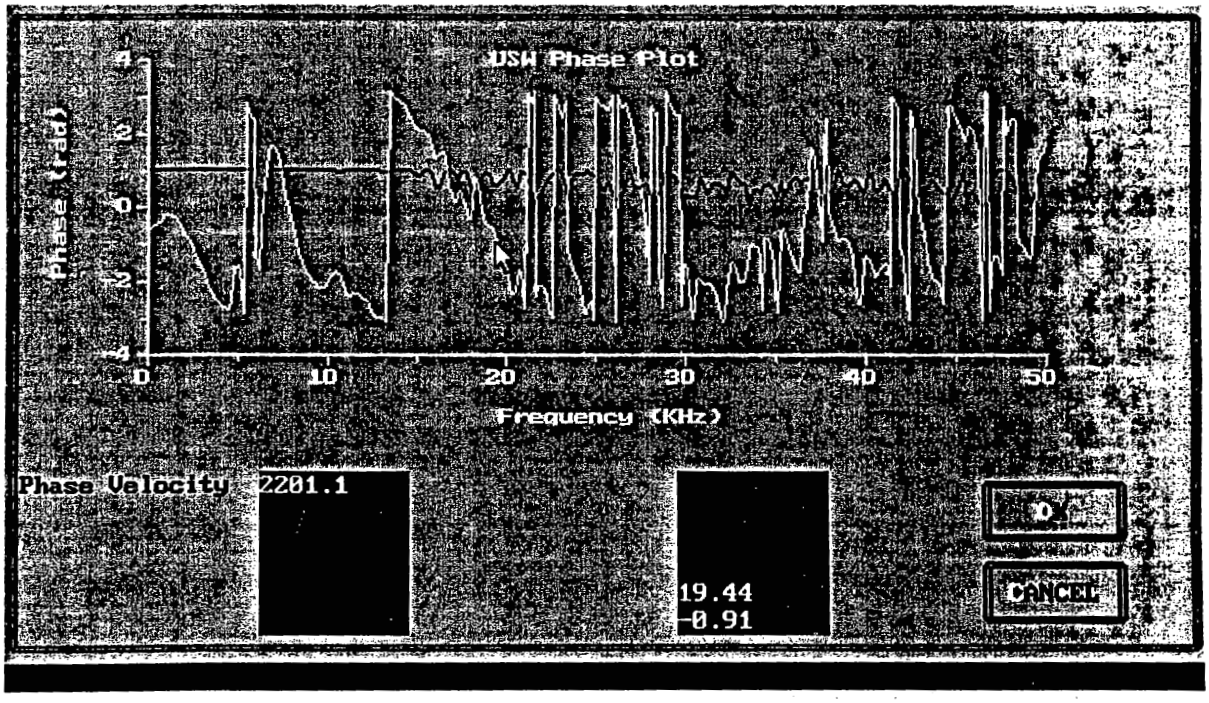


Figure 36. USW phase plot from reanalysis.

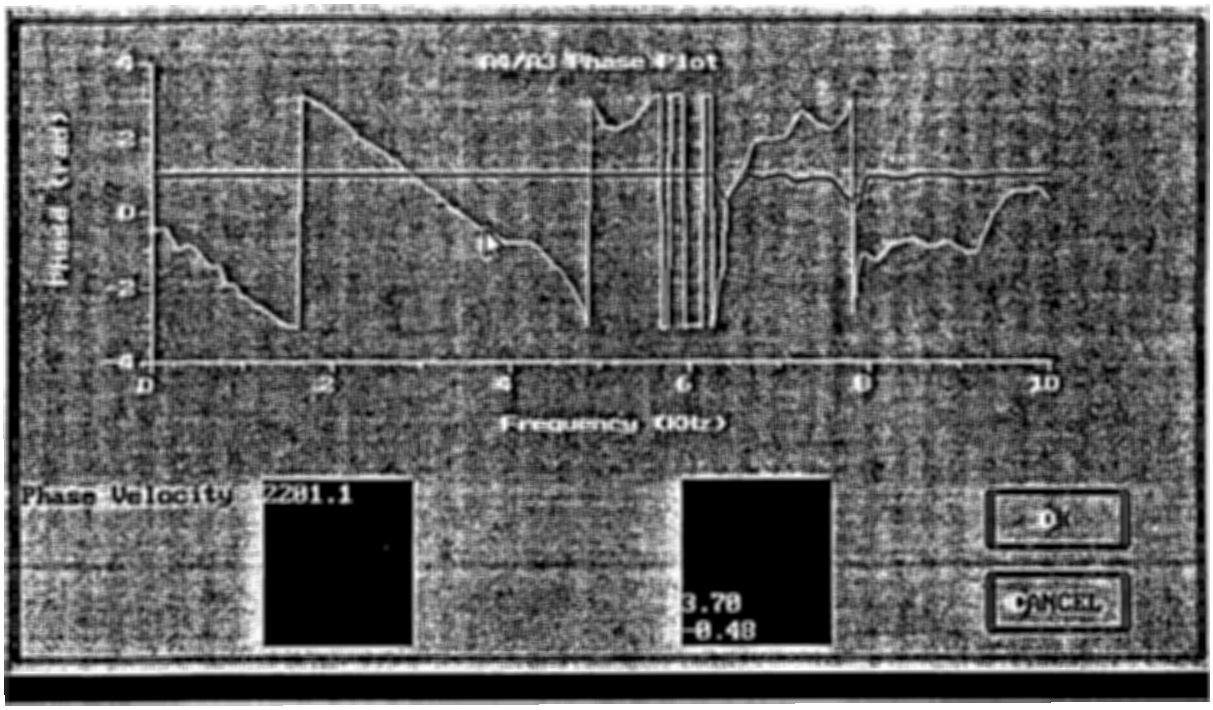


Figure 37. Phase plot for A3 and A4 receivers from reanalysis (used in SASW).

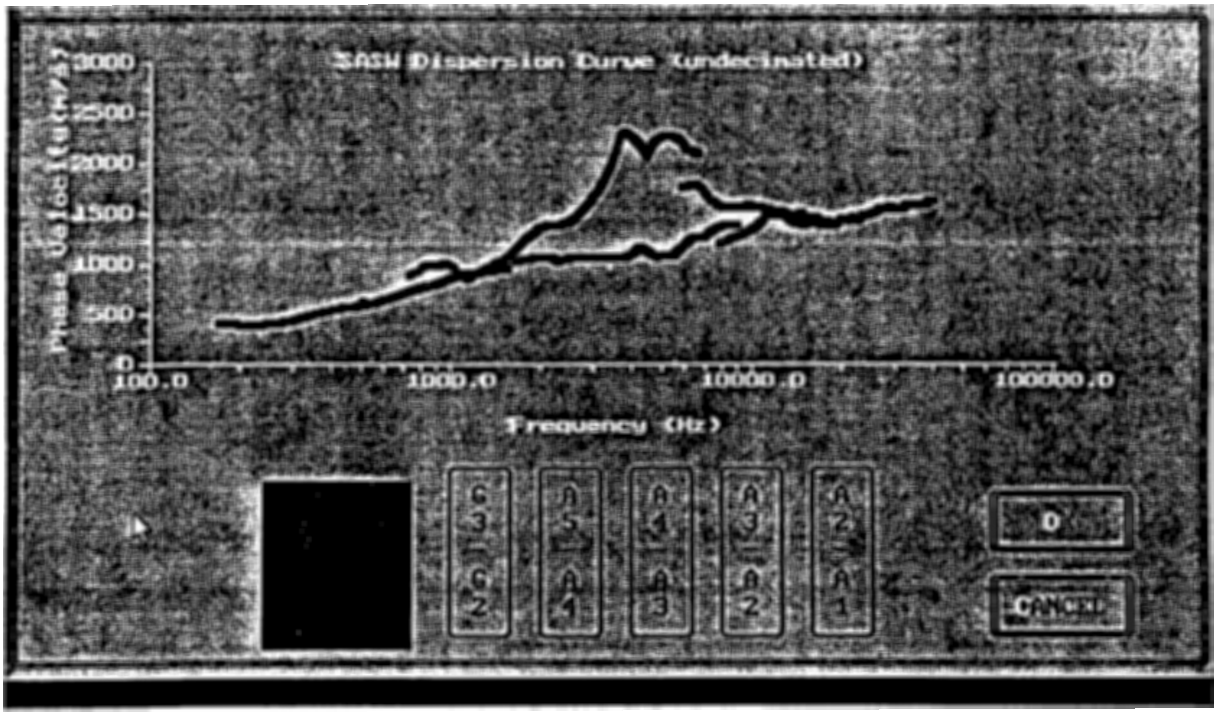


Figure 38. Dispersion curves for all receiver spacings.

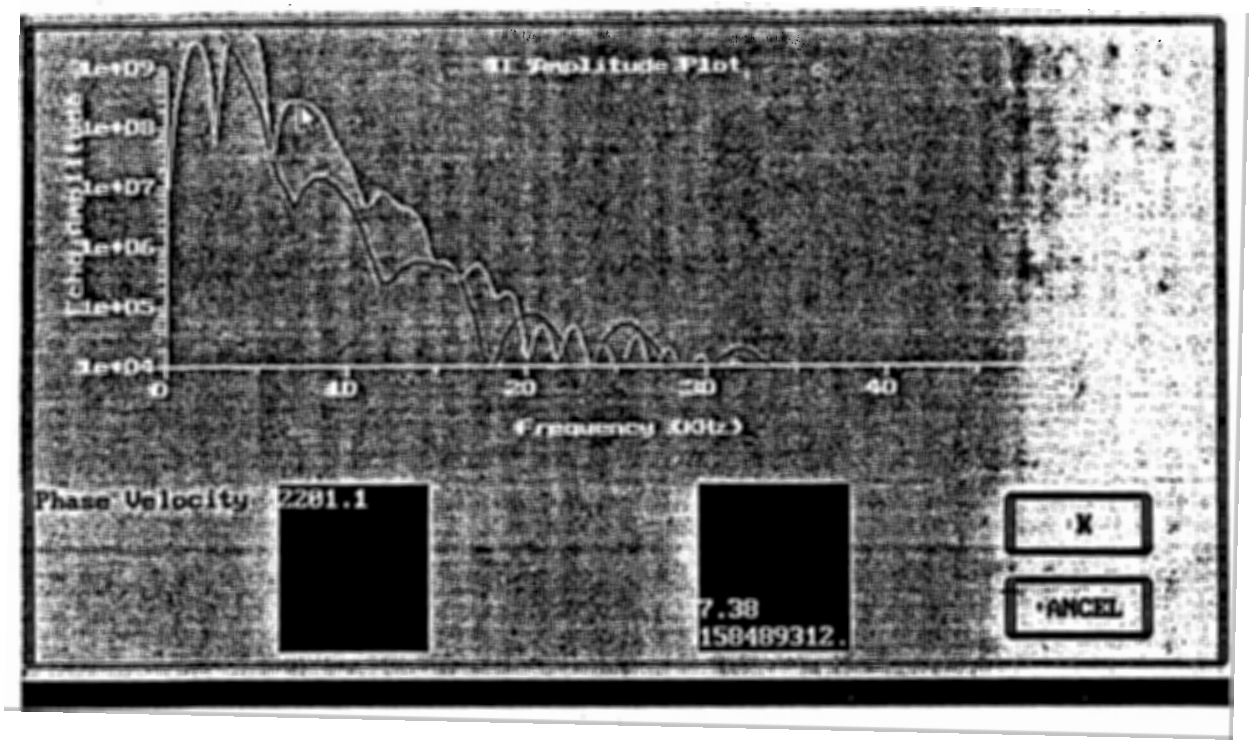


Figure 39. Impact Echo amplitude plot.

The process of generation of the dispersion curve illustrated in Figure 41 is repeated for the five spacings of the SASW test (A1-A2, A2-A3, A3-A4, A4-A5 and G2-G3). As any new section of the curve is developed, it is being added to the already generated sections of the curve. (The generation starts with the shortest transducer spacing, A1-A2, or a section of the dispersion curve in a shortest wavelength range is generated.) This process allows the operator to see whether the dispersion curves for different receiver spacing match in a reasonable manner. (They should differ to a minor extent. However, the explanation of the reasons of such differences exceeds the scope of this study and the report.) In this particular case, the shortest wavelength curve (A1-A2 spacing) does not match the rest of the curve, and the operator can exclude it from further analysis. Once the dispersion curves for all receiver spacings are constructed, an average dispersion curve that is going to be used in the inversion is generated (Figure 42). The average dispersion curve is defined by 30 to 40 points. The manually generated curve is compared to the one previously automatically generated by the SPA software.

In the last step of the SASW test, Reinterp goes through a number of iteration steps of inversion. As shown in Figure 43, the generated experimental dispersion curve (diamonds with a full line), is compared to the dispersion curve from the forward modeling for an assumed pavement profile. Properties of the assumed pavement profile are given in the top portion of the figure. In this particular case, a three-layer system was assumed with the thickness in meters in the second column, Poisson's ratio in the third column, and the shear wave velocity in meters/second in the fourth column. The least square iteration procedure adjusts properties of the assumed pavement profile until the root mean square (RMS) error is minimized. Typically, the lowest error is achieved after only a few iteration. It takes less

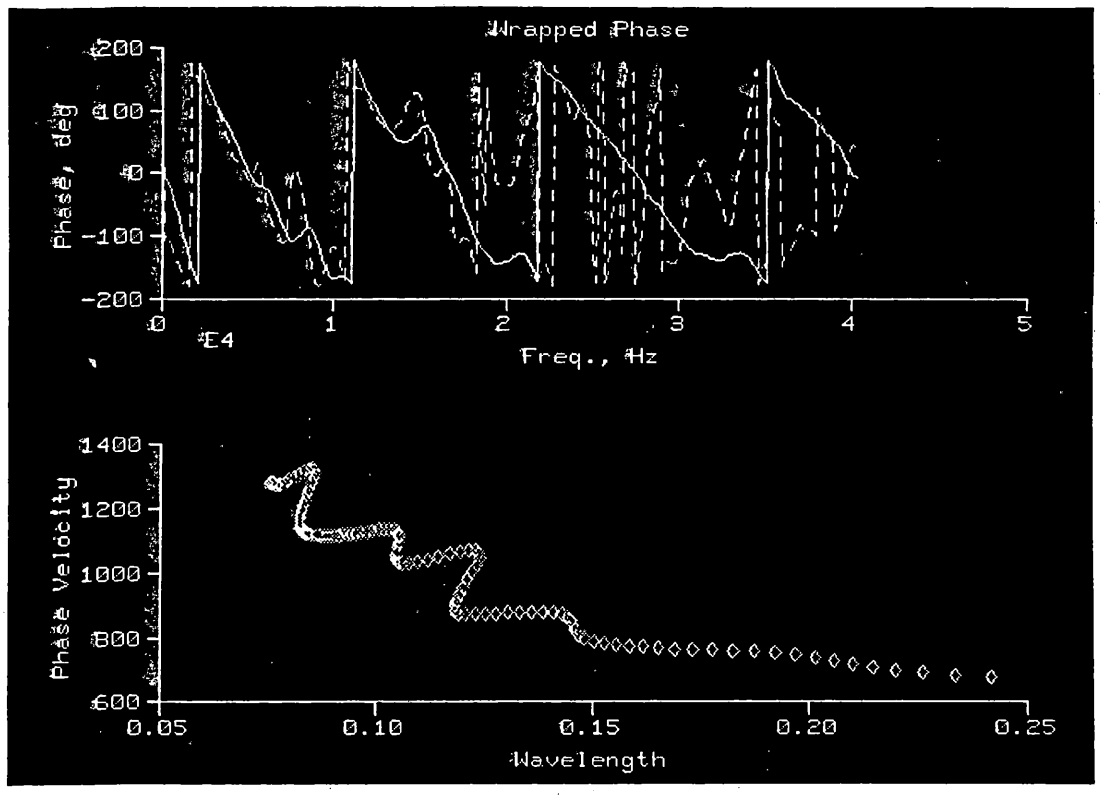


Figure 40. Phase of the cross power spectrum and dispersion curve - USW.

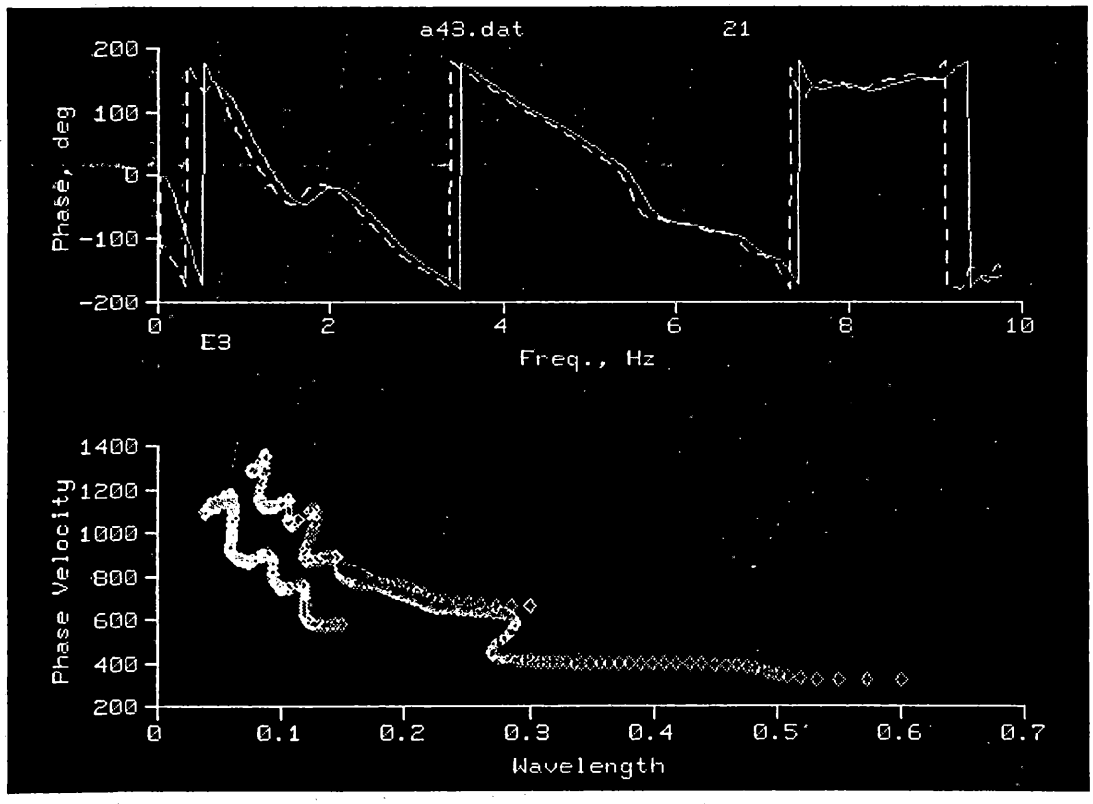


Figure 41. Phase of cross power spectrum and dispersion curve for A3-A4.

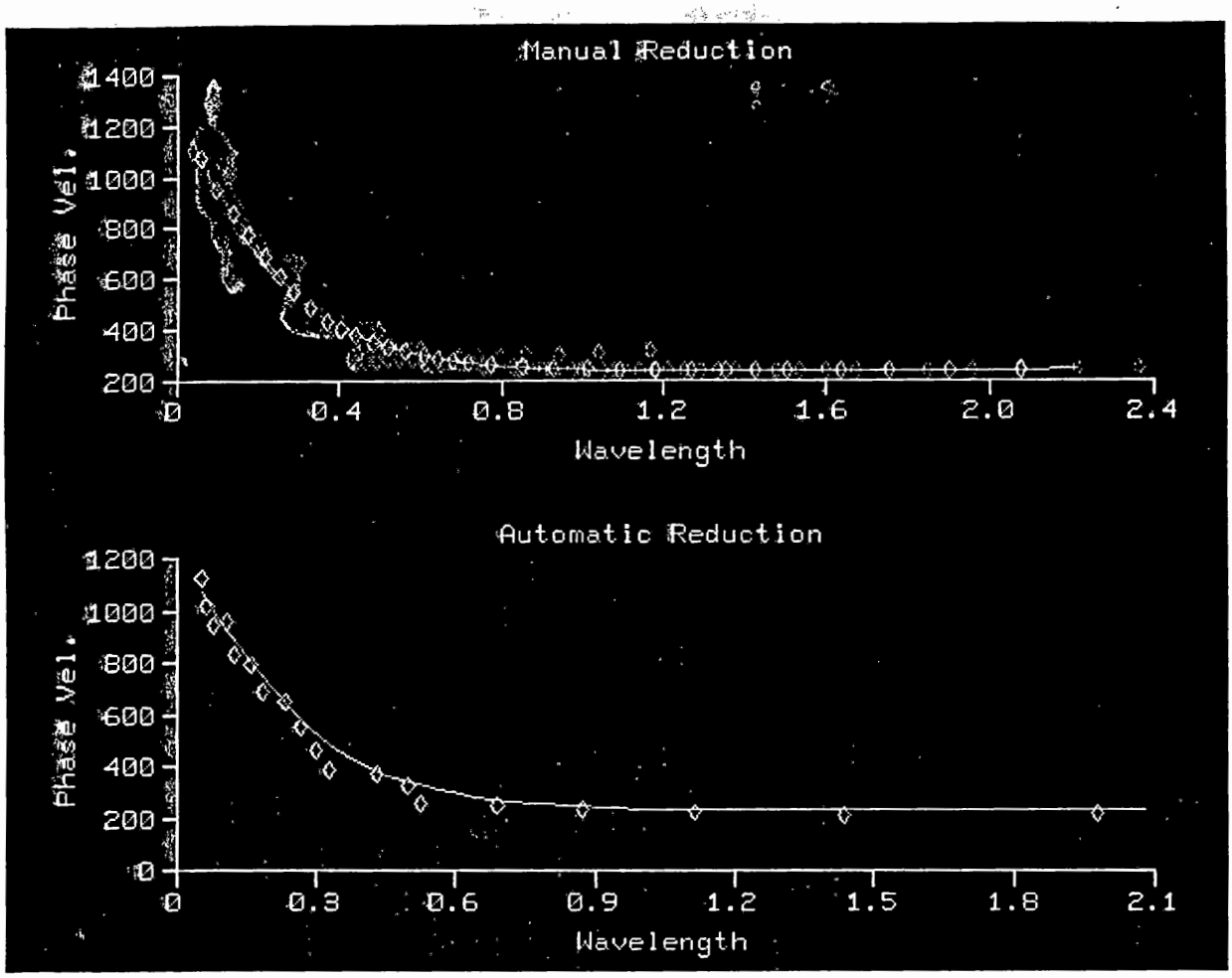


Figure 42. Dispersion curves from manual and automatic reduction.

than a second on a Pentium III - 500 MHz for a single iteration, or less than five seconds for all iterations in the automated mode run. As shown in Figure 44, a good match between the experimental and theoretical dispersion curves was achieved, and the assumed profile is considered to be the backcalculated profile. Reinterp provides also an improved Impact Echo analysis.

**Impulse Response Analysis by IR**

IR program is used for evaluation of the shear modulus of the subgrade and the damping ratio of the pavement system. As such, when the objective of SPA testing is to evaluate the pavement using the Impulse Response technique only, the testing sequence can be reduced to Bank 4 only. This flexibility of SPA controls is illustrated by the image from the menu View Waveforms option in Figure 45, where the testing sequence consisted of Banks 0 and 4. Prior to running IR program, the information about the slab tested and the SPA transducers and load cell used should be provided in file ir.msc. Specifically, the following should be the content of file ir.msc:

- Line 1 - Length, width and thickness of the slab in meters.
- Line 2 - Young's modulus off PCC in Gpa, Poisson's ratio of subgrade.

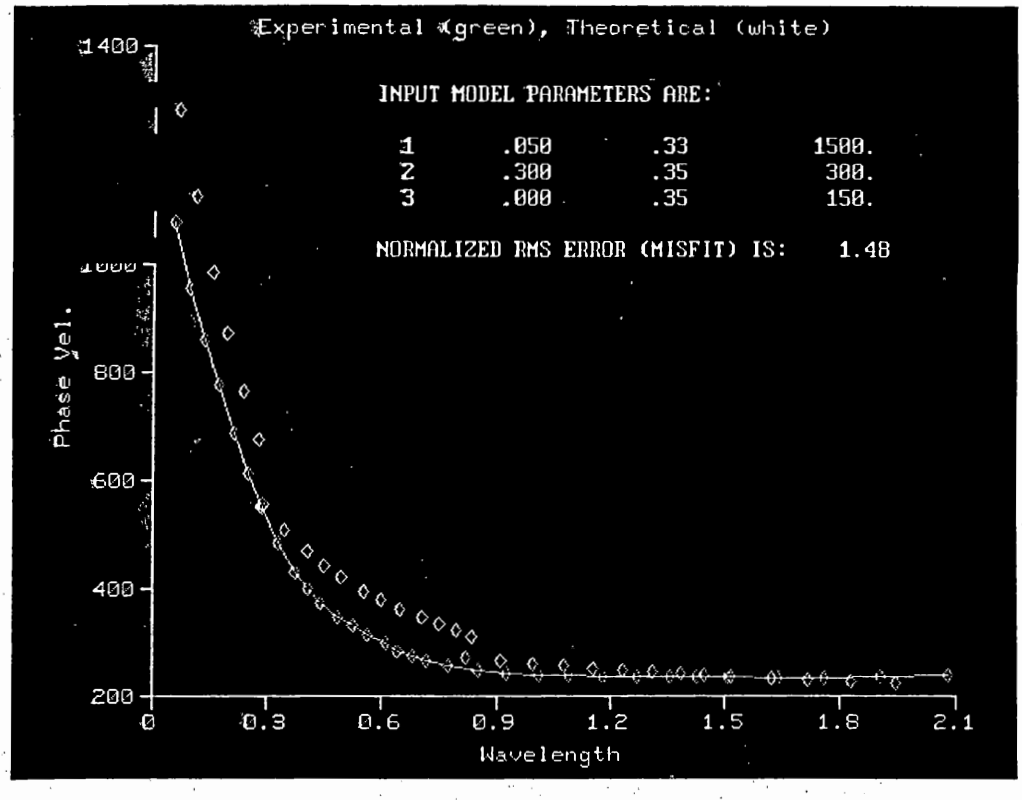


Figure 43. Inversion - First iteration.

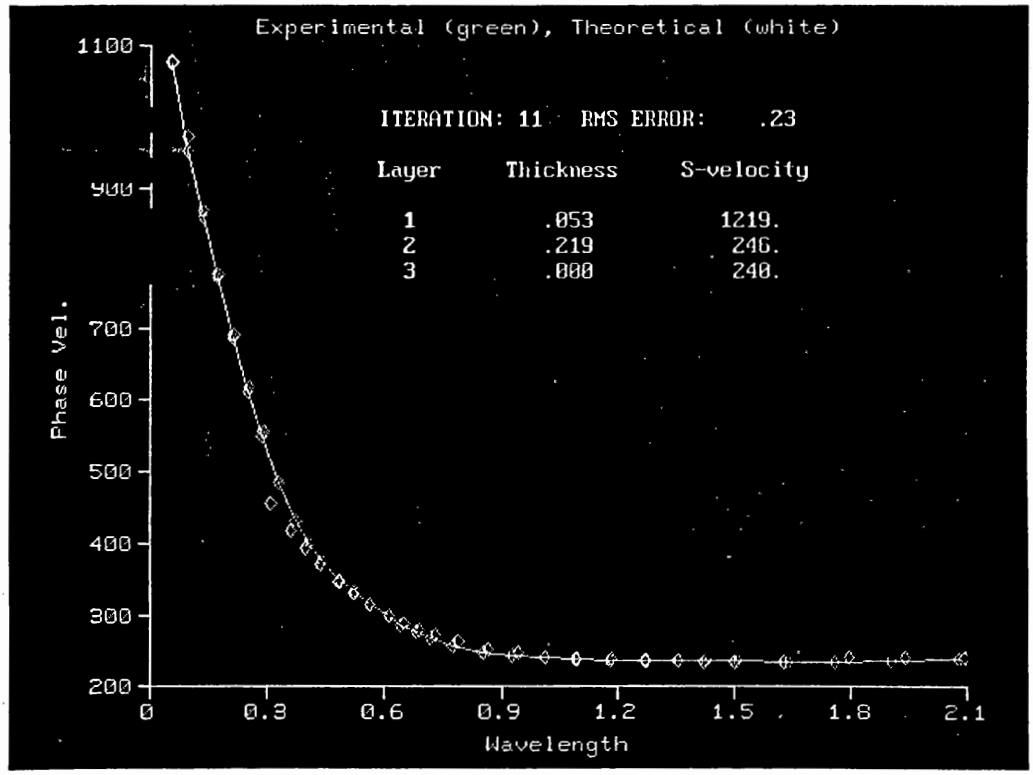


Figure 44. Inversion - Last iteration.

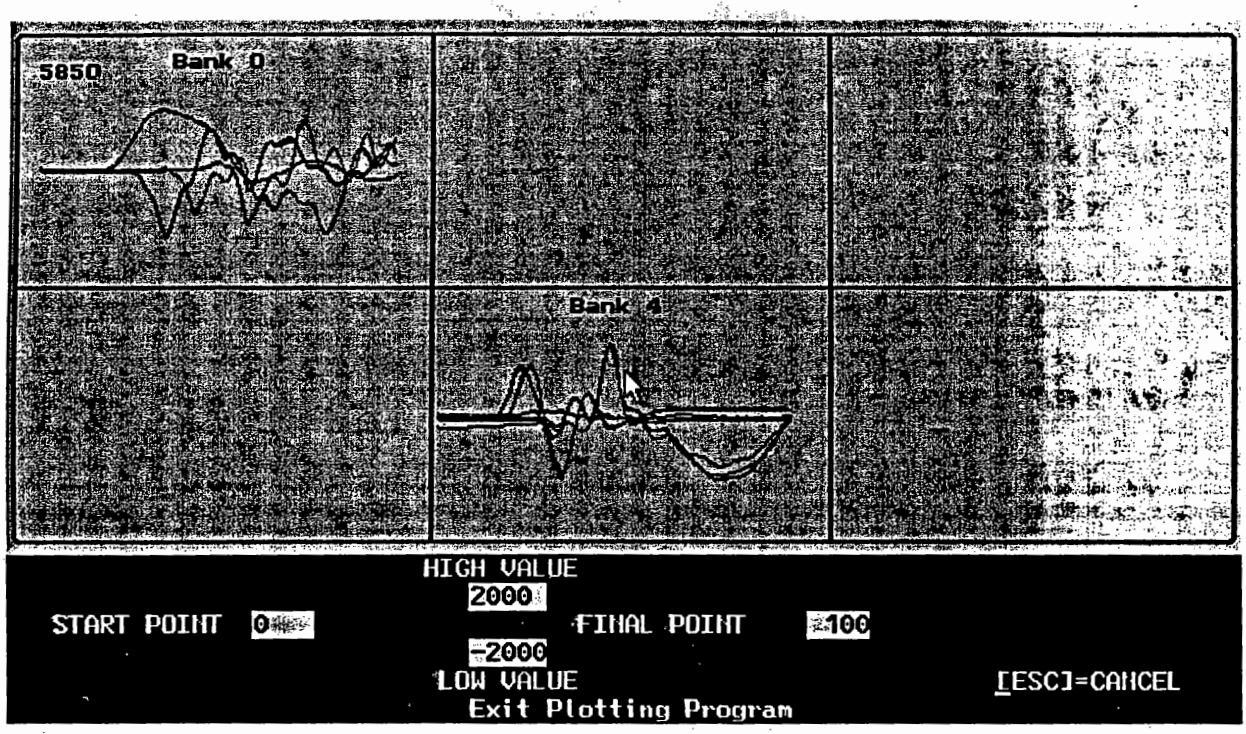


Figure 45. Waveforms for Banks 0 and 4.

- Line 3 - Calibration factors for the first geophone and the low frequency hammer load cell.
- Line 4 - Location of test on the slab (M =middle, C=center or E=edge).
- Line 5 - Number of data banks collected.

Once the program is executed an image like the one in Fig. 46. appears. The solid line in the graph represents the best fit to the experimental impedance curve (dashed line). The information provided below the graph, but can not be seen herein, contains: the subgrade modulus, (S)tatic stiffness, (D)amping ratio, natural (F)requency, (L)ocation of the test, as well as general information about the test. Any of the four parameters (S, D, F or L) can be changed to achieve a better fit. The changes made within a particular run are used for that particular point. Permanent changes to default values are made in lr.msc file. The summary of the results will be in a sub directory with the name identical to the number of the record. The files within the subdirectory are:

- Comments.txt — contains the comments entered during the field test,
- lr.dat — contains the original field data that contains real, imaginary of stiffness spectrum and coherence value at each frequency,
- lr.dbg — contains the amplification factors of the data acquisition board during field test,
- lr.pcs — contains the measured and fitted data for plotting, and
- lr_sum.out — is the summary of the output file.

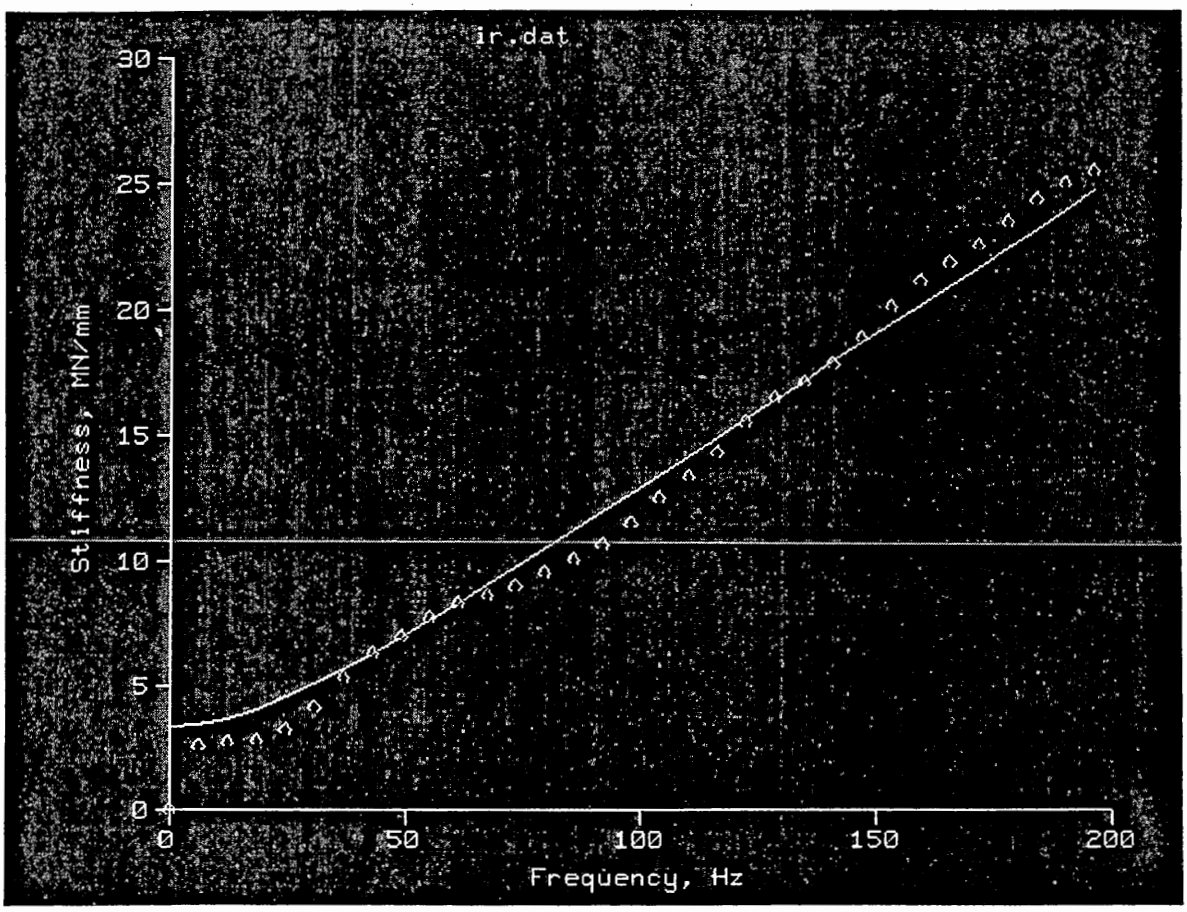


Figure 46. Matching of experimental and theoretical impedances.

## EVALUATION OF THE SPA IN PAVEMENT PROFILING

The main use of the SPA is pavement profiling in terms of the definition of the change of elastic moduli with depth. A number of road sections were tested with an objective of evaluating the ability to define the pavement profile accurately and consistently. The following sections describe results of several tests conducted on roads in New Jersey. The tests described were conducted with three separate objectives:

1. To evaluate consistency in data collection,
2. To evaluate consistency and accuracy in evaluation of properties of the paving layer, and
3. To evaluate the ability and accuracy in measurement of pavement base and subgrade properties.

From a number of tests conducted results of two test are described in this report. The first one is at rest areas of Rt. I-295 near mile post 49.7, and the second one on Rt. 1 in North Brunswick.

### Testing on Rest Areas of Rt. I-295, New Jersey

The testing was conducted on July 20, 1999 on both south and north bound rest areas of Rt. I-295 near mile post 49.7. Based on the coring results the pavement can be described as a 10 cm thick AC paving layer on a gravelly base. The rest areas consist of three parking zones: car parking areas on the right side, a truck parking area on the left side and a car parking area/drive thru area in the middle. The testing was conducted in the middle parking areas for the both north and south bound rest areas, as shown in Figure 47. The condition of the pavement based on the visual inspection can be described as good, with very little or no cracking, as shown in Figure 49.

The primary objective of the testing was evaluation of pavement profiling capabilities of the SPA. Specific objectives of the testing included evaluation of repeatability and consistency of SPA hardware and software in data collection and data analysis with respect to the pavement profiling. To achieve objectives of this task, the testing was conducted in the following sequence:

- The first series of tests was conducted along lines of test points 1 to 13 on the south bound rest area, and 1 to 8 along the north bound rest area, with every test point being tested three times in a sequence.
- The second series of tests involved twice repeated testing along the same two test lines within a period of about 2 hours.
- The final series of tests involved testing along the middle lines (test points 14-26 on the south bound side, and 9-16 on the north bound side) and long the parking zones (test points 27-34 on the south bound side and 17-24 on the south bound side).

A schematic of the tested areas and position of SPA test point and core locations is shown in Figures 48 and 49. Asphalt thicknesses obtained from cores are listed in Table 4.

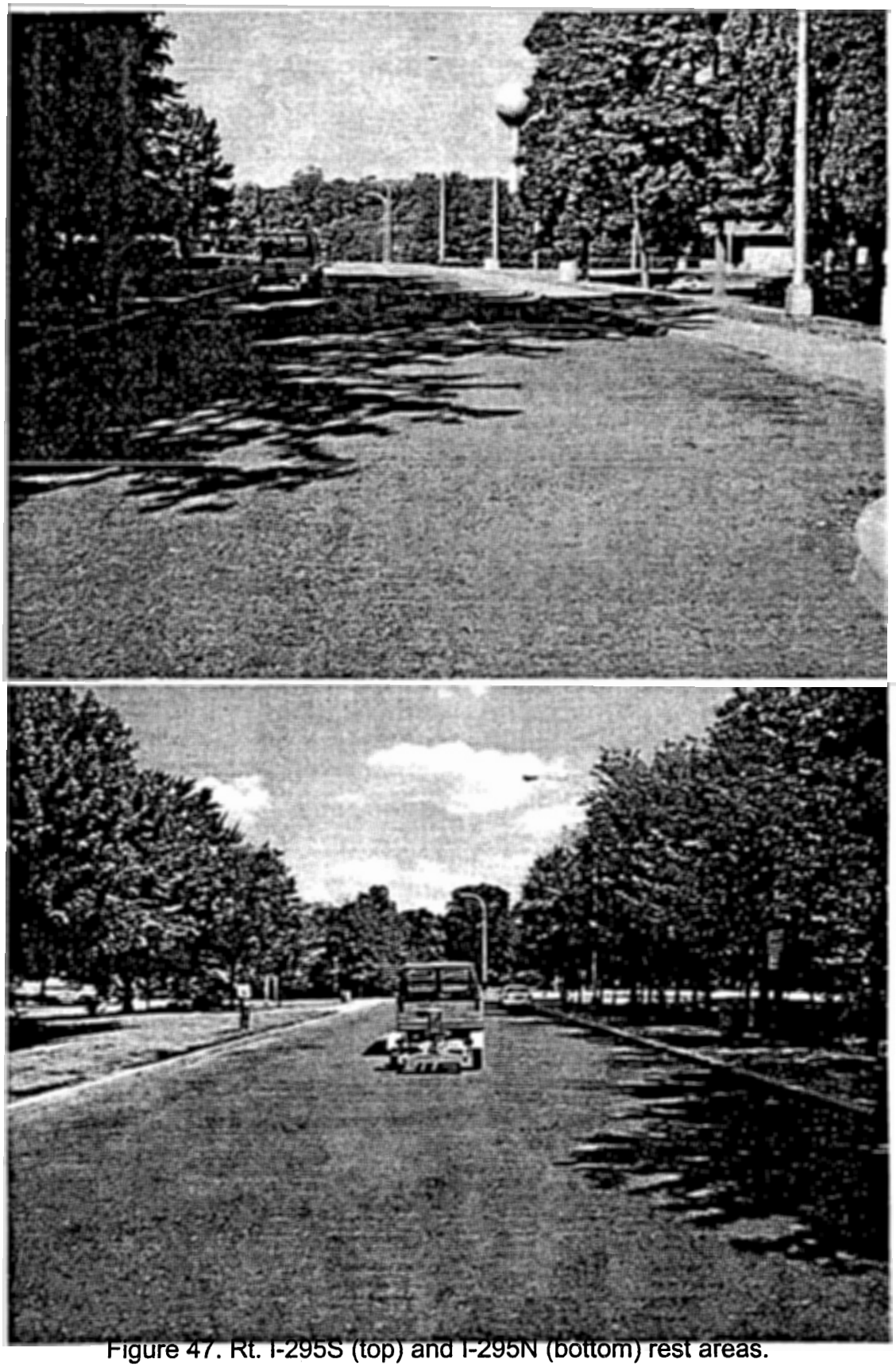

Figure 47. Rt. I-295S (top) and I-295N (bottom) rest areas.

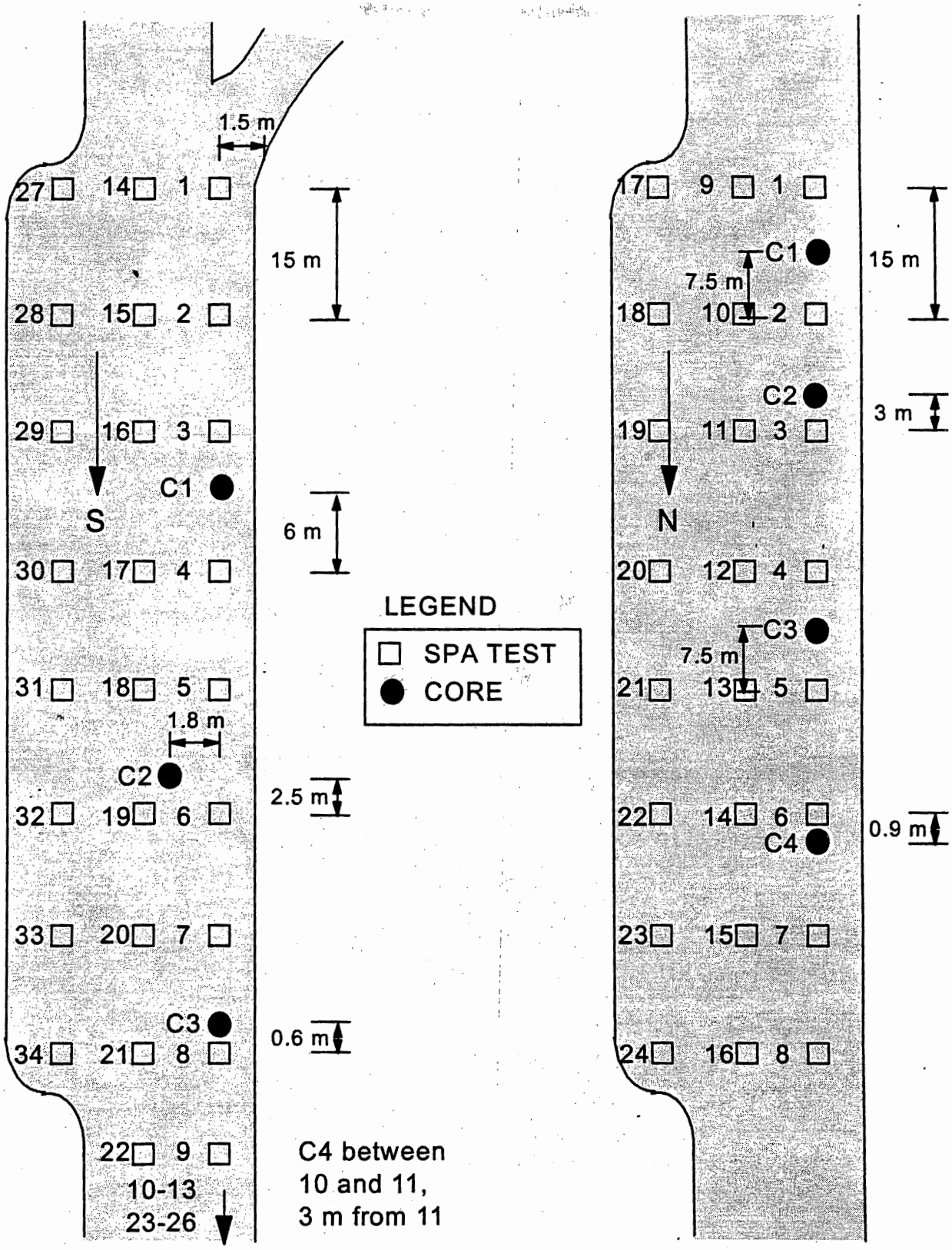


Figure 48. Schematics of south (left) and north (right) bound rest area test and core locations.

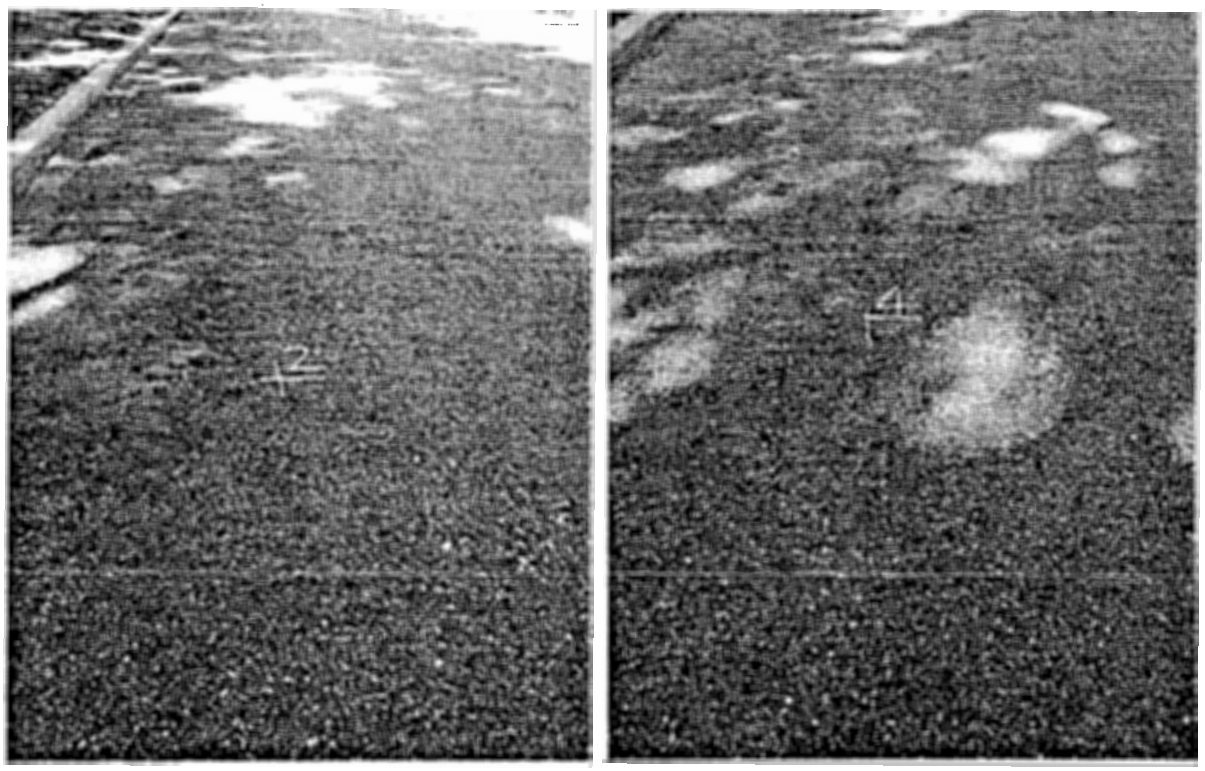

Figure 49. Pavement condition in the south bound rest area.

Figure 50. SPA testing in the rest area.

**Table 4. Asphalt Layer Thickness from Cores in cm**

| Core Location | South Bend Rest Area | North Bend Rest Area |
|---|---|---|
| 1 | 11.5 | 11.5 |
| 2 | 7.5 | 7.5 |
| 3 | 10.8 | 12.7 |
| 4 | 11.5 | 11.5 |

**First Series - Multiple Hit Comparison**

The first series of tests was conducted along the lines of test points 1 to 13 on the south bound rest area and 1 to 8 on the north bound rest area. The testing involved repeated testing at a test point, three tests per point, for the purpose of evaluation of consistency and repeatability both SPA hardware and software. To analyze the repeatability of the hardware in impact generation, signal detection and recording, hammer load cell and transducer signals were compared on the level of:

- time histories,
- linear spectra, and
- cross power spectra.

The data provided in this section provide a comparison of signals from multiple impacts during a single test. The following section provide a comparison of signals from three subsequent tests at a same test point.

In general, the signal generated and recorded is repeatable. The conclusion will be illustrated through a comparison of load cell and transducer signals from three hits of a single test. To meet repeatability of the signal, three requirements have to be satisfied. Firstly, the hammers need to generate impacts consistently in terms of their time history and frequency content. Secondly, the hammer induced signal must not be significantly affected by external sources. And thirdly, the transducers should consistently record the generated signals. An example of hammer and transducer consistency is illustrated by time histories and corresponding spectra for Bank 0 in Figures 51 and 52. Bank 0, as described in the SPA section, represents a record including the high frequency hammer and accelerometers 1, 2 and 3. Time histories (Figure 51) of both the hammer load cell and accelerometers look very similar, except for the magnitude that increases from Hit 1 to Hit 3. Similar can be said for the spectra, shown in Figure 52, where the shape of the spectra is about the same with a magnitude increasing from Hit 1 to Hit 3. Because the primary interest of this testing was the SASW method, on the data collection side was of interest how any inconsistencies affect the phase of the cross power spectrum that is used in the generation of the dispersion curve. Magnitude and phase of the cross power spectra for accelerometers 1 and 2, and 2 and 3, are shown in Figure 53. While the magnitude of the cross power spectrum is not utilized in the data analysis, it is a good indicator of the distribution of energy of the signal with frequency. In this particular case, significant energy exists for frequencies up to about 5 kHz for accelerometer pair 1-2, and up to 4 kHz for 2-3

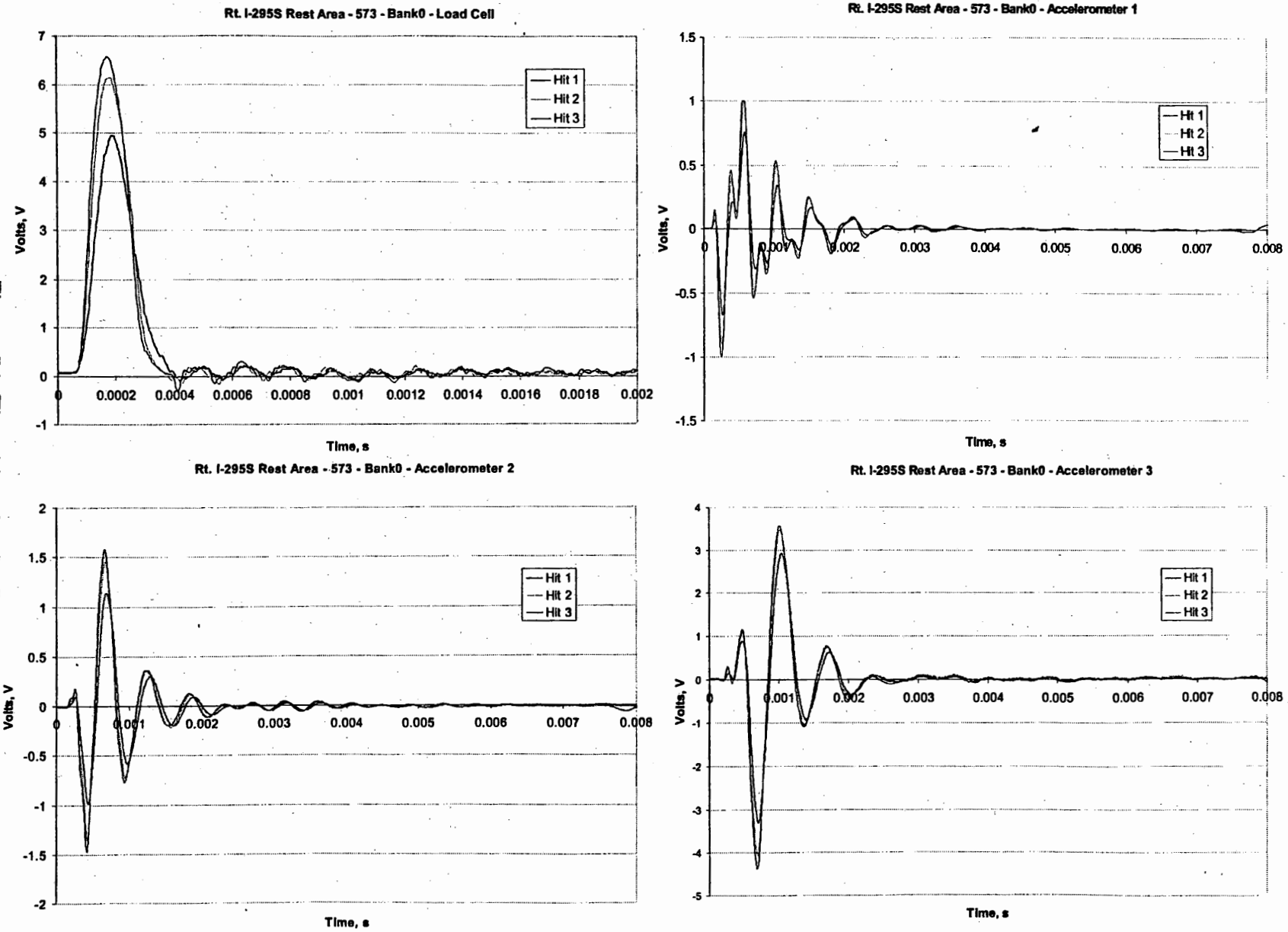


Figure 51. Time histories for Bank O.

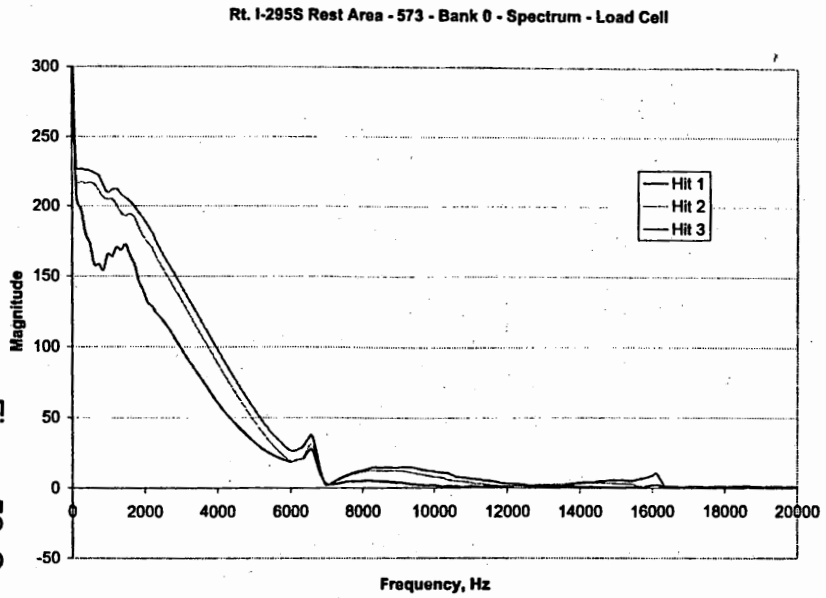


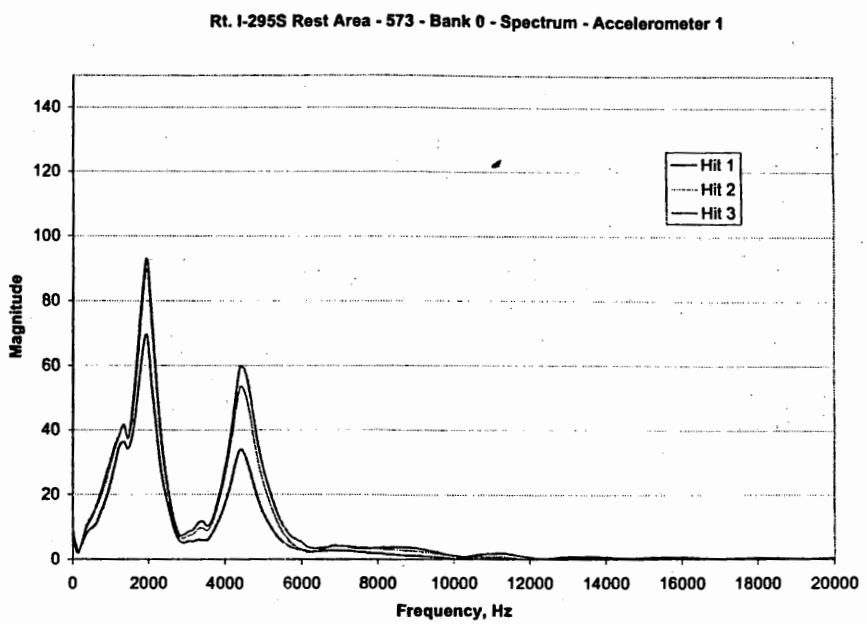


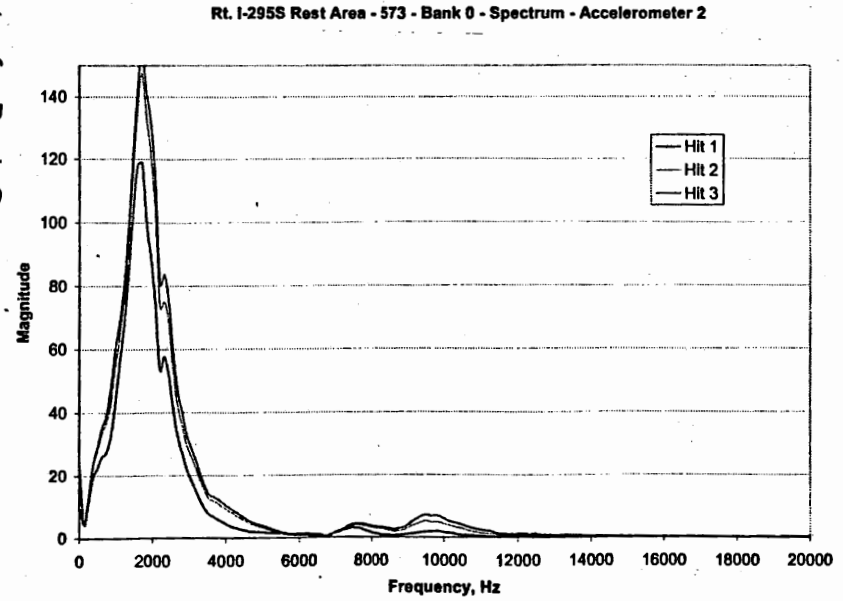


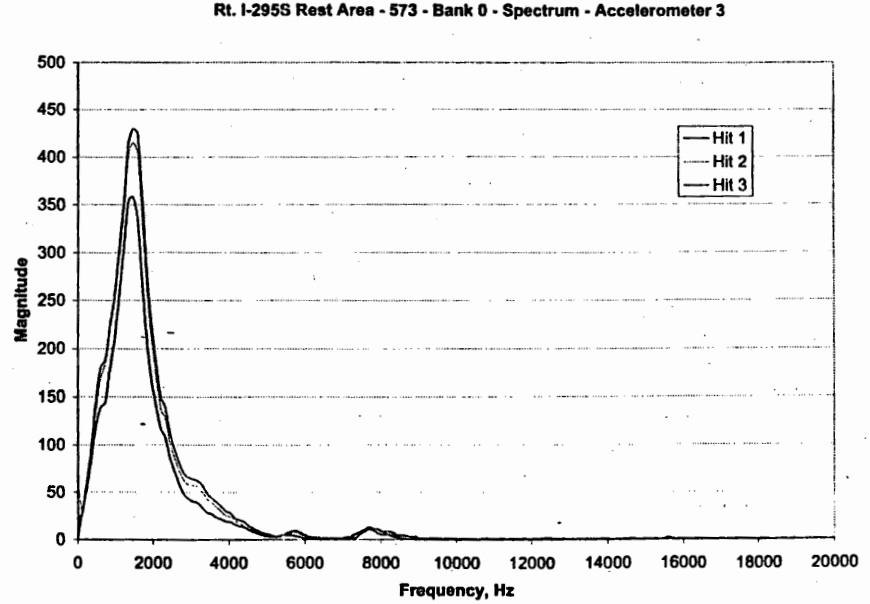


Figure 52. Spectra for Bank O.

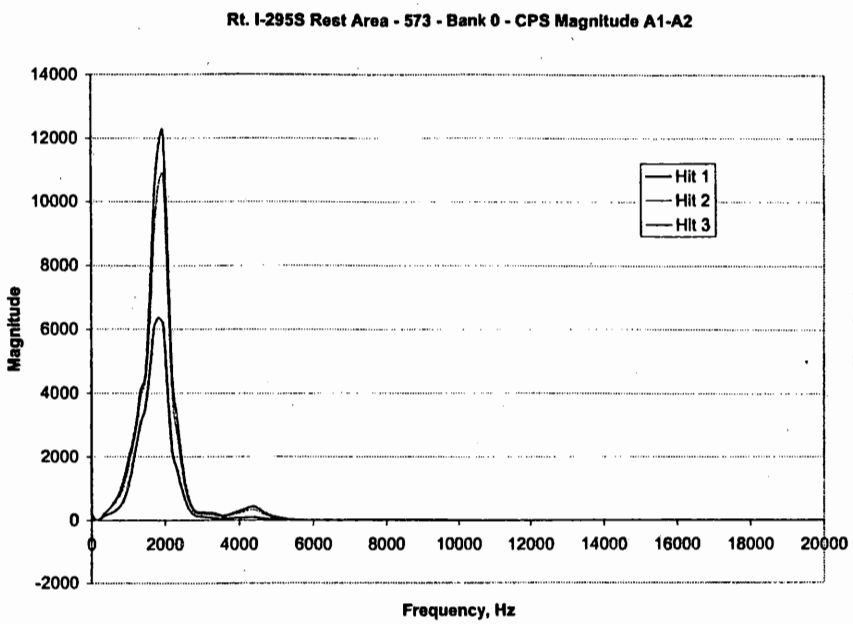


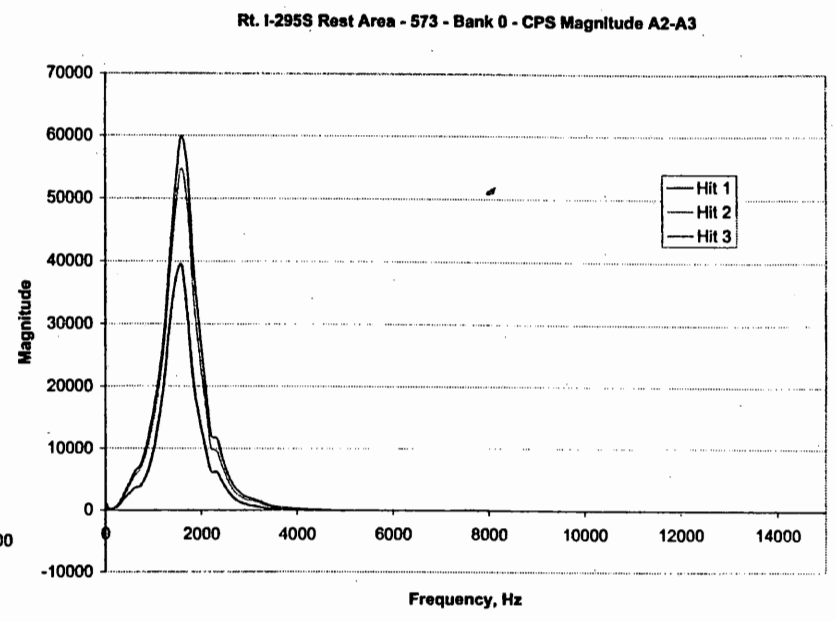


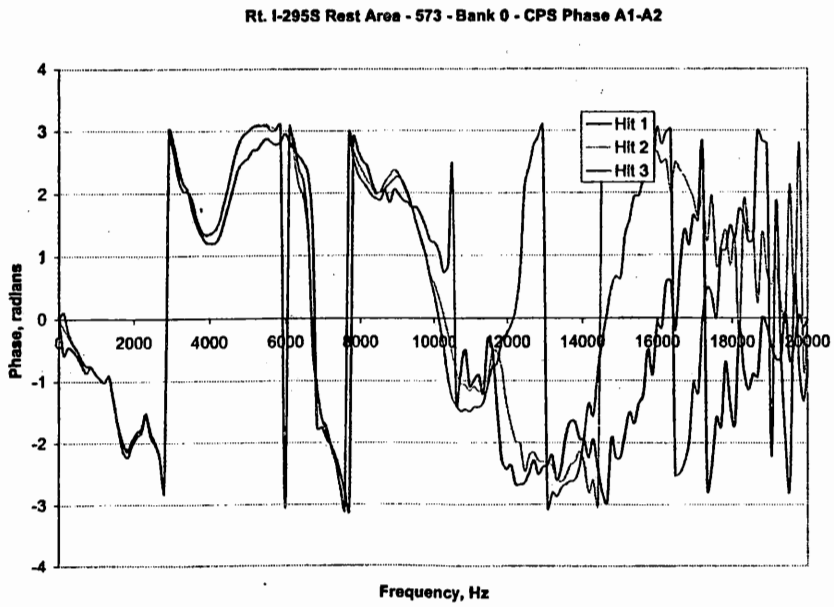


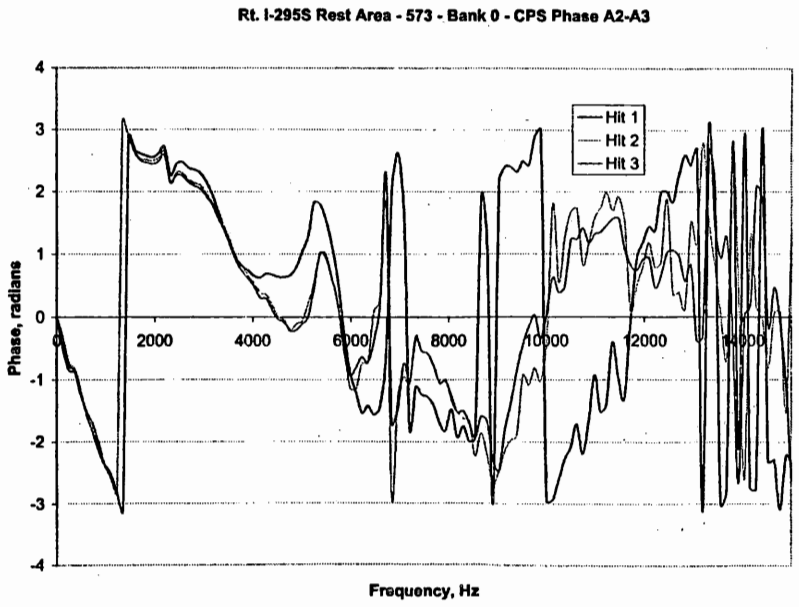


Figure 53. Cross power spectra for Bank O.

pair. Therefore, it could be anticipated that there is a good agreement below those frequencies in the phase of the dispersion curve, as is the case in Figure 53. The response in a relatively low frequency range in this case can be described as that a dominant part of the paving layer response is coming from flexural oscillations of the layer, instead of compression and shear deformation induced wave propagation that should cover a much broader frequency range. As a result, accuracy in measurement of properties of the upper most part of the paving layer is reduced.

Several inconsistencies and problems were observed also, as shown in Figure 54. Accelerometer 5 in Bank 1 had a noise of a significant level. The low frequency hammer had a secondary impact, and Geophone 3 had significant vibrations of an unknown origin. However, none of the three observed problems will necessarily lead to a problem in data reduction, as illustrated by the phase of the cross power spectrum for Geophones 2 and 3 in Figure 54. In this case an important part of the phase curve between about 100 and 400 Hz shows high repeatability.

**First Series - Subsequent Test Point Testing**

The second comparison of the first series of tests involved a comparison of repeated testing at test points 1 to 13 on the south bound side, and 1 to 8 on the north bound side. The objective of this part of testing was to examine the repeatability of testing at a same test point location, by comparing time histories, linear and cross power spectra, and obtained pavement layer properties from three subsequent tests. Any differences on the data collection level (time histories, linear and cross power spectra) would be an indication of inconsistencies in impact generation and/or transducer coupling.

Observations and conclusions of this study are similar to those for a comparison of results obtained in the multiple hit comparison study. As shown in Figures 55, 56 and 57, time histories, linear spectra and magnitude and phase of the cross power spectra for Bank 0 of three tests at test point 11 of the south bound rest area are comparing well in a frequency range of significant energy. Those frequency ranges are 0 to about 8 kHz for A1-A2 combination, and 0 to about 4 kHz for A2-A3 combination. Similar differences in time histories for Banks 1 and 4 do not cause discrepancies in the phase of the cross power spectra, as shown in Figures 58 and 59. This is an important feature of some of the seismic techniques, that a measurement of elastic wave velocities is not affected by variations in the impact source characteristics.

Software consistency was examined through a comparison of layer properties obtained from the three tests. For this purpose the pavement was backcalculated as a four course pavement. The base layer was described as a two course layer for computational reasons. The thickness of the paving layer is shown in Figure 60. A good agreement between the evaluated thicknesses can be observed. However, the thickness is about 20 to 40% less than the actual paving layer thicknesses obtained from the cores. The shear wave velocity measured in the paving layer in most cases is repeatable, as shown in Figure 61. Differences in Young's moduli of the paving layer for the three tests are more pronounced than of the shear wave velocity, as shown in Figure 62. This is simply a result of a fact that the modulus is proportional to a square of the velocity. It should be also mentioned that the

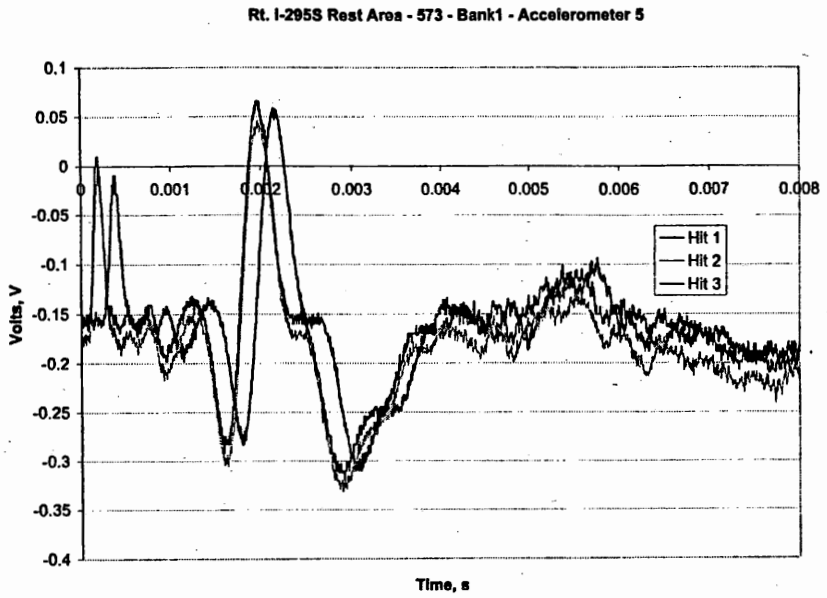


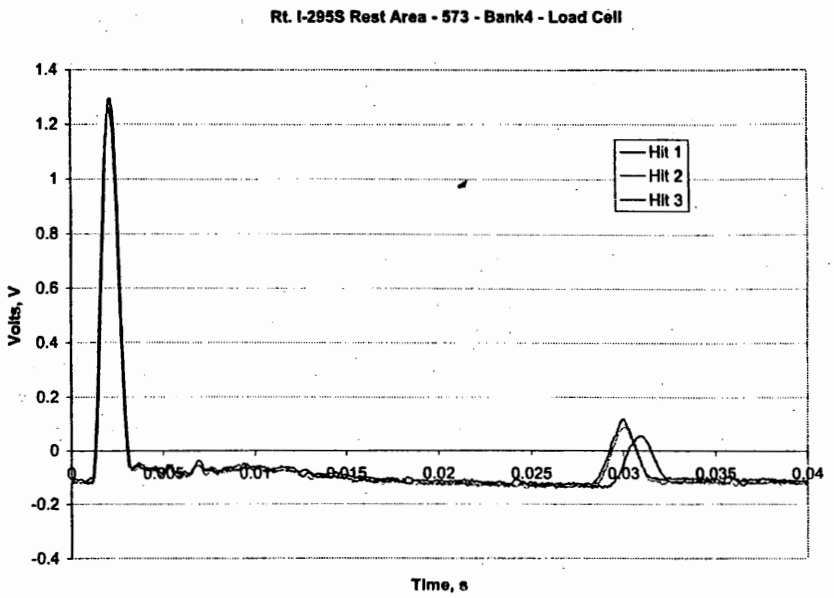


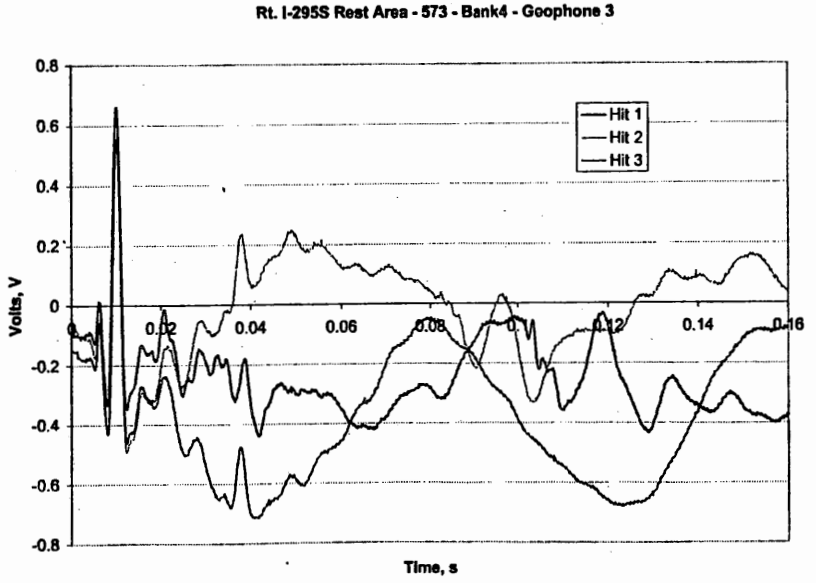


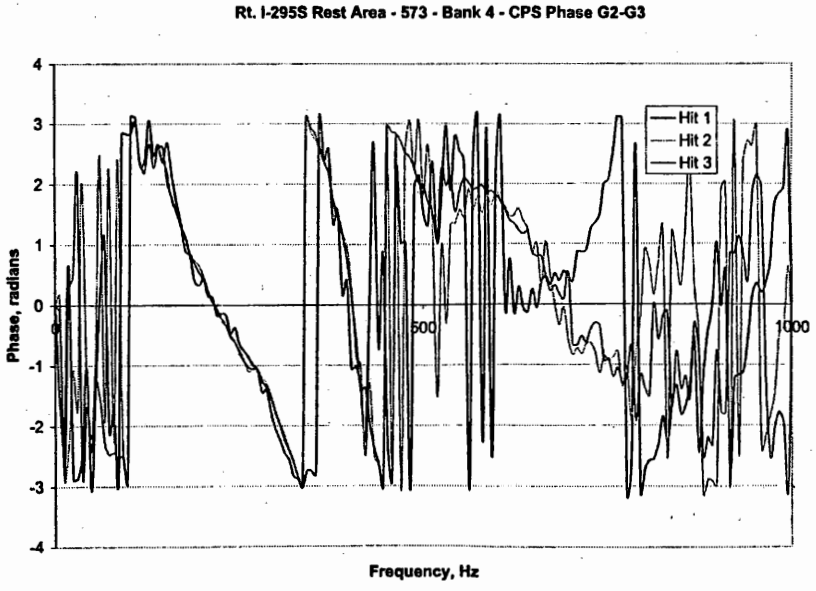


Figure 54. Signal inconsistencies.

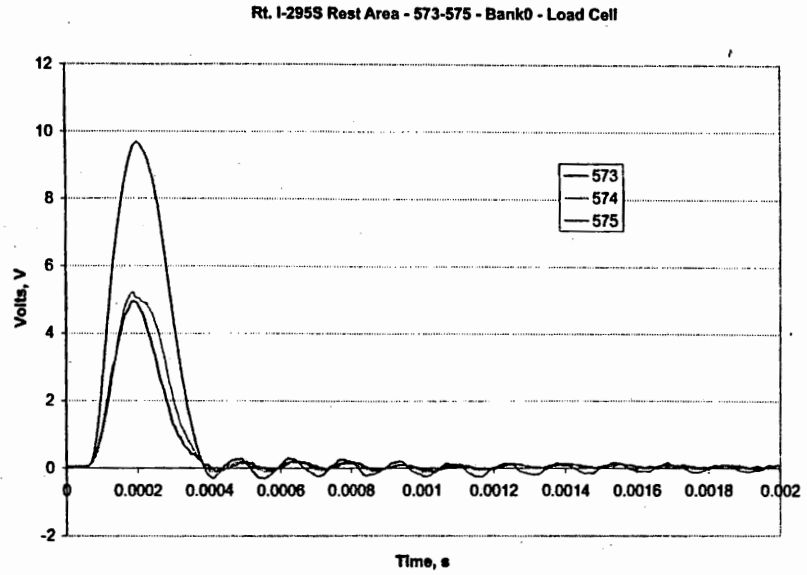


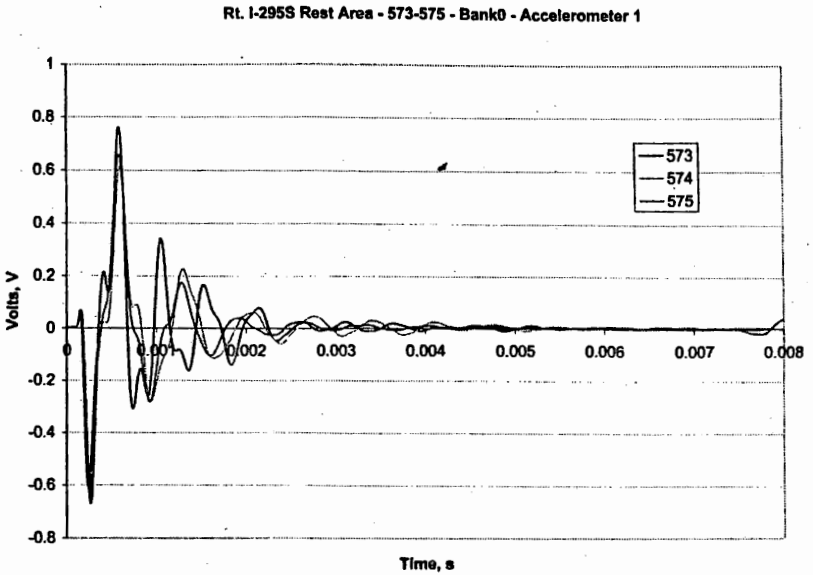


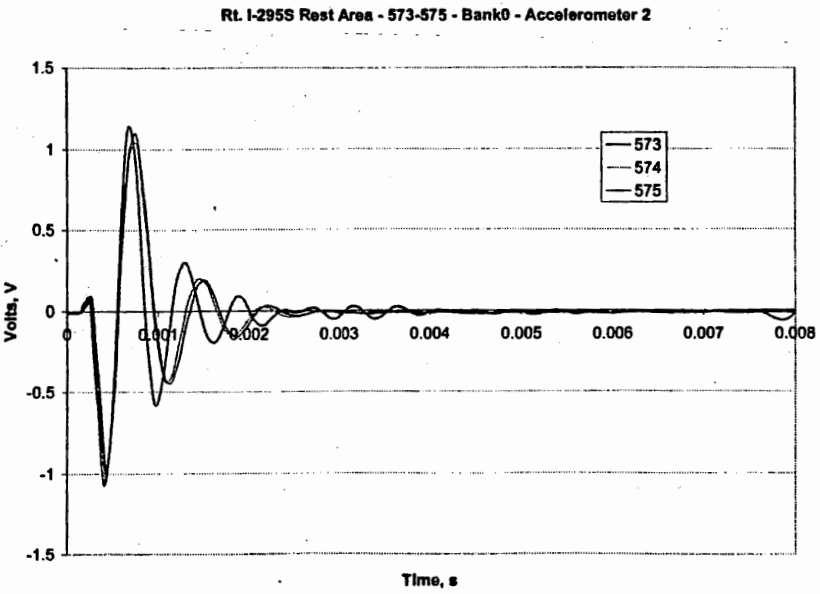


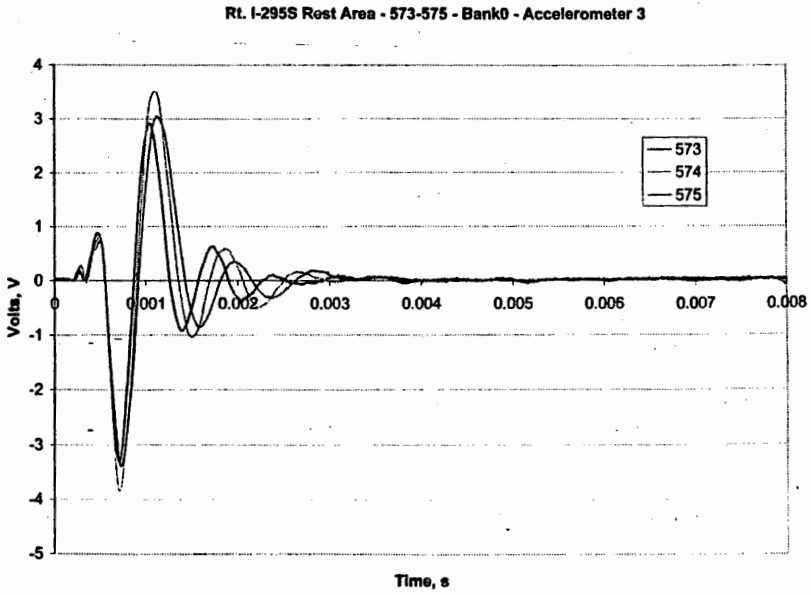


Figure 55. Time histories for Bank 0 - subsequent testing.

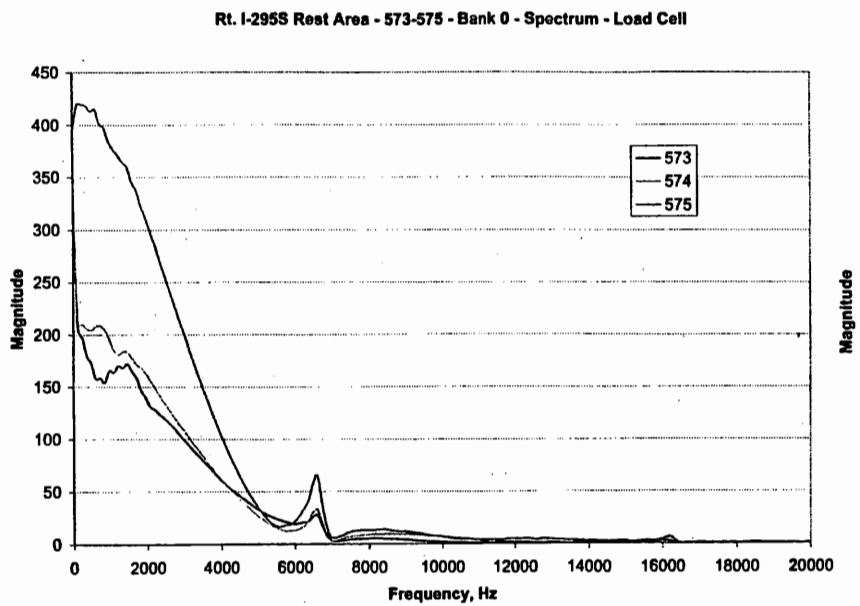


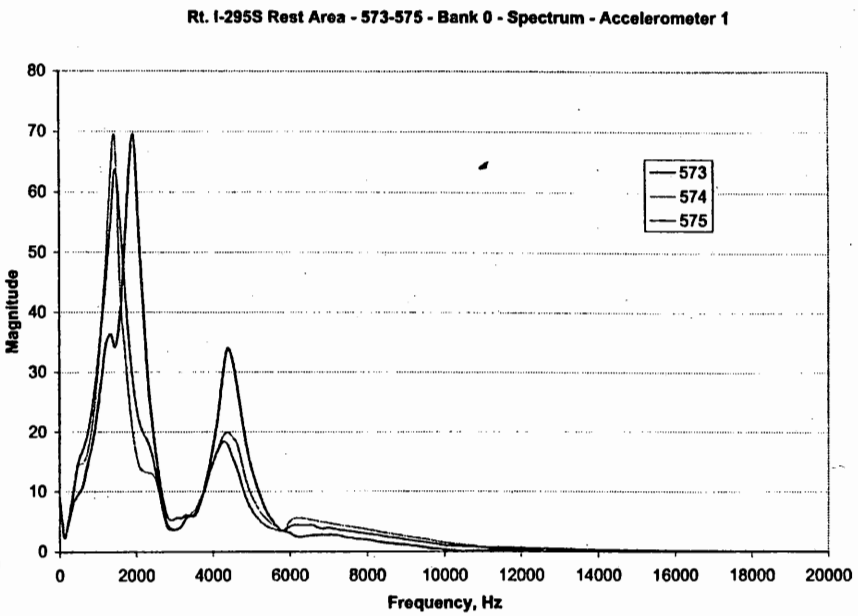


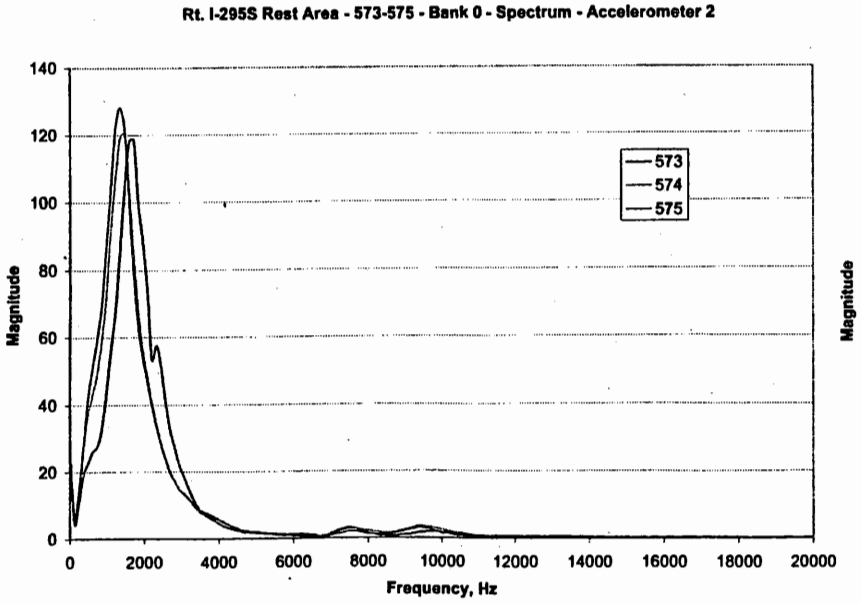


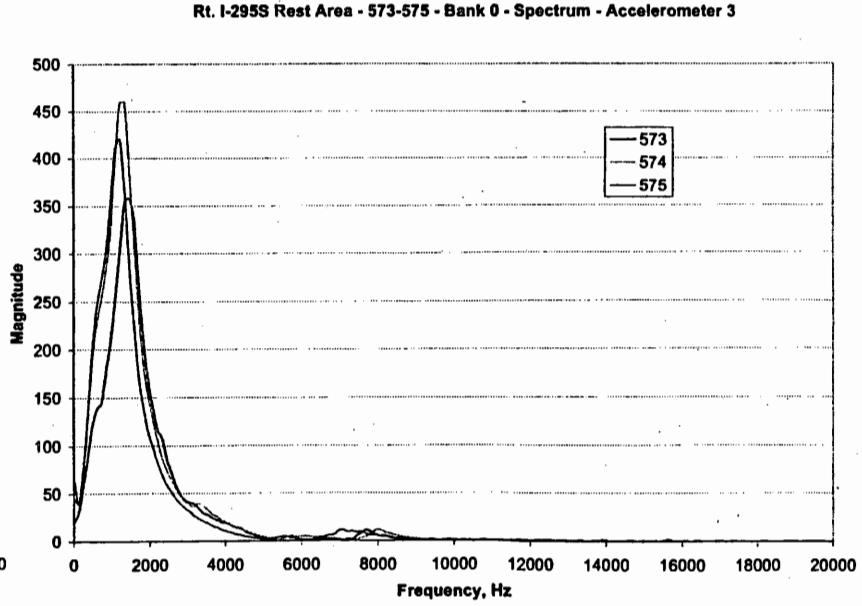


Figure 56. Spectra for Bank 0 - subsequent testing.

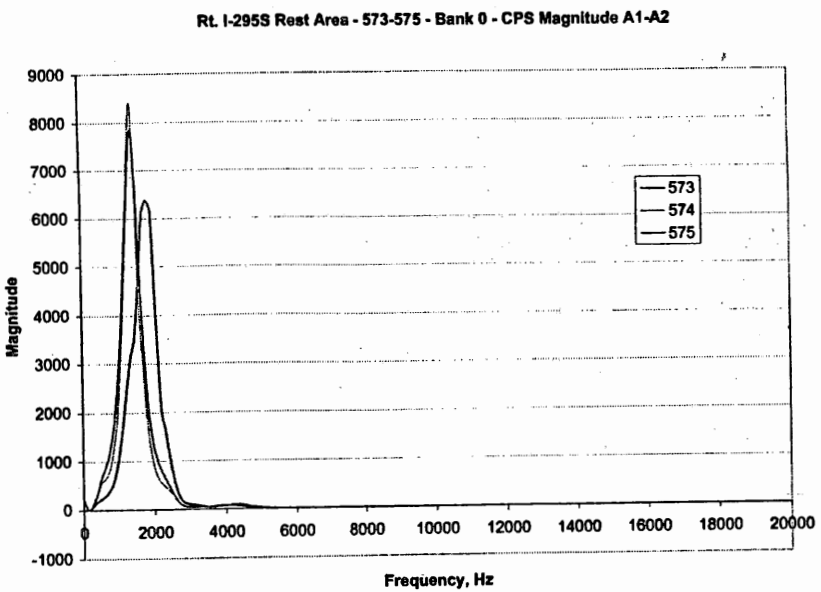


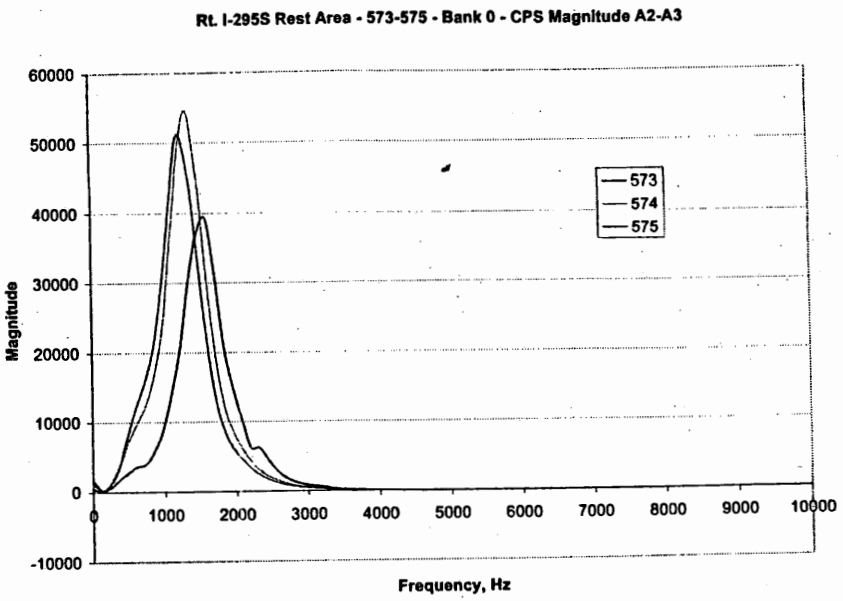


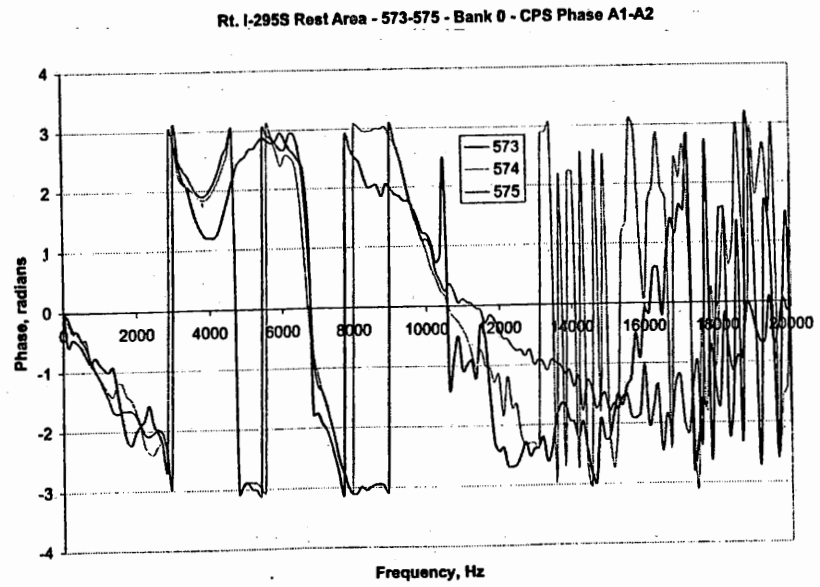


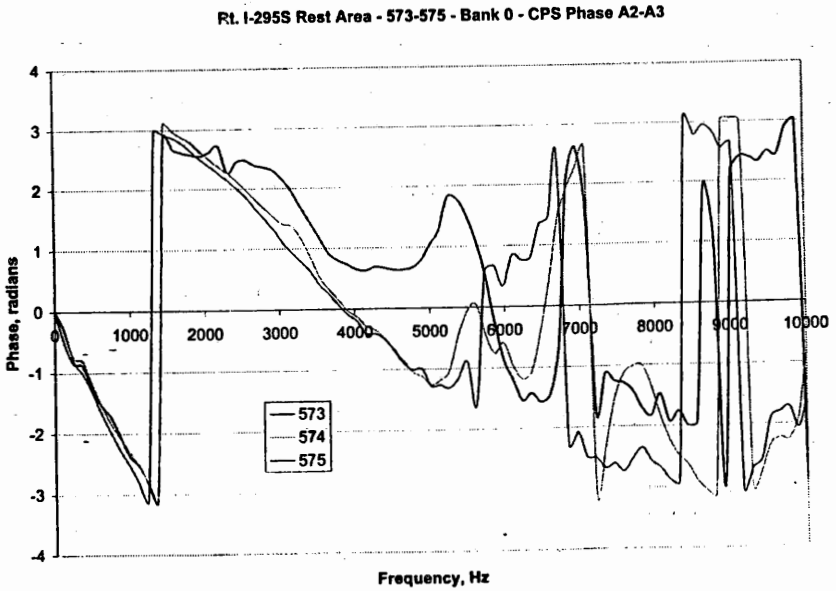


Figure 57. Cross power spectra for Bank 0 - subsequent testing.

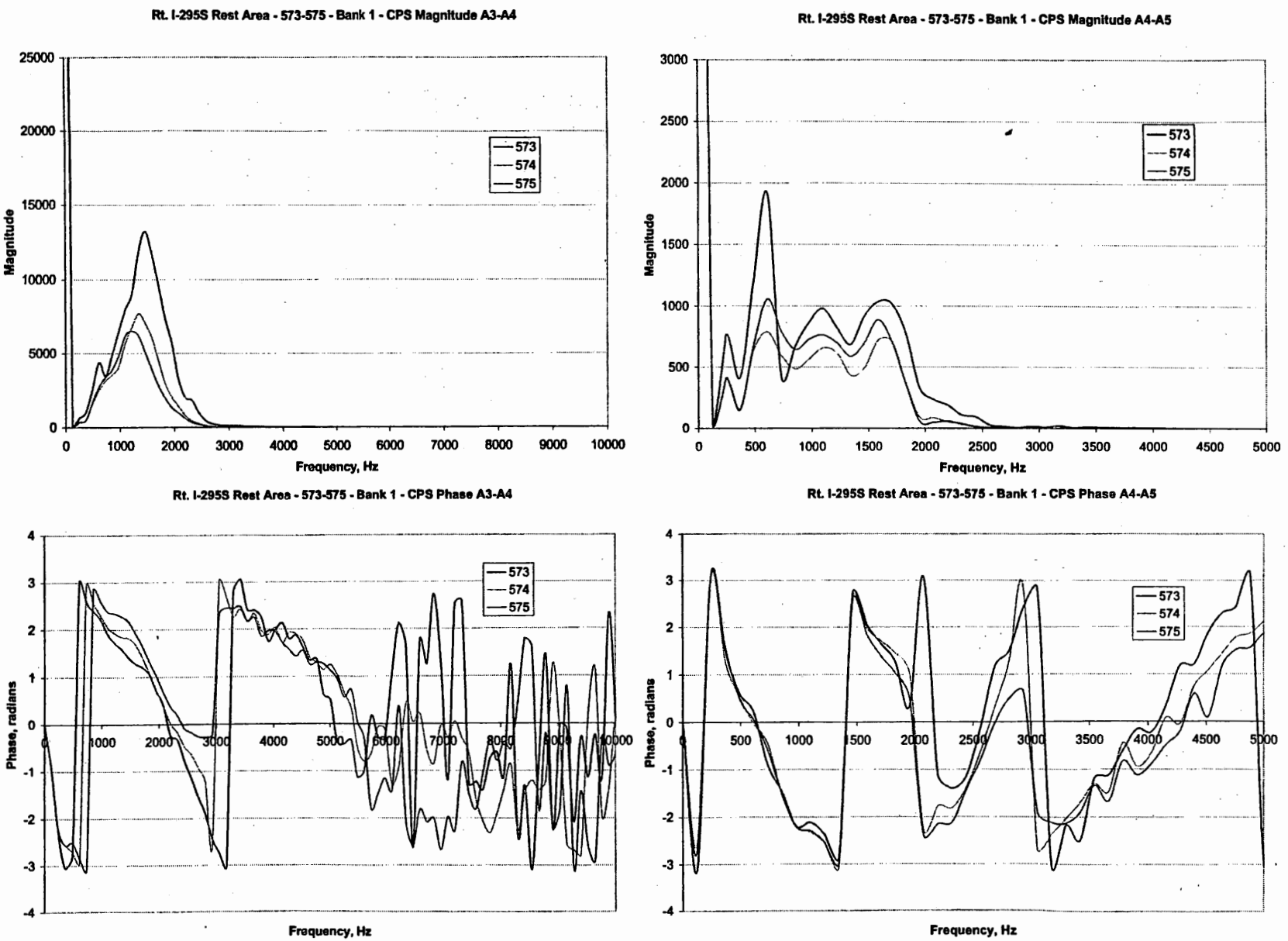


Figure 58. Cross power spectra for Bank 1 - subsequent testing.

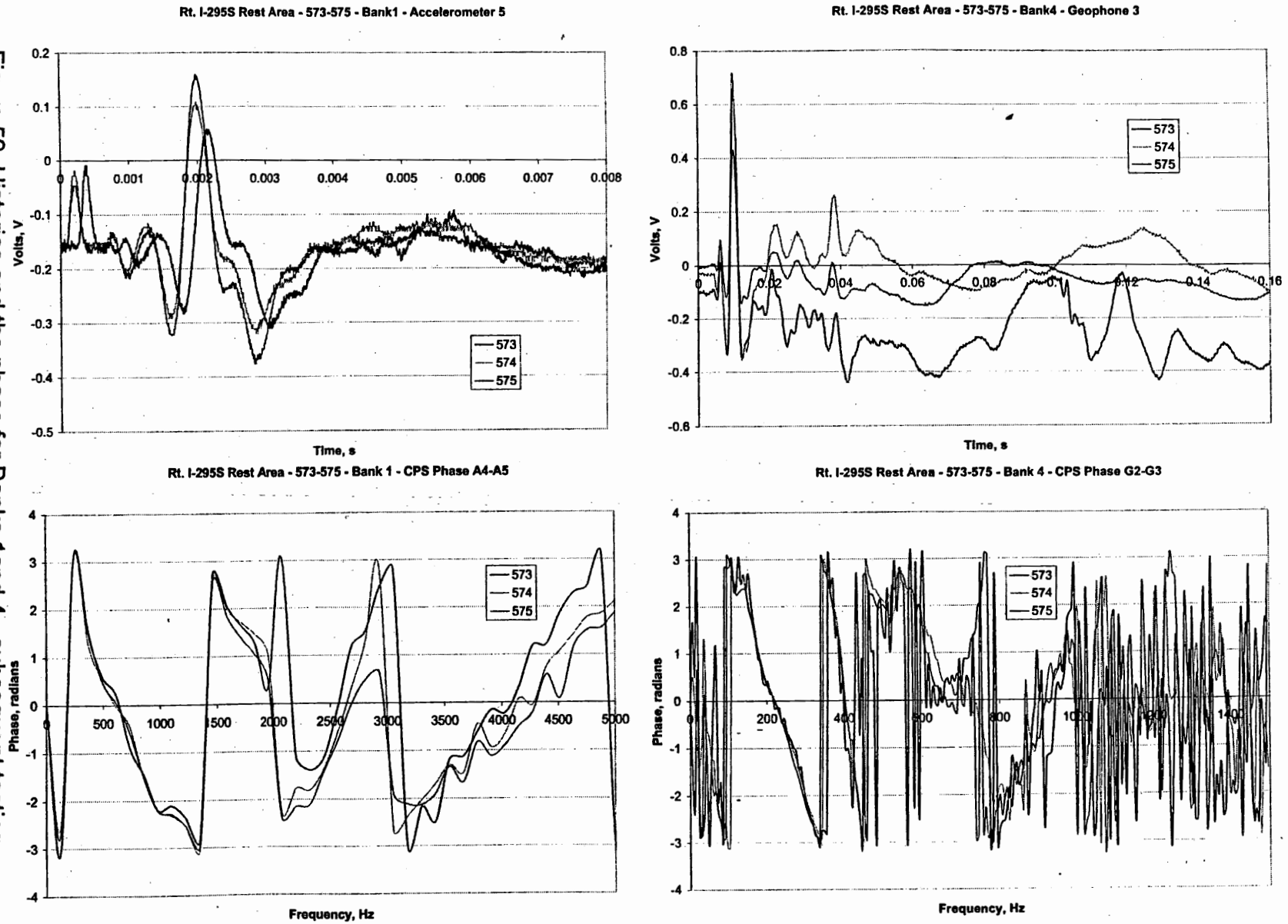


Figure 59. Histories and the phase for Banks 1and 4 - subsequent testing.

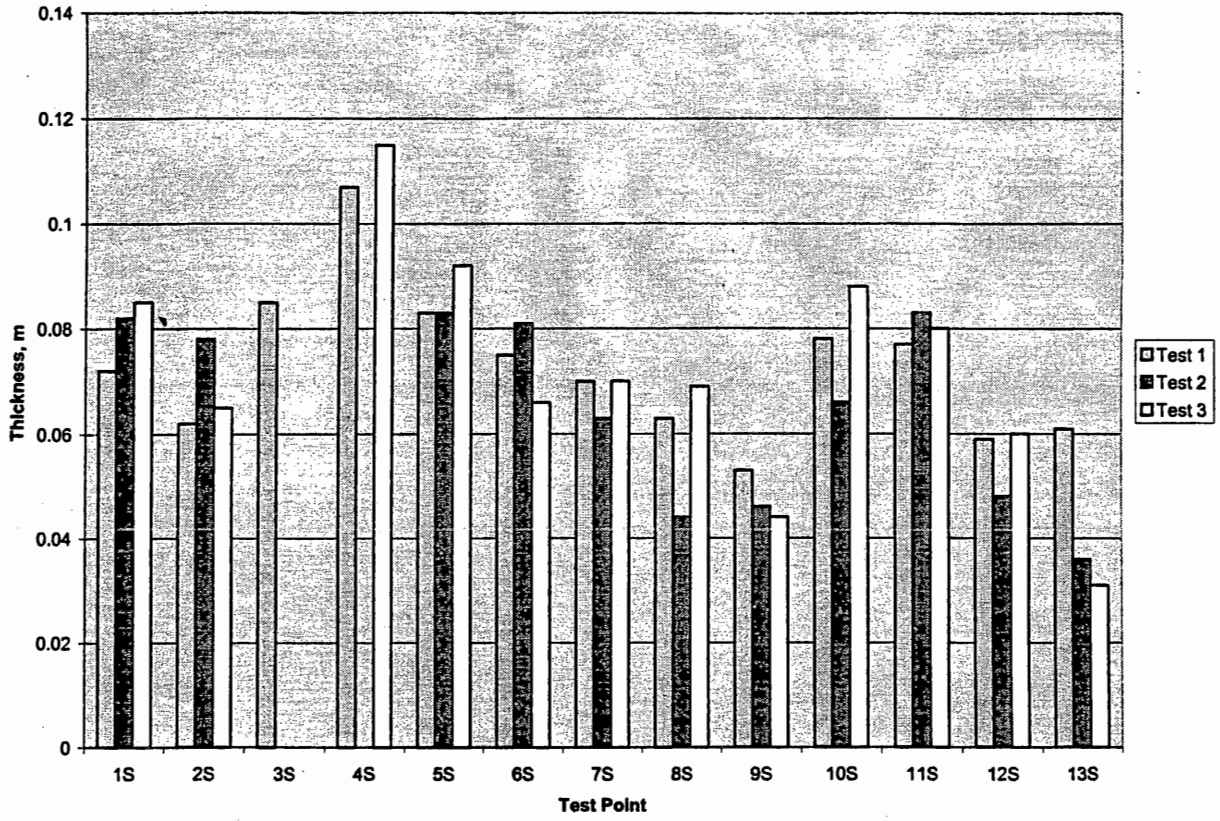


Figure 60. Paving layer thickness.

moduli are not corrected for frequency. A correction factor that would make it comparable to moduli measured by a falling weight deflectometer is about 3. Shear moduli of the base and the subgrade, shown in Figures 63 and 64, vary much more than the elastic modulus of the paving layer. The variation is somewhat attributed to flexural vibrations of the paving layer. A low frequency range of flexural vibration matches the range of surface waves used in evaluation of properties of deeper layer. This certainly raises the question of finding the minimum paving layer thickness for which the evaluation of pavement layer properties by the SASW test would not be affected by flexural deformations of the paving layer. The thickness of the base layer varied between 20 and 40 cm. This large variation in the thickness is attributed to the backcalculation. Several studies have shown that, if the contrast in rigidity of the base layer and the subgrade is not sufficiently high, the base thickness is difficult to determine by the SASW test.[39]

## Second Series - Repeated Testing at Close Points

The second series of tests involved twice repeated testing at test points 1 to 13 on the south bound side, and 1 to 8 on the north bound side. The objective of this part of testing was to examine the repeatability with time and minor changes in a test point location. In this part of the study the first record from the first series is compared to two records taken within the next two hours. Since the temperature conditions did not change significantly during this period, temperature effects were not considered to be a factor. Similar to the first series the

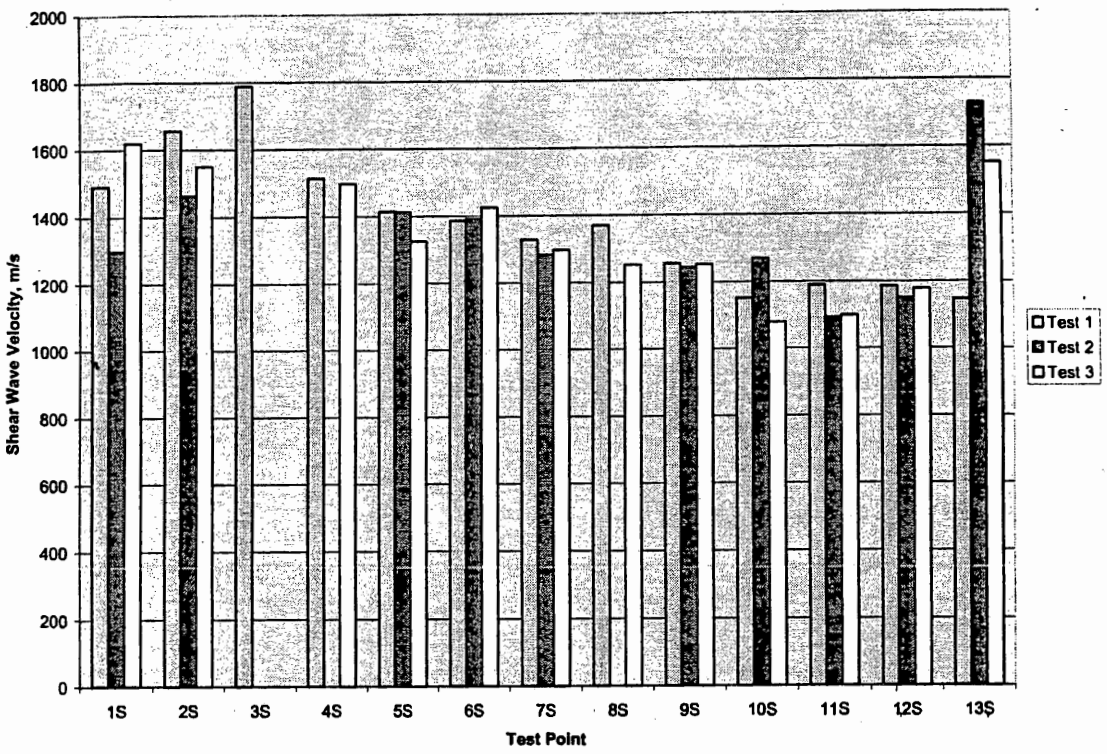


Figure 61. Shear wave velocity of the paving layer.

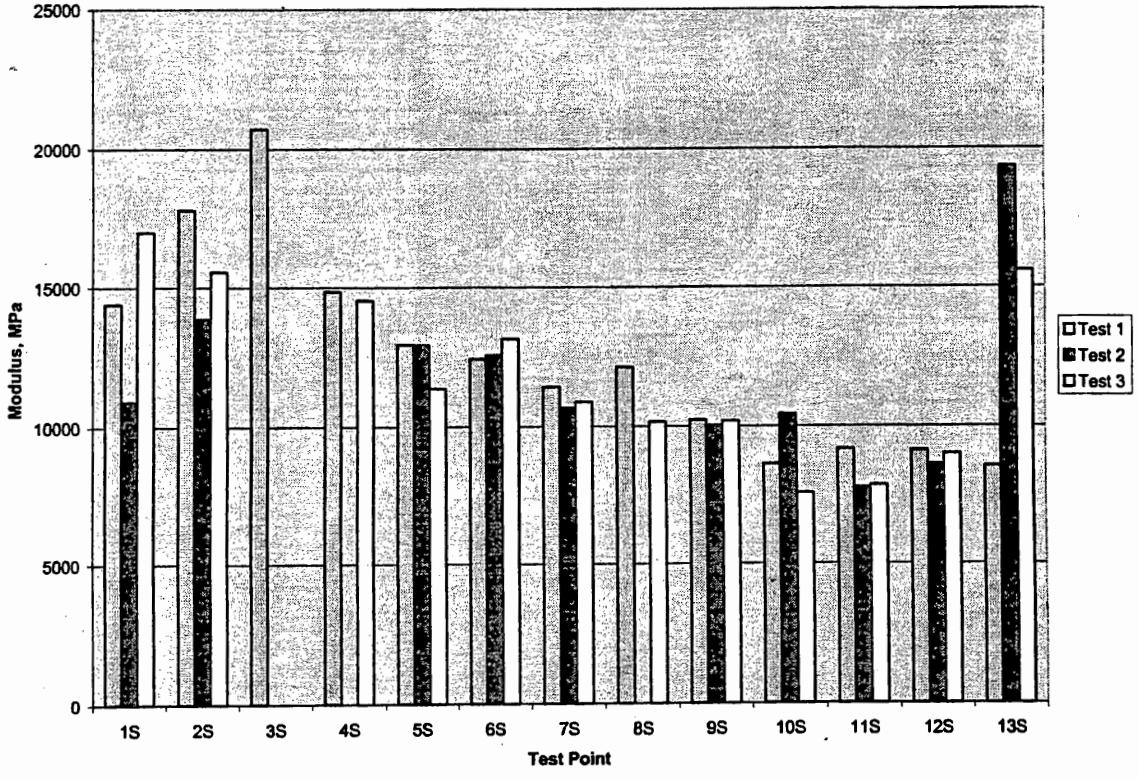


Figure 62. Young's modulus of the paving layer.

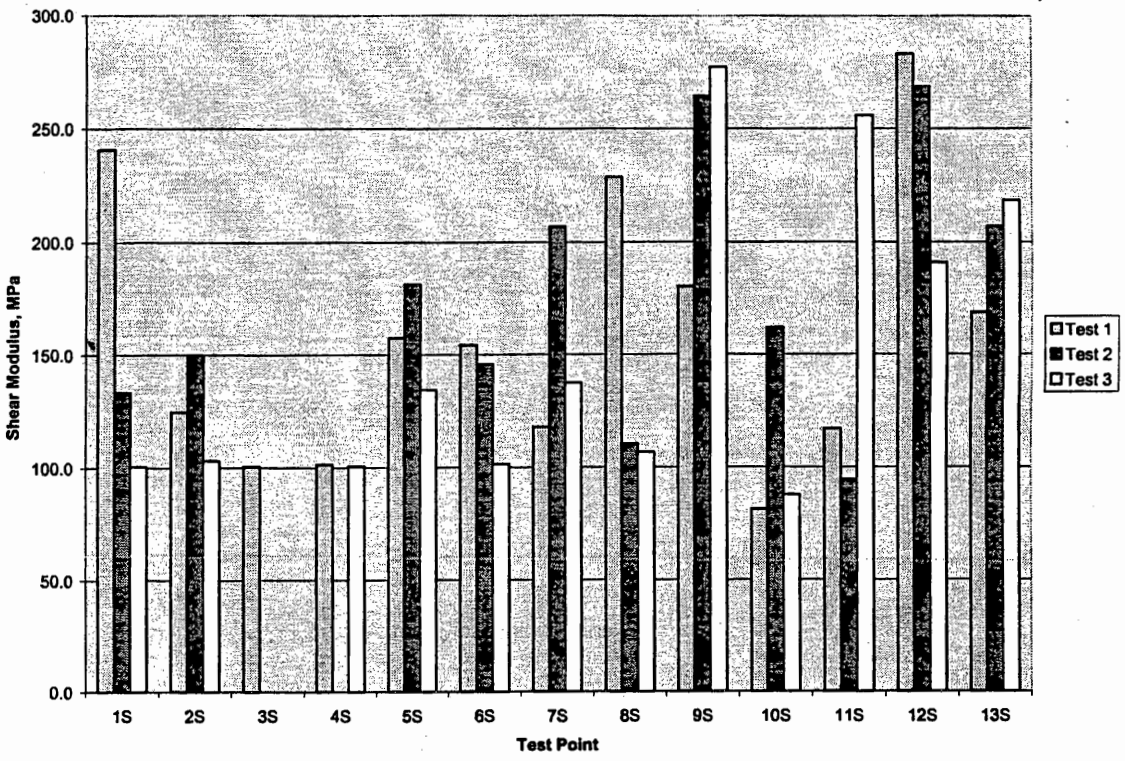


Figure 63. Base shear modulus.

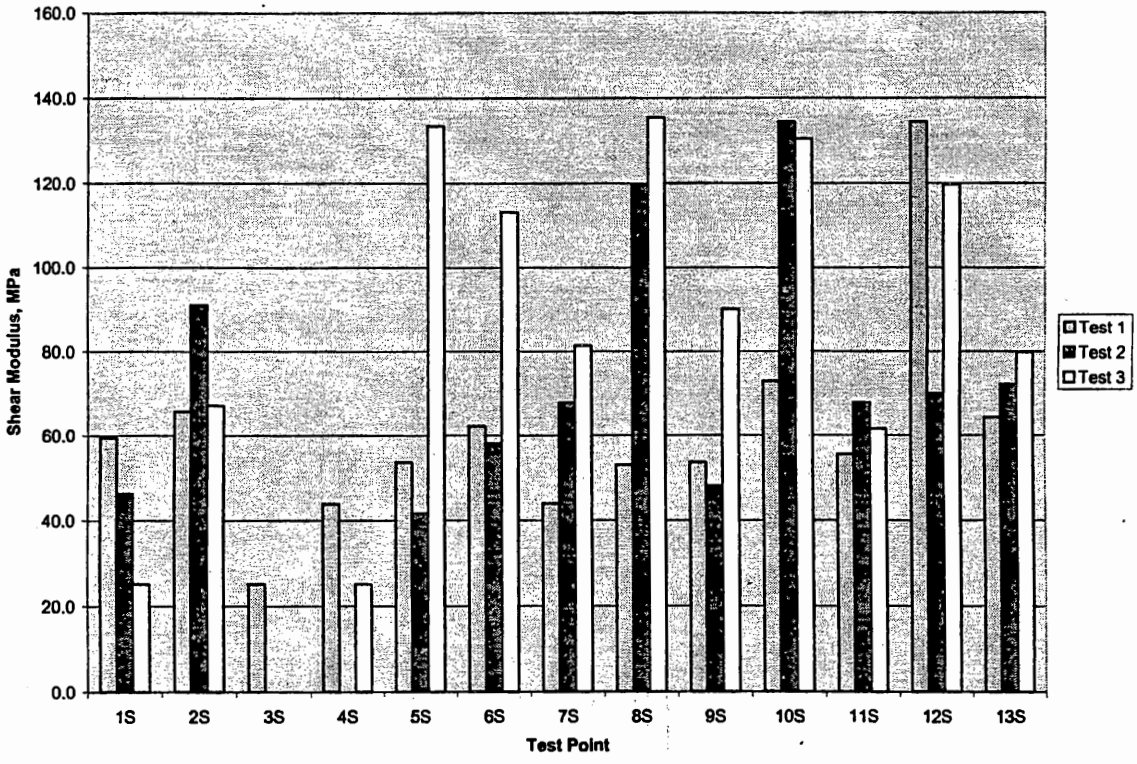


Figure 64. Subgrade shear modulus.

comparison on the hardware side was made on the level of time histories, linear and cross power spectra, and on the software side on the level of backcalculated pavement layer properties.

Differences between records from the three tests are more pronounced than in series one tests for three consecutive hits, or three consecutive tests. This is illustrated by data and obtained pavement layer properties for test point 11 of the south bound rest area. Time histories, linear spectra and cross power spectra for Bank 0 are shown in Figures 65, 66 and 67. There are clear differences in the magnitude of the hammer impact and consequently the response between the first (573) and the last two tests (600 and 621). However, there is also a difference in the frequency content of the response, as can be observed in both time histories and spectra. The phase cross power spectrum curves for receiver pair A1-A2 are very close up to 5 kHz. This frequency range matches the range of significant wave propagation energy, as can be observed in the cross power spectrum magnitude plot in Figure 67. On the other hand, the phase curves of A2-A3 pair have significant differences for frequencies above about 1 kHz. A comparison of cross power spectra for the remaining three receiver pair combinations used in SASW testing (A3-A4, A4-A5 and G2-G3), shown in Figures 68 and 69, seems to indicate good matching between the phase curves in what can be described a useful frequency range.

Results and conclusions of backcalculation of pavement modulus profiles are similar to those from the first series tests. There is a good agreement between thicknesses of the paving layer from the three tests (Figure 70), however, the backcalculated thicknesses are all lower than those obtained from the cores. Similarly, there is a good agreement in measured shear wave velocities of the paving layer (Figure 71) and some differences in calculated Young's moduli (Figure 72). Finally, differences between the shear moduli obtained from the three tests increase going from the paving layer to the base layer (Figure 73) and the subgrade (Figure 74). Again, signficant variations in the base layer thickness are attributed to a low contrast in rigidity of the base layer and the subgrade.

**Third Series - Evaluation Along Two Additional Test Lines**

The third series of tests involved testing along the center and right curb lines for two purposes. The first purpose was to compare the pavement layer properties to those from the first series tests, and the second to develop as an illustration composite plots of each of the tested rest areas. An example of such composite plots are the spectral plots for paving layer thickness and shear modulus for the south bound rest area in Figure 75.

While the study on Rt. I-295 rest areas was instructive in terms of evaluation the repeatability and consistency of data collection on the hardware side, and data analysis on the software side, observations made should not necessarily lead to definite conclusions about the same. The primary reason why definite conclusions should not be made is that measurements were made on a pavement a relatively thin AC layer. Low frequency flexural oscillations of the AC layer seem to dominate the dynamic response of the pavement on one hand, while generation of high frequency surface wave components is dampened.

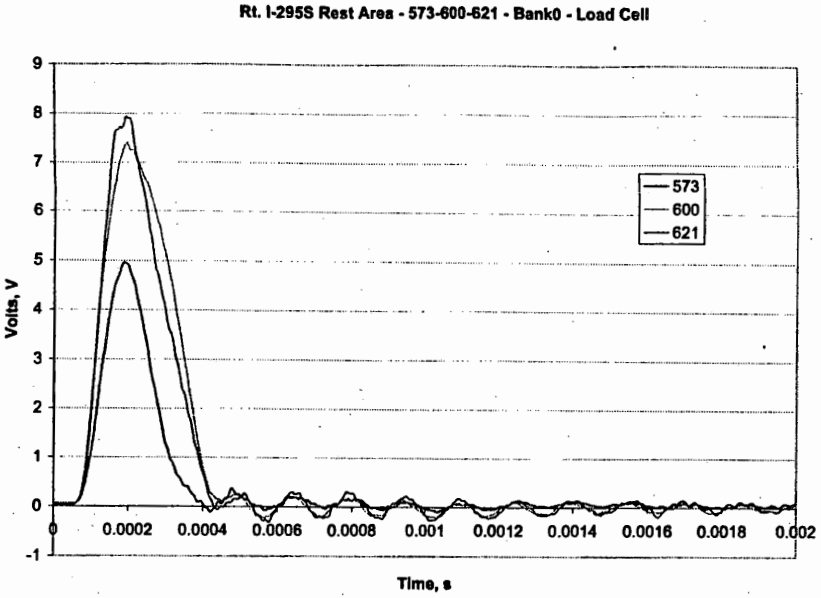


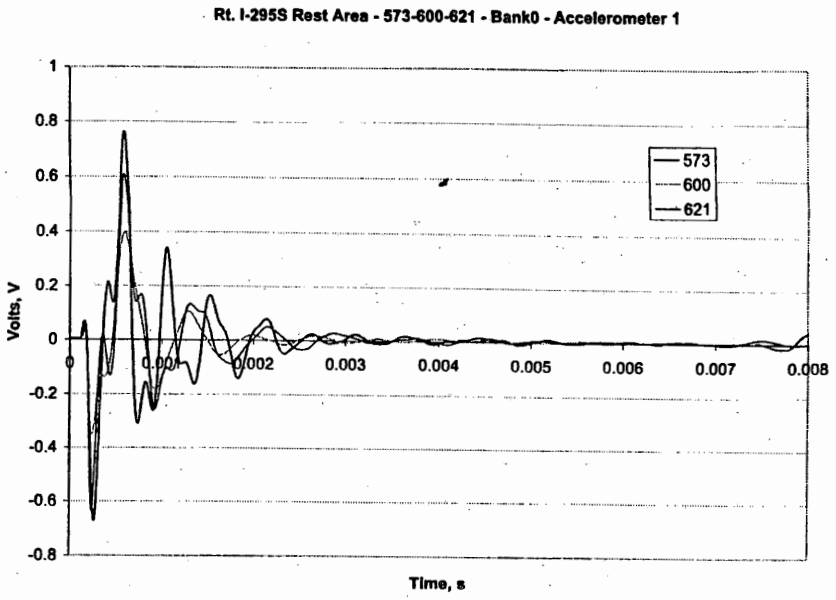


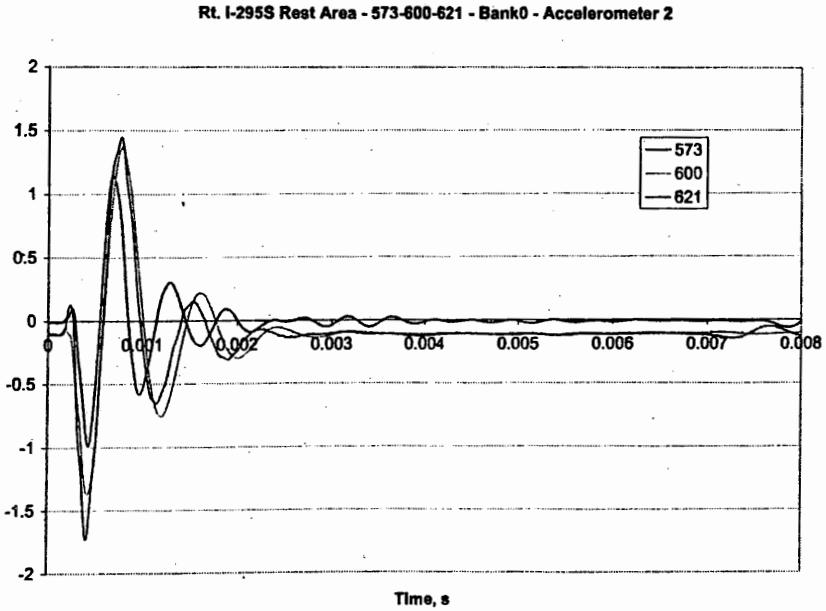


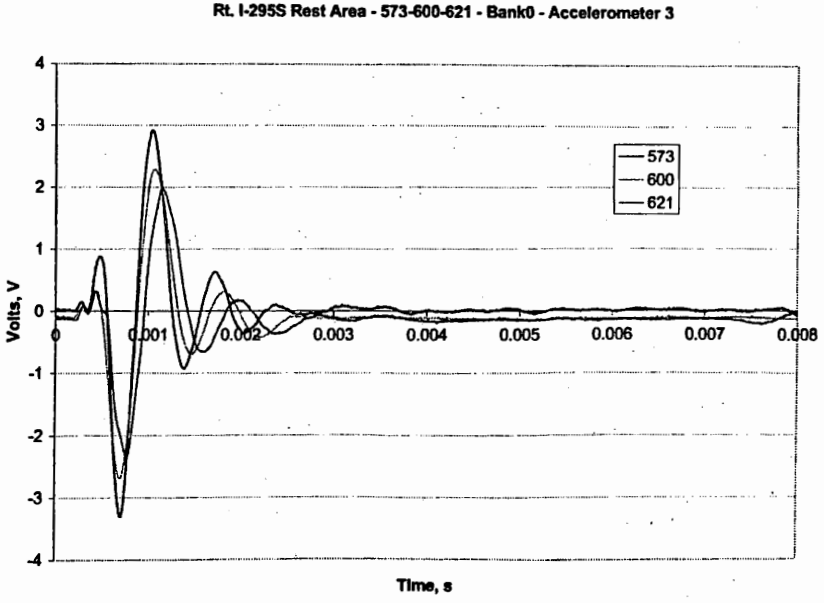


Figure 65. Time histories for Bank 0 - repeated testing at close points.

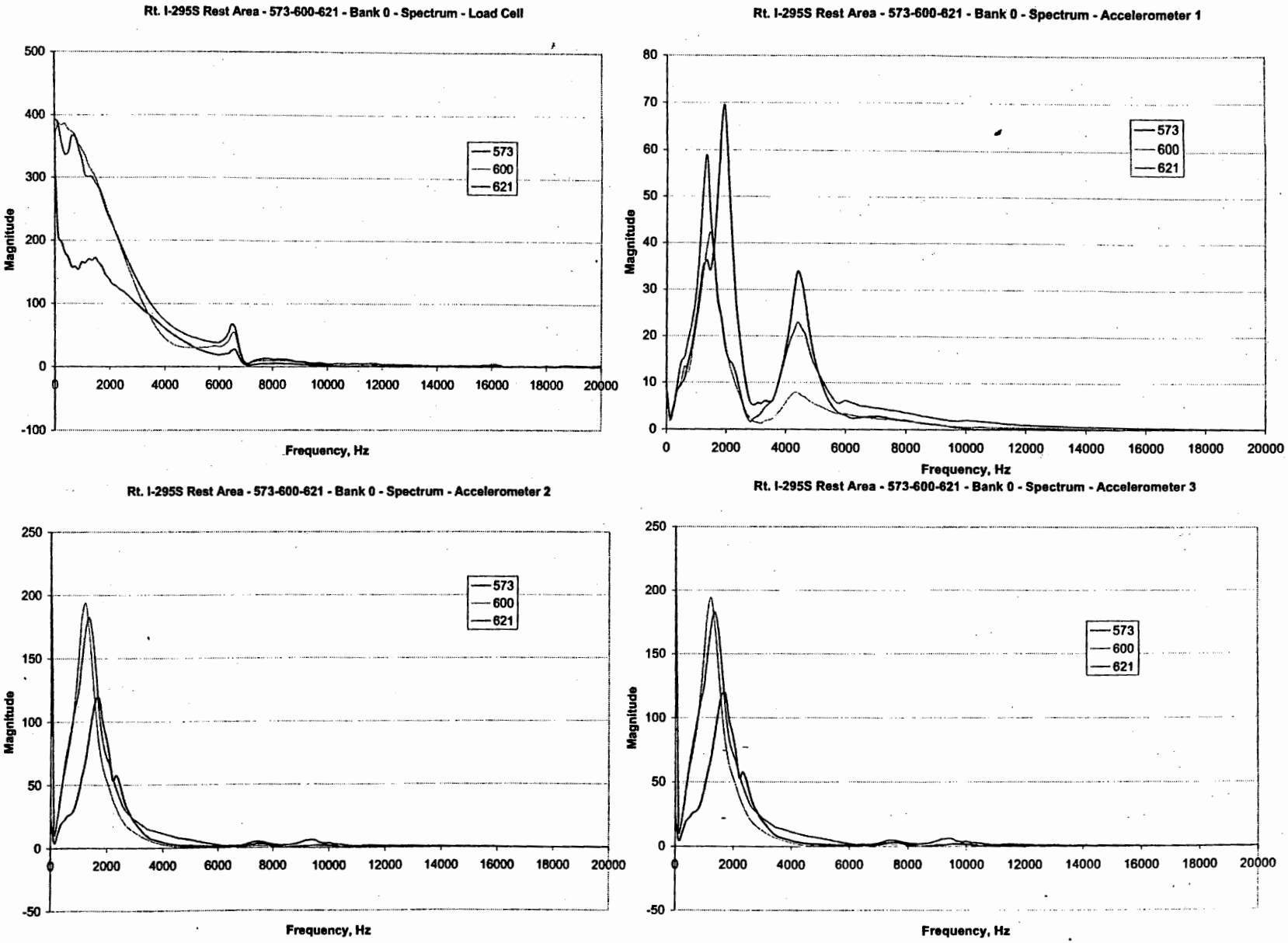


Figure 66. Spectra for Bank 0 - repeated testing at close points.

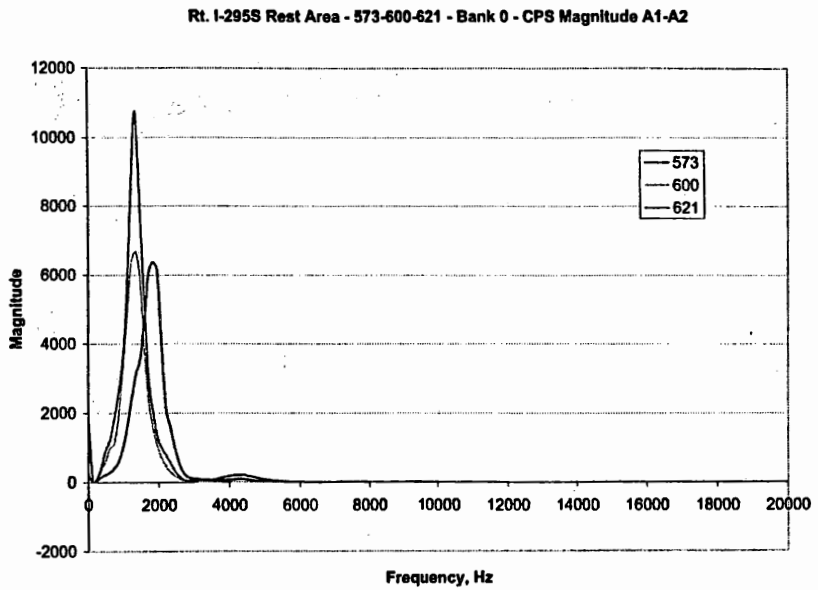


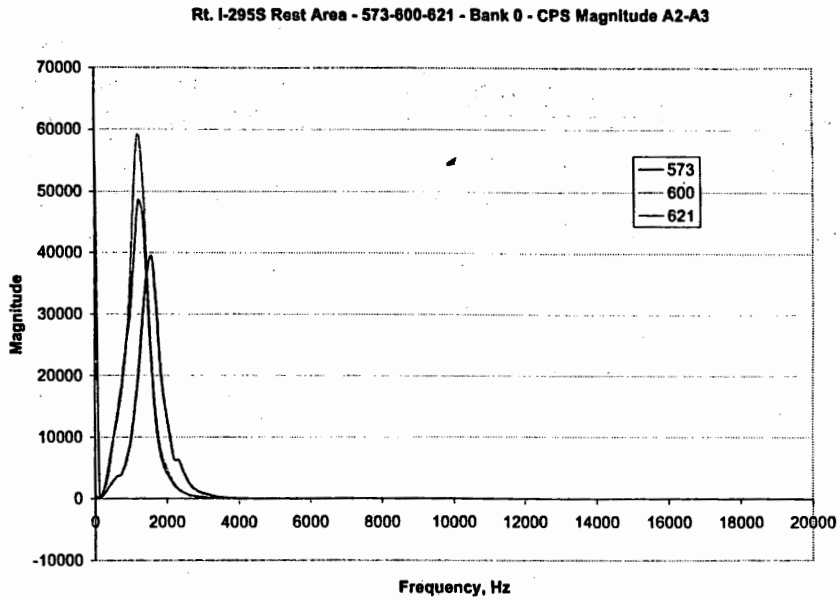


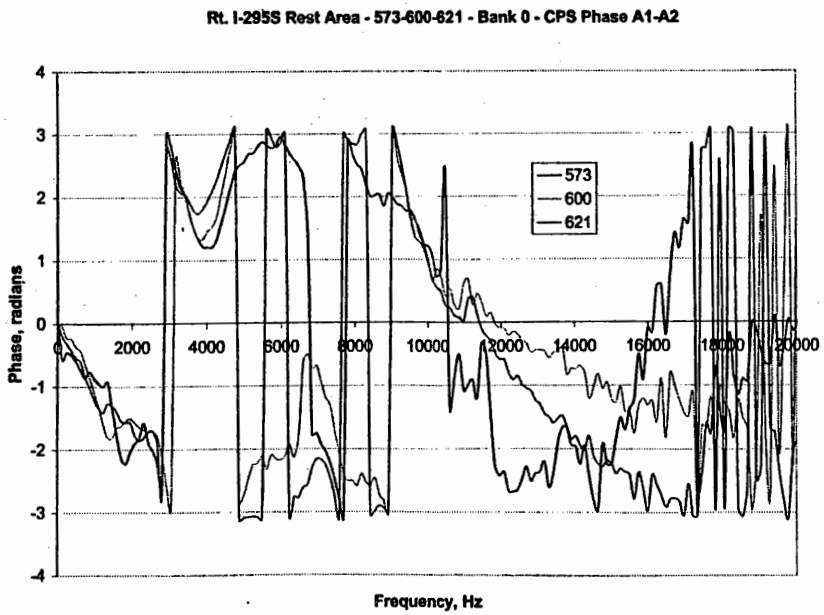


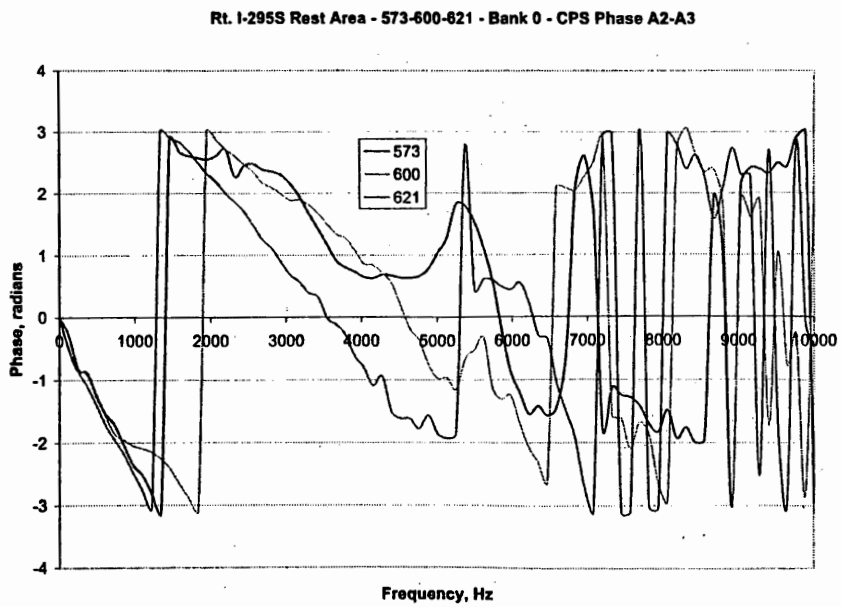


Figure 67. Cross power spectra for Bank 0 - repeated testing at close points.

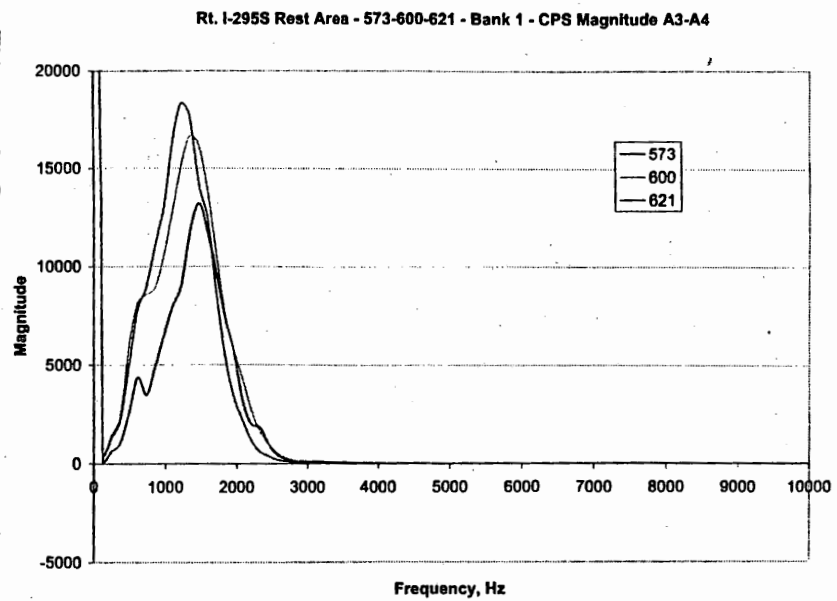


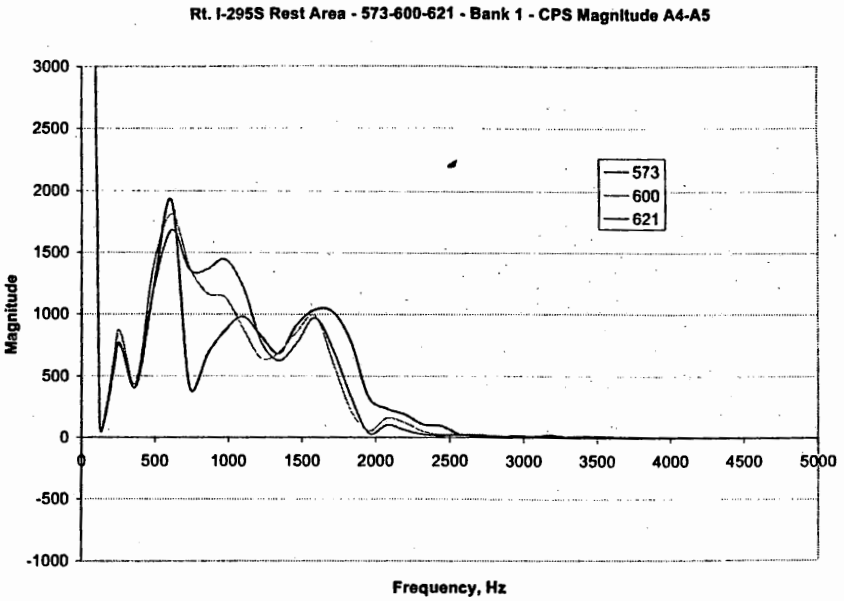


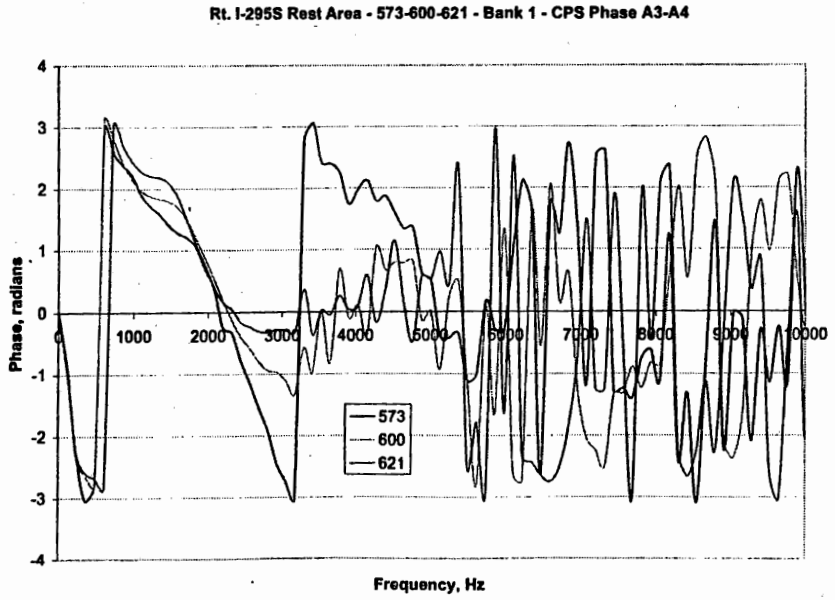


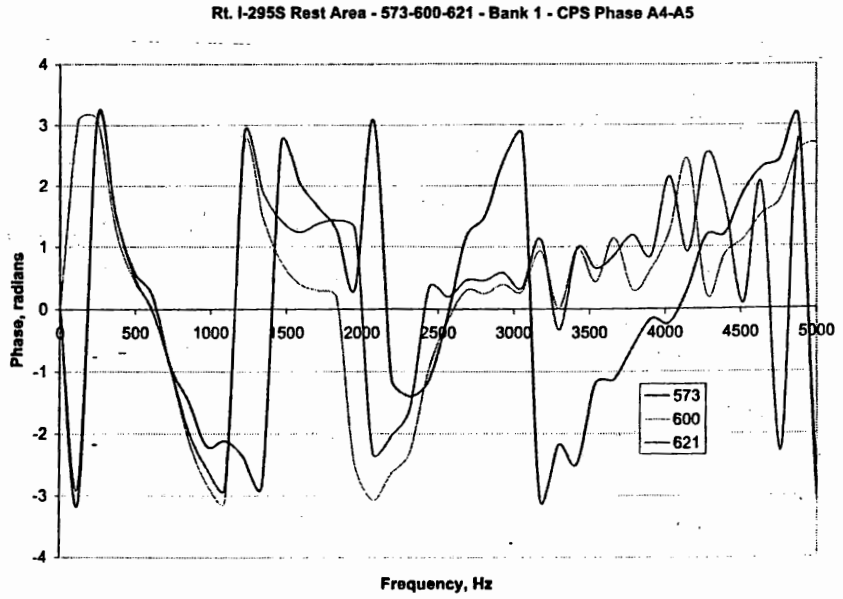


Figure 68. Cross power spectra for Bank 1 - repeated testing at close points.

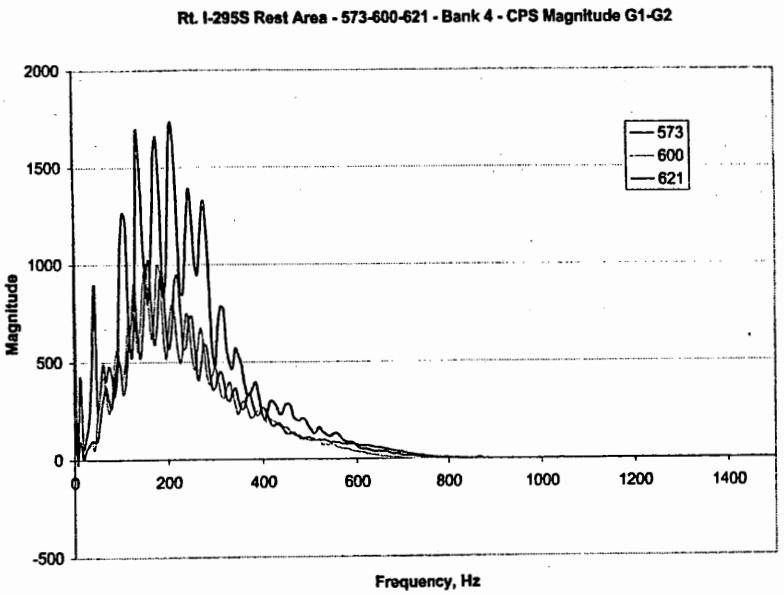


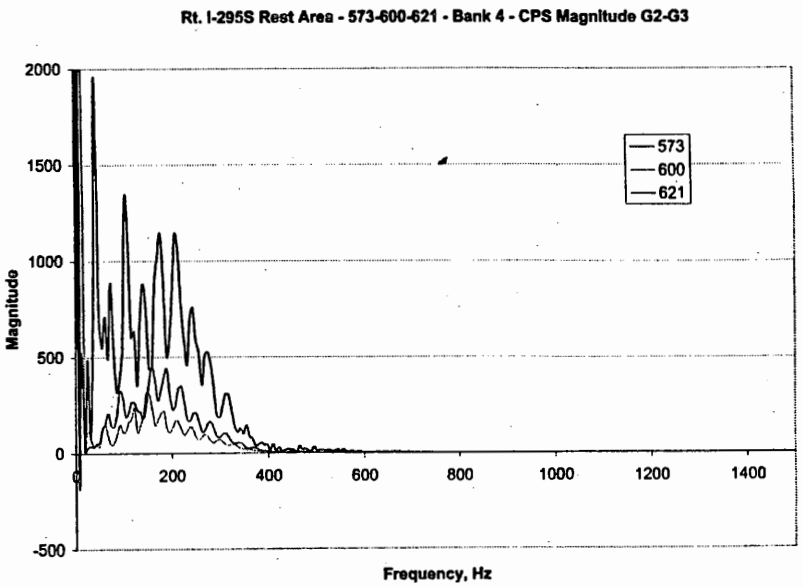


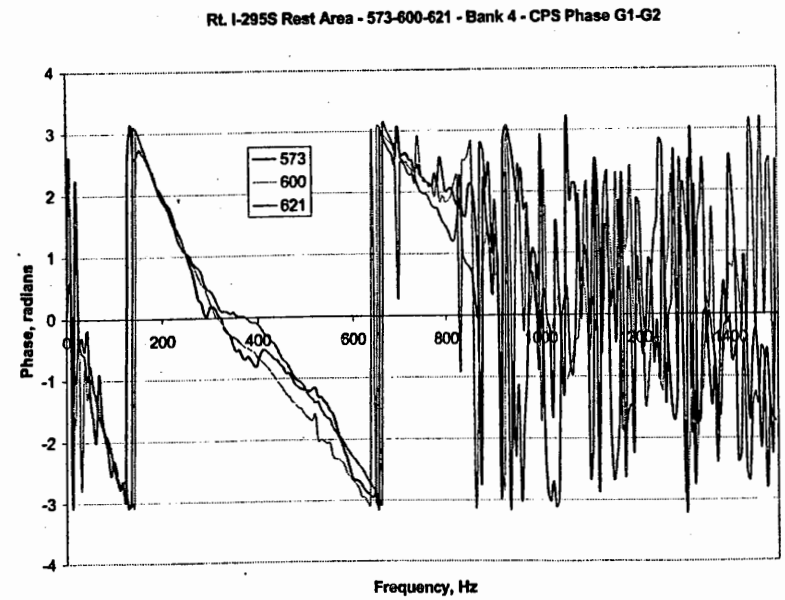


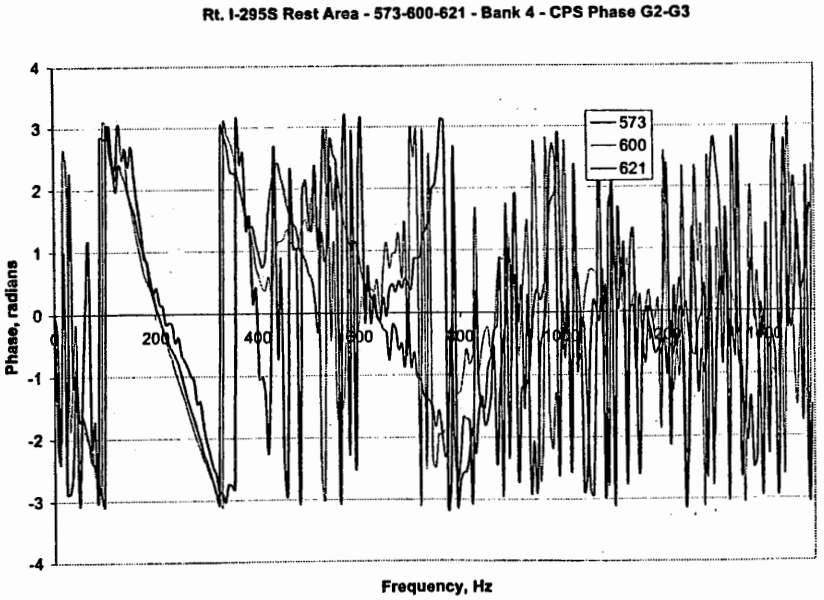


Figure 69. Cross power spectra for Bank 4 - repeated testing at close points.

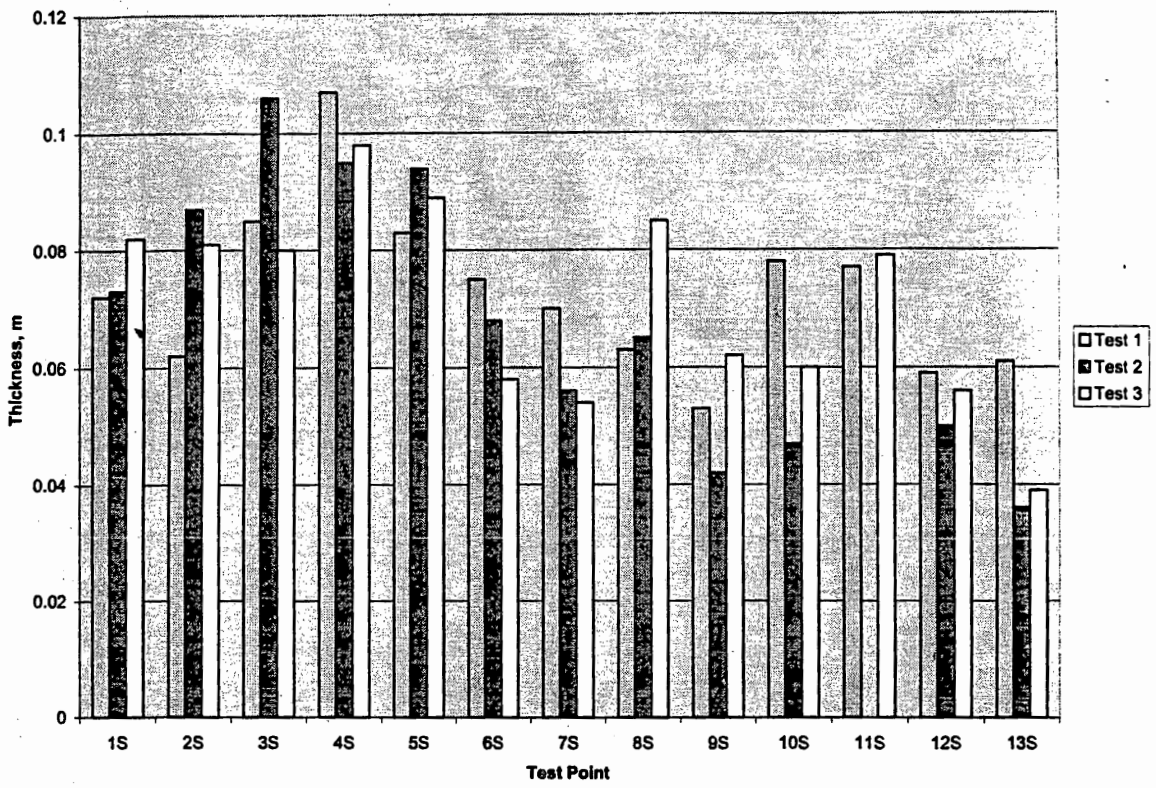


Figure 70. Paving layer thickness for the south bound area from the second series tests.

**Rt. 1 in North Brunswick Testing**

A 330 m section of Rt. 1 in North Brunswick was evaluated by the SPA (Figure 76). The section consisted of three subsections with different base materials, as described in Figure 77. Section A had a 100% dense graded aggregate (DGA) base, section B a 100% recycled asphalt concrete (RAP) base, and Section C had as a base a 75% DGA and 25% RAP blend. The objective of the evaluation was to determine properties of RAP and RAP mixed with DGA bases, to a traditionally used DGA base. The evaluation was done on a 7 m wide test section. The section comprises a 3.6 m wide right shoulder and a 3.4 m wide slow lane. Both the shoulder and the slow lane were tested at 25 locations each, in 15 m intervals. The shoulder and the slow lane have an identical design profile consisting of a 5 cm bituminous concrete surface course, a 17.5 cm bituminous stabilized base course, a 15 cm base course, and a 20 cm I-3 subbase course. There was parallel testing by a FWD (Figure 78), however those results are not presented herein.

Elastic moduli of surface and base AC courses, and of the base, are shown in Figure 79. Backcalculated moduli for the three sections are in the same range. However, due to a large data dispersion, a comparison does not provide a clear answer on how the sections containing RAP compare to the DGA sections. It seems that a problem similar to the problem encountered during Rt. I-295 testing, difficulty with evaluation of properties of a thin base layer, or a base layer with a low rigidity contrast with the subbase or the

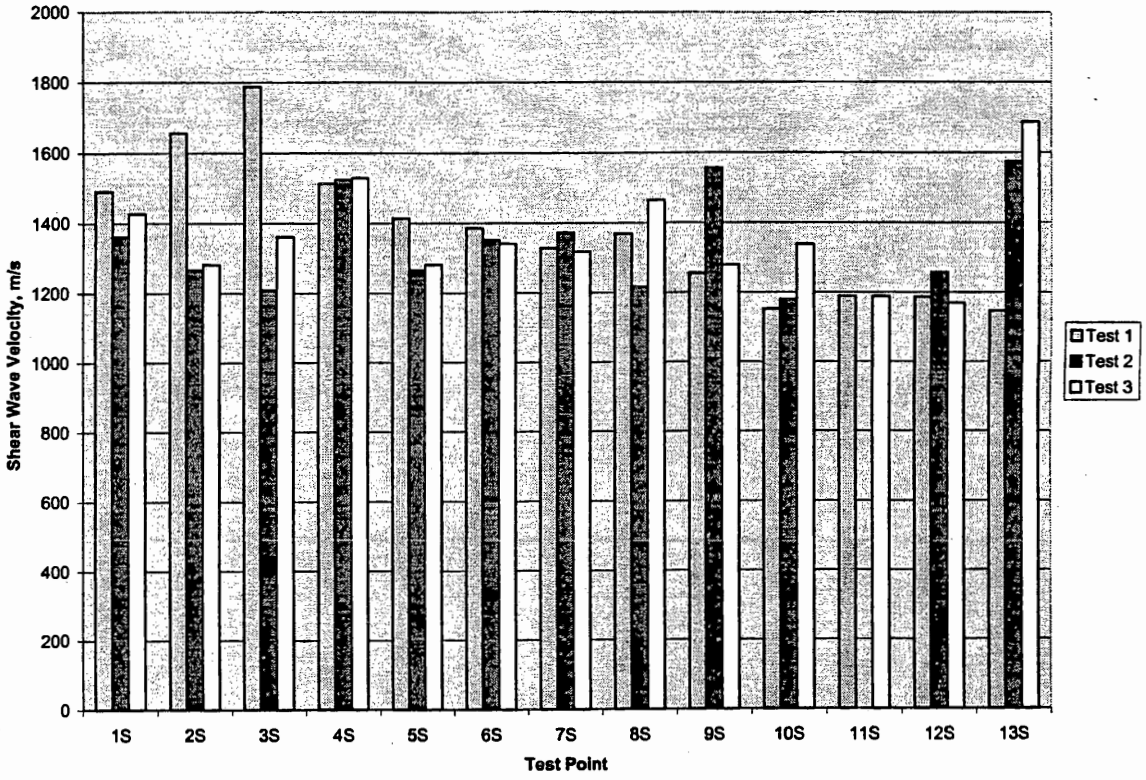


Figure 71. Shear wave velocity of the paving layer for Series 2 tests.

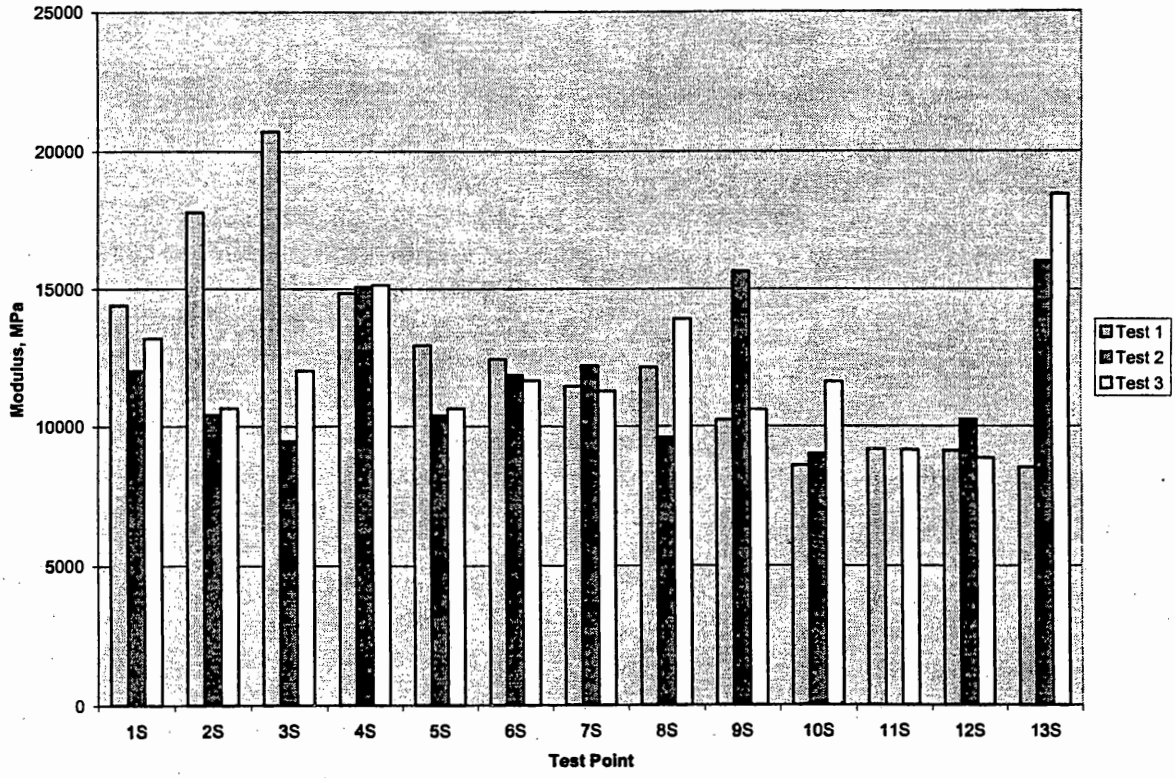


Figure 72. Young's modulus for the paving layer for the Series 2 tests.

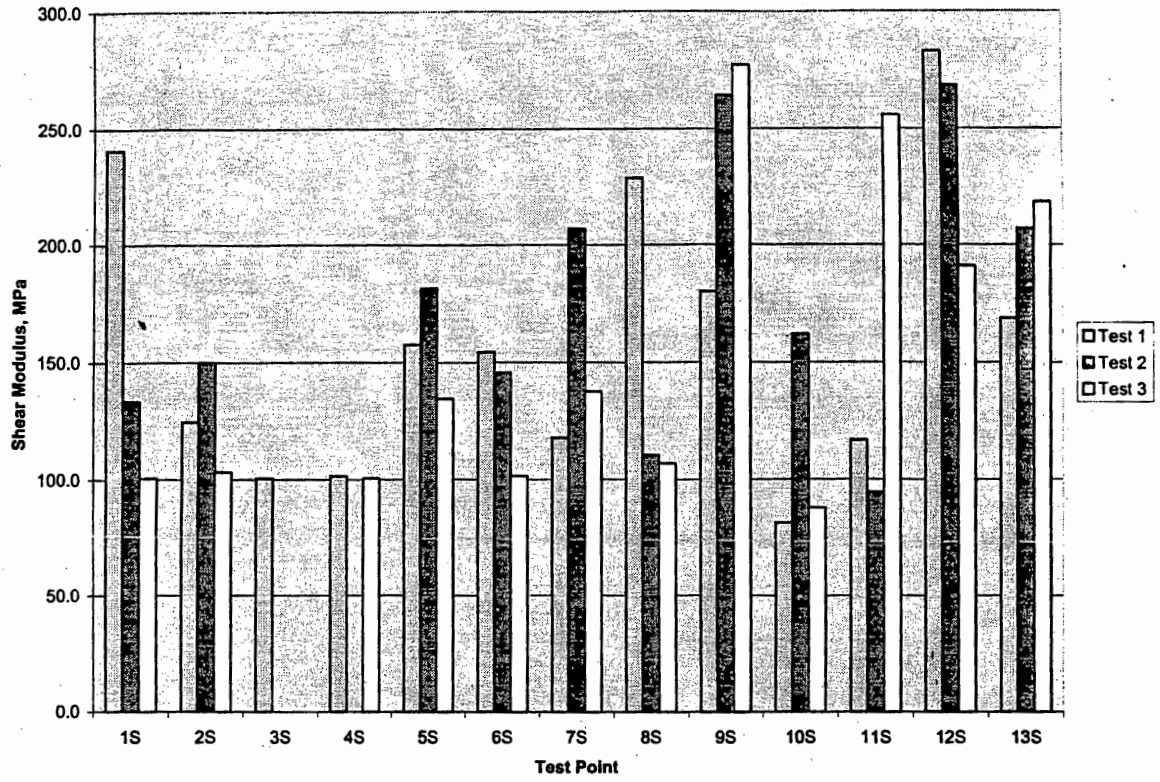


Figure 73. Base layer shear modulus for Series 2 tests.

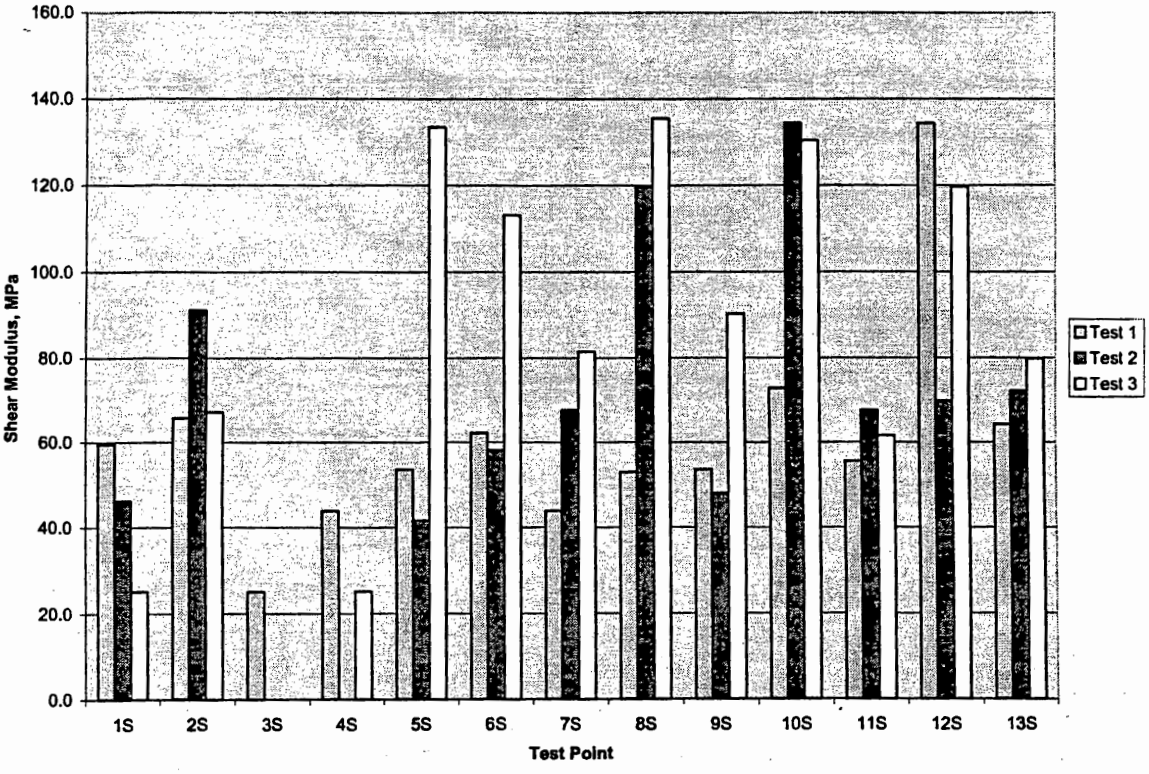


Figure 74. Subgrade shear modulus for Series 2 tests.

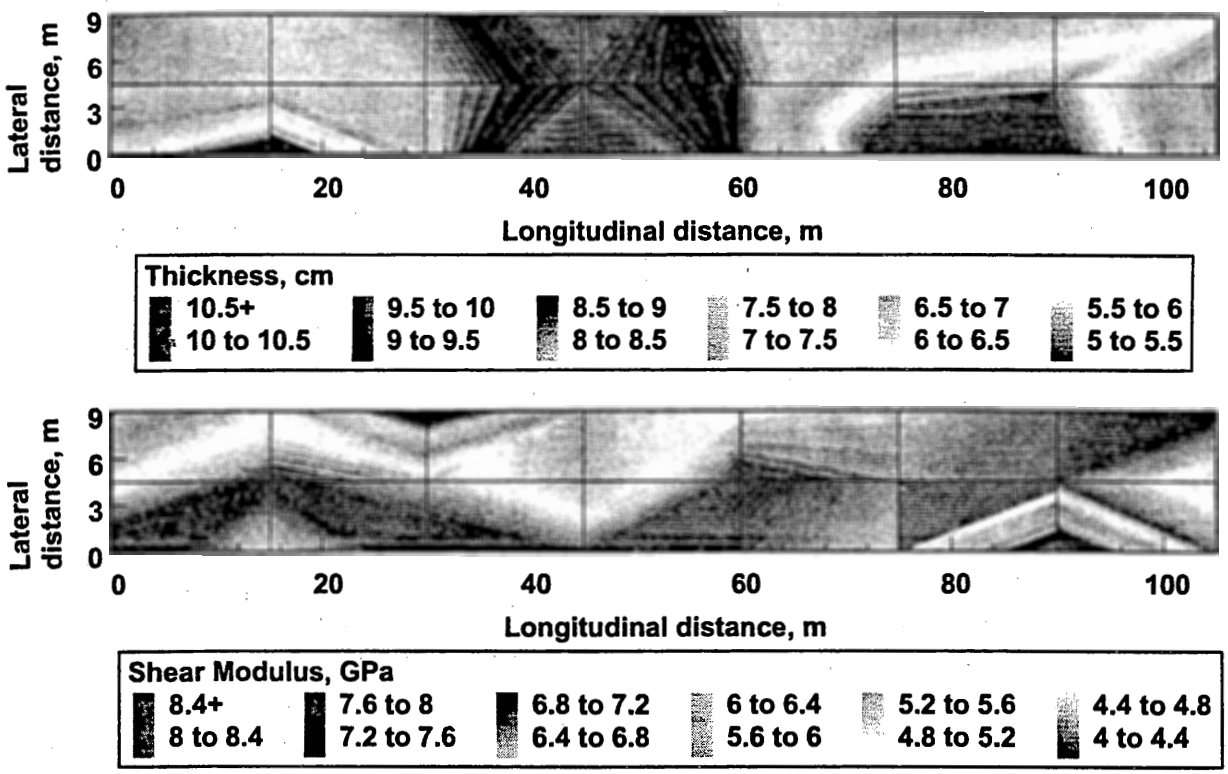


Figure 75. Paving layer thickness (top) and shear modulus (bottom) distributions from Series 3 tests on the south bound rest area.

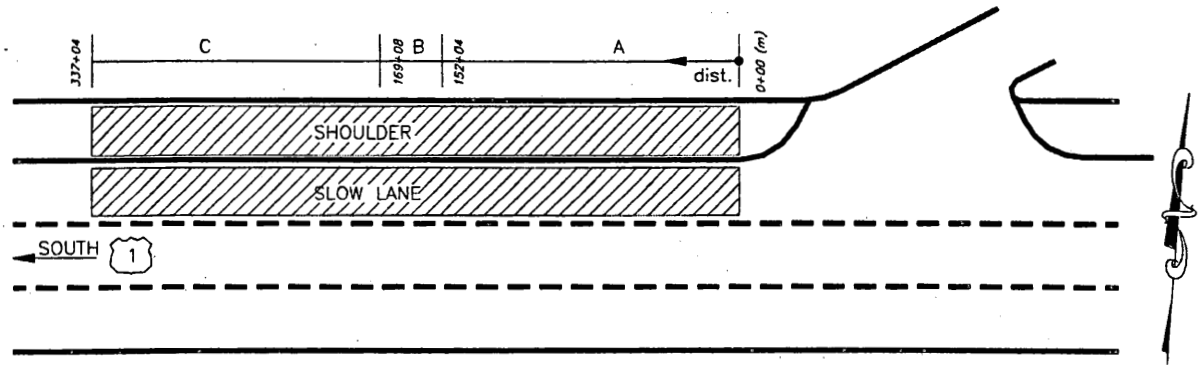


Figure 76. Schematic of the test section.

subgrade, is encountered again. The shear modulus of the subgrade is evaluated by the impulse response (IR) technique, because the IR obtained modulus had much a smaller dispersion then the modulus backcaclulated from the SASW test. Typical backcalculated pavement profiles for the shoulder and slow lane are shown in Figure 80. The IR obtained modulus for both the shoulder and the slow lane is shown in Figure 81. Overall, there is a good agreement between a backcalulated and design thickness of a combined surface and base AC, and the design thickness of the same.

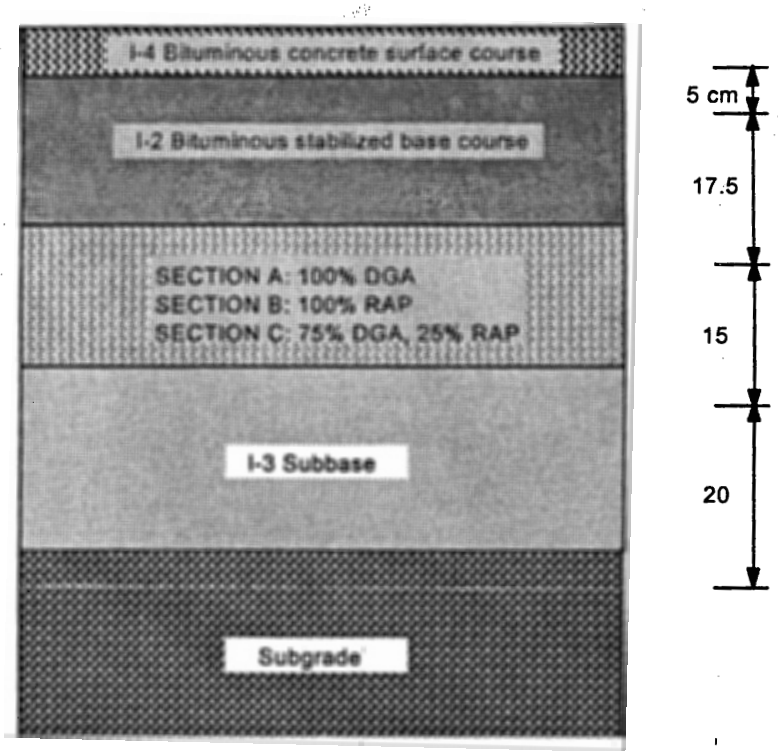


Figure 77. Rt. 1 pavement profile.

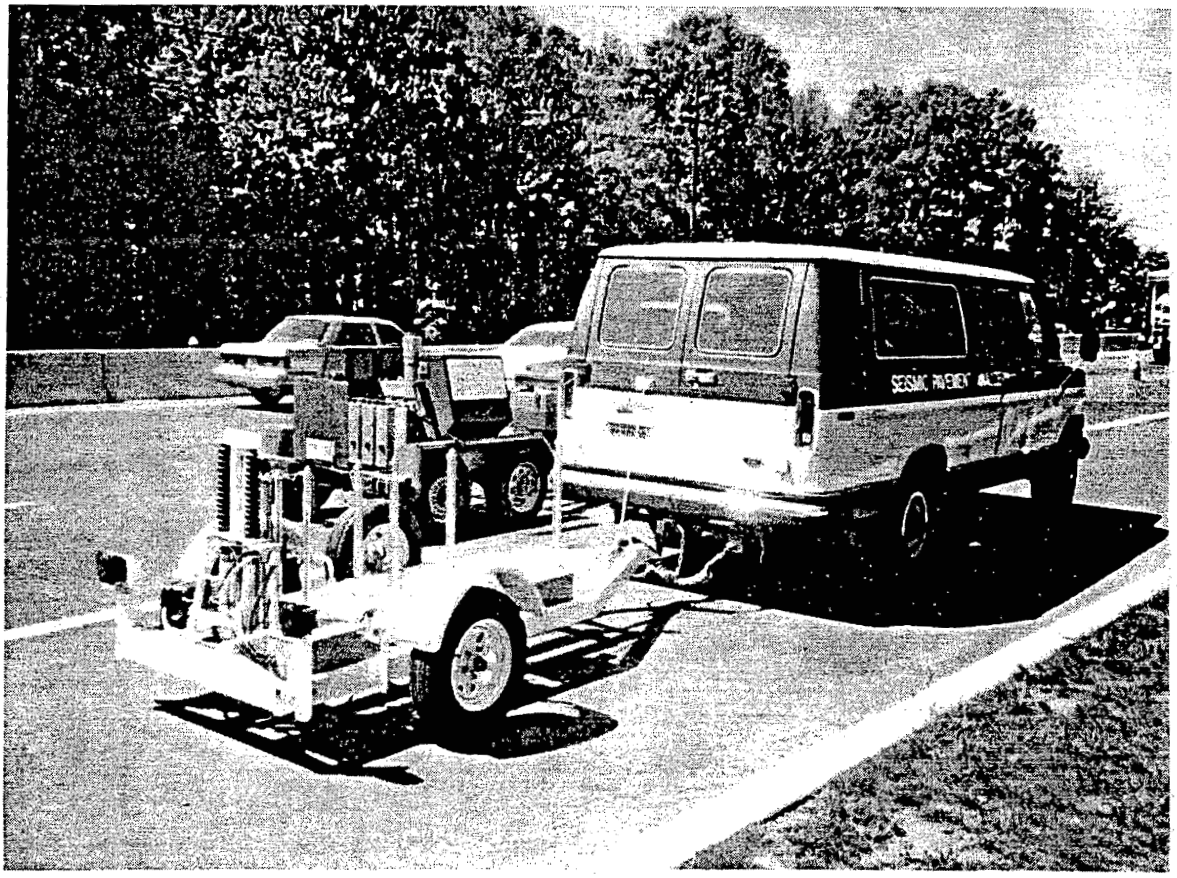

Figure 78. SPA (front) and FWD (back) testing on Rt. I-1S in North Brunswick.

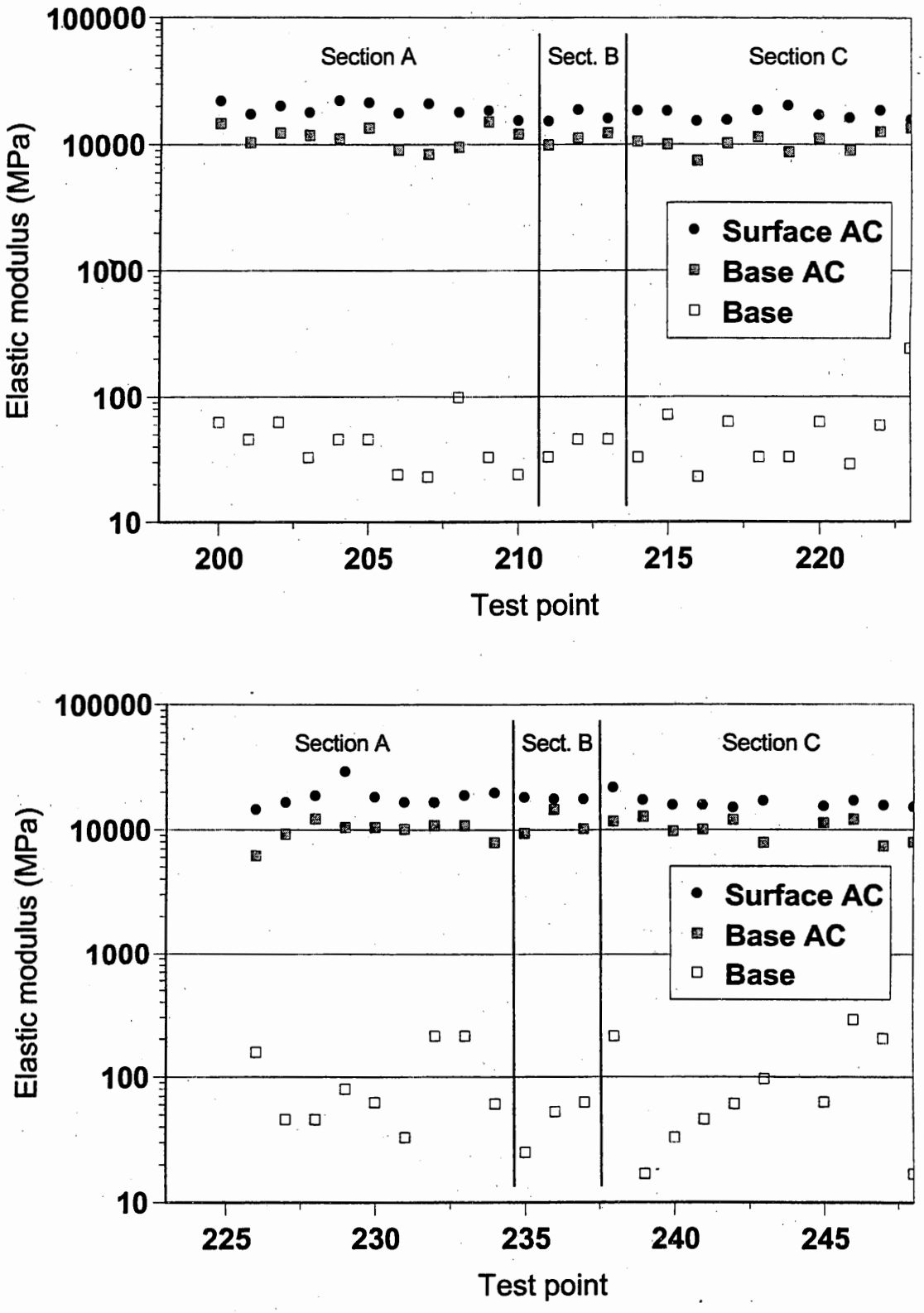


Figure 79. Elastic modulus for the paving and base layers. Shoulder (top), slow lane (bottom).

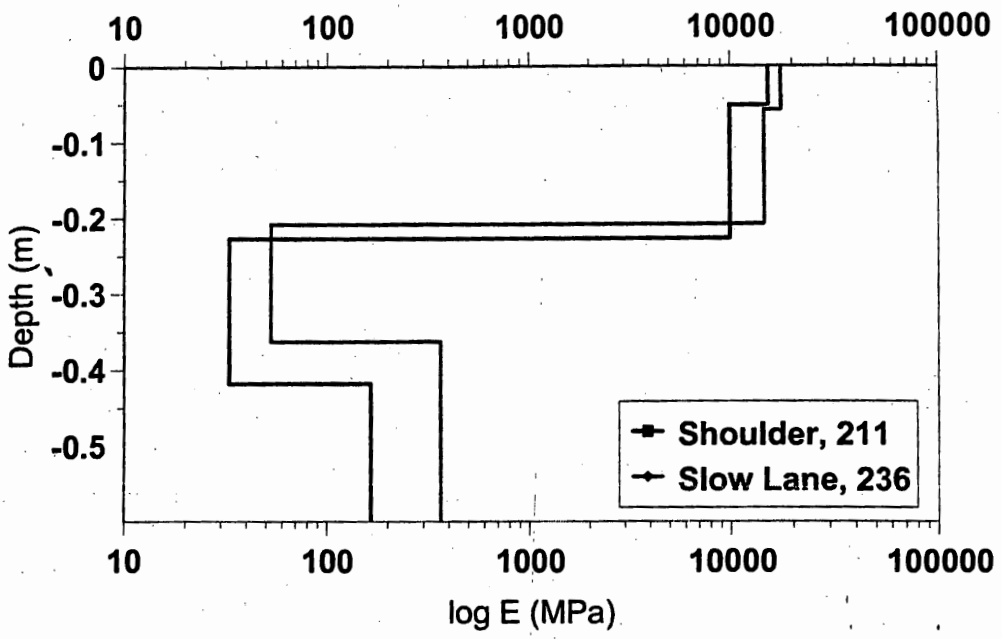


Figure 80. Typical backcalculated pavement profiles.

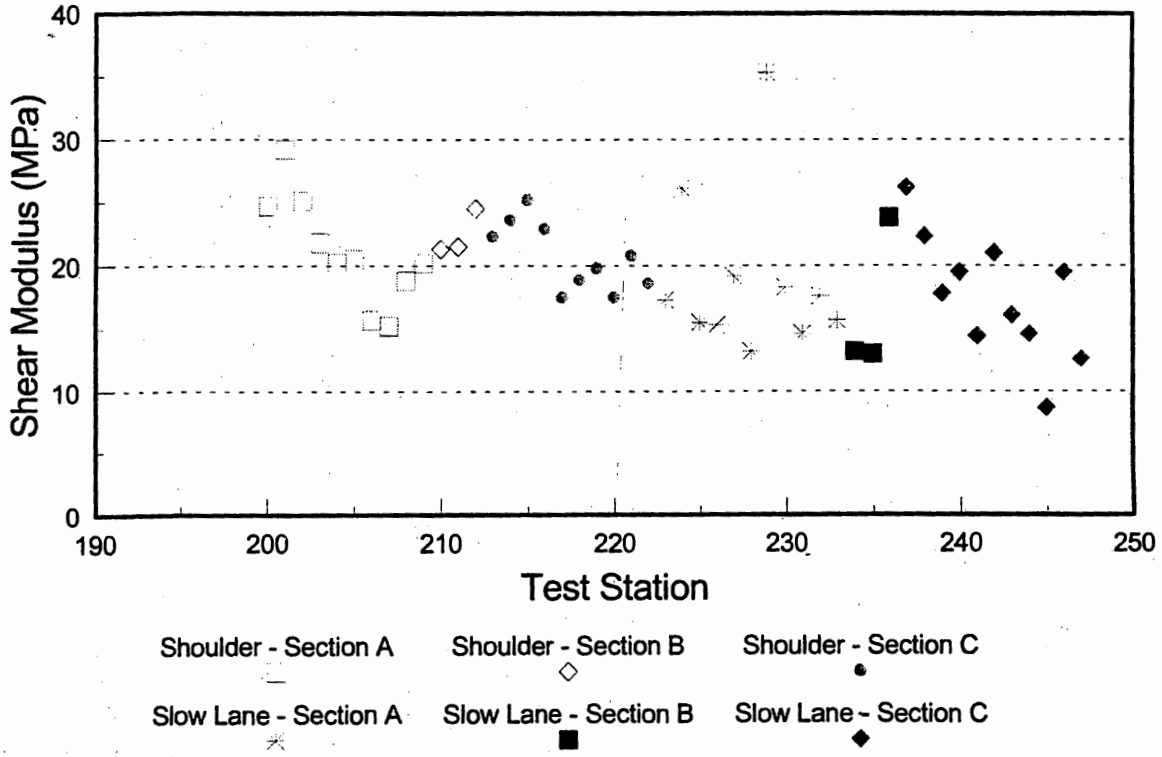


Figure 81. Shear modulus of the subgrade from the IR test.

## OTHER APPLICATIONS OF SPA

The SPA has potential for application in problems of detection of defects in pavements, like voids under rigid pavements and delamination in PCC overlays.[40,41] This section provides a description and results of application of the SPA in verification of effectiveness of rigid pavement undersealing by Impulse Response method, and evaluation of joint transfer on rigid pavements.

### Verification of Pavement Undersealing on Rt. I-287S

The IR method was implemented in evaluation of effectiveness of pavement undersealing on a section of interstate expressway Rt. I-287S South of Mahwah (between mile posts 53 and 50), New Jersey. The pavement is a 225 mm reinforced concrete pavement, on a non-stabilized open graded (NSOG) aggregate base. Since a significant settlement of some of the slabs and loss of support under joints was observed, New Jersey Department of Transportation (NJDOT) decided to implement a slab undersealing program. The program involved injection of a polyurethane foam under weakened joints, and under entire slabs where an overall slab settlement was observed. The injection process is illustrated in Figure 82. A number of 2.5 cm diameter holes are drilled through a slab (top left), an injection nozzle inserted into it (bottom) and the foam from a tank (top right) injected until a certain pressure is achieved. The foam sets within few minutes, so that the roadway can be reopened for traffic within 15 minutes. Penetration of a hardened foam into the NSOG layer can be observed on the left side of the core shown in Figure 83.

The undersealing verification program was done by IR testing using the SPA and by a Falling Weight Deflectometer (FWD). The testing was conducted on a slow lane section between mile posts 55 and 53, and on a fast lane section between mile posts 52 and 51. On the slow lane section of the roadway, the IR testing was done both prior and after the undersealing. On a fast lane section the testing was conducted only after the undersealing was completed. The testing involved evaluation of the shear modulus of the subgrade (subgrade modulus) at three points, two joints and the midpoint, of each of the 23.5 m long pavement slabs. The SPA testing at a joint, where both the low frequency hammer and the first geophone, as described in the section on the IR method, are placed within 30 cm of a joint, is shown in Figure 84 and the top of Figure 85. At the end of the slab the geophone would be closer to the joint, at the beginning of the slab the hammer. Testing at the middle of a slab is shown at the bottom of Figure 85. As in any other SPA testing, it took about a minute to complete testing at a single point. (If the testing is conducted for the sole purpose of IR testing, the test time can be reduced to about 30 seconds.)

#### IR Testing of the Slow Lane Starting at MP 55

A schematic of the slow lane section is shown in Figure 86. The first testing was conducted on April 25, 2001, before slab undersealing. The testing encompassed, for the most of the slabs, evaluation of the subgrade modulus at three slab points: at both joints and the slab midpoint. Several short slabs next to the bridges were tested just at at joints. The first testing was conducted on 71 slabs. The second testing was conducted on April 30, on the

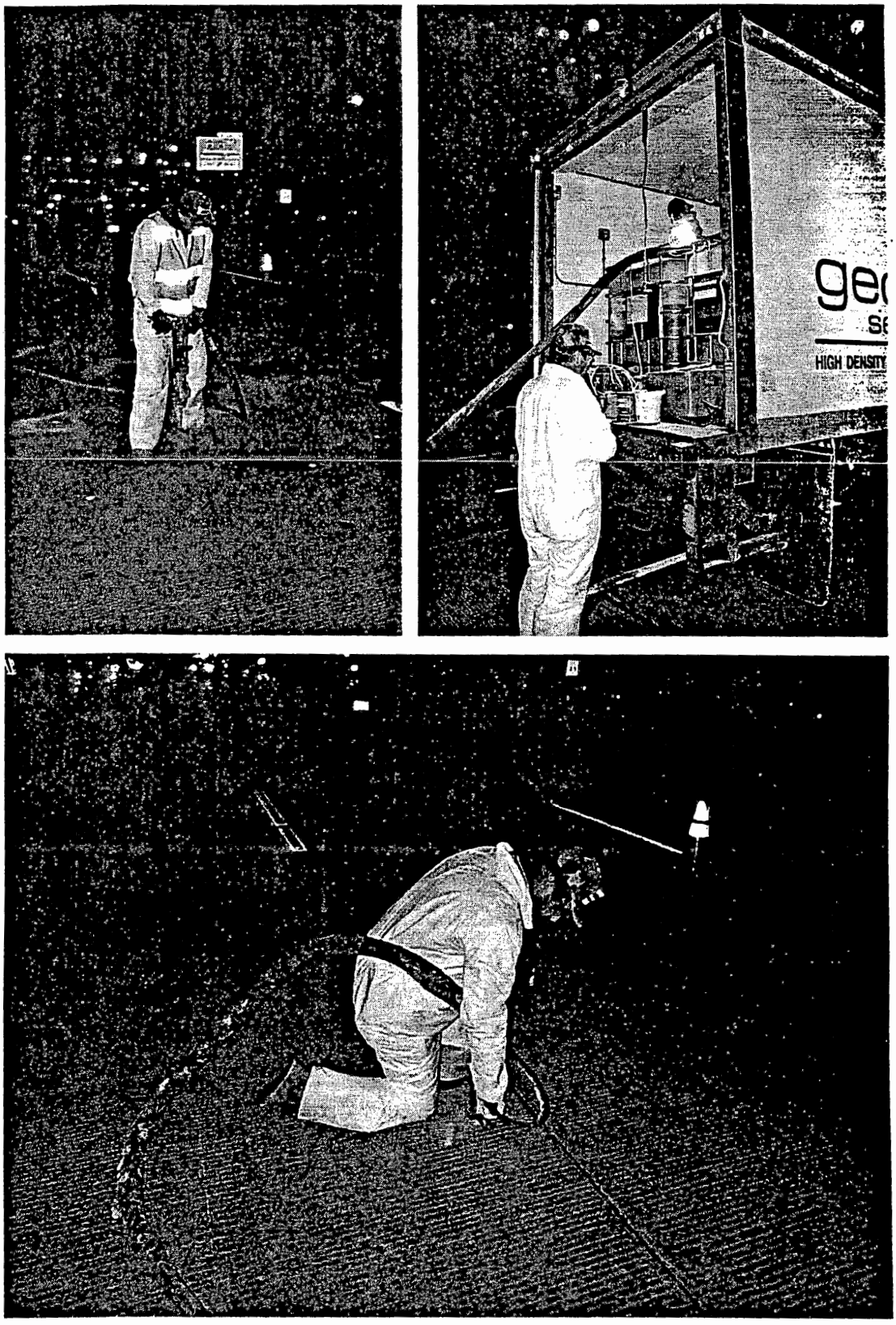


Figure 82. Pavement undersealing: drilling (top left), grout tanks (top right), and injection (bottom).

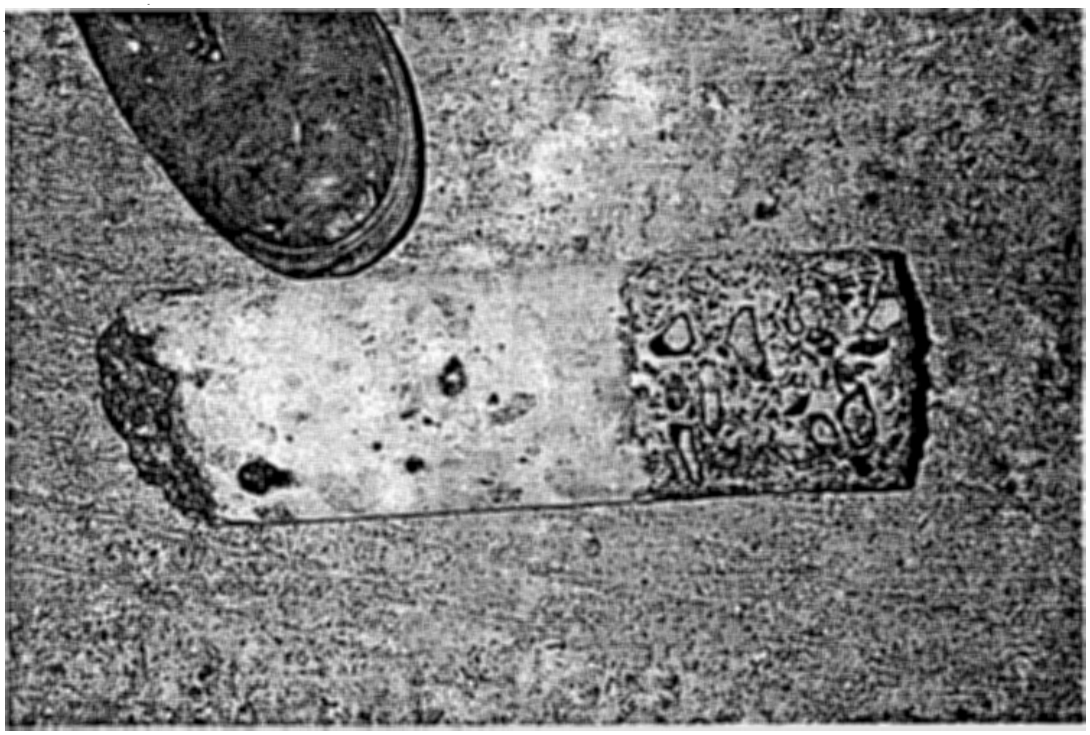

Figure 83. Core taken from a grouted joint.

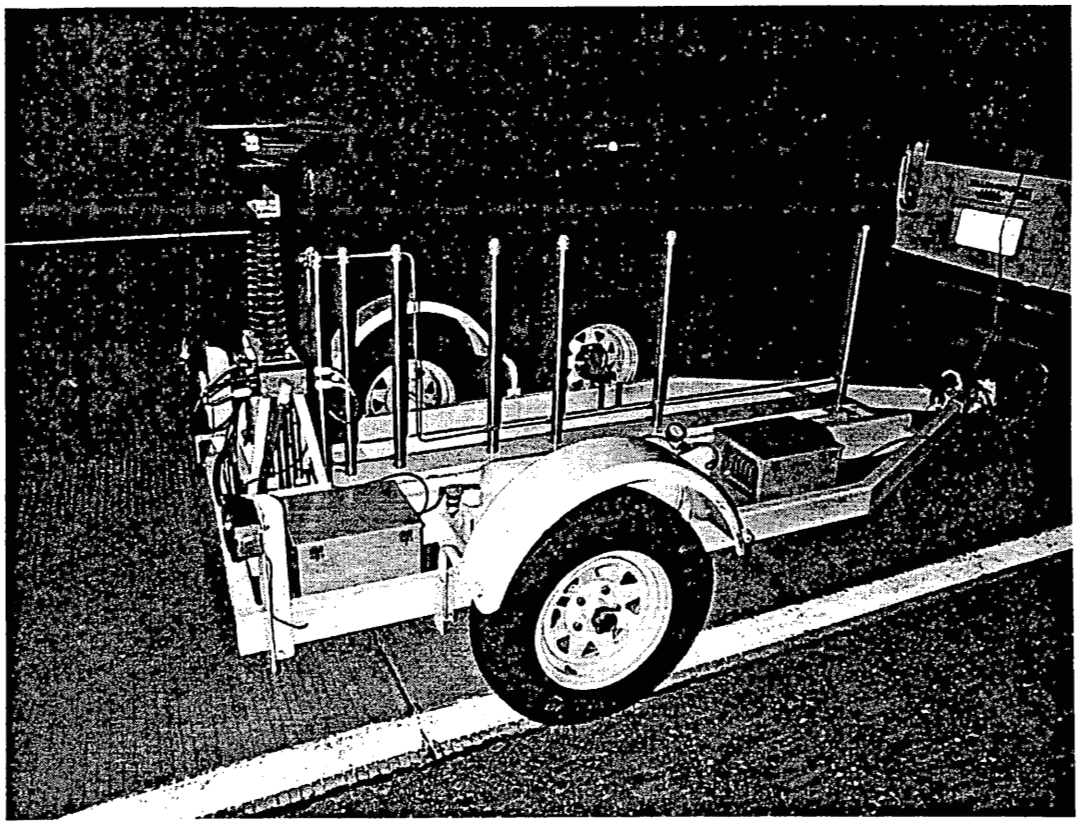

Figure 84. SPA in position for testing at a joint.

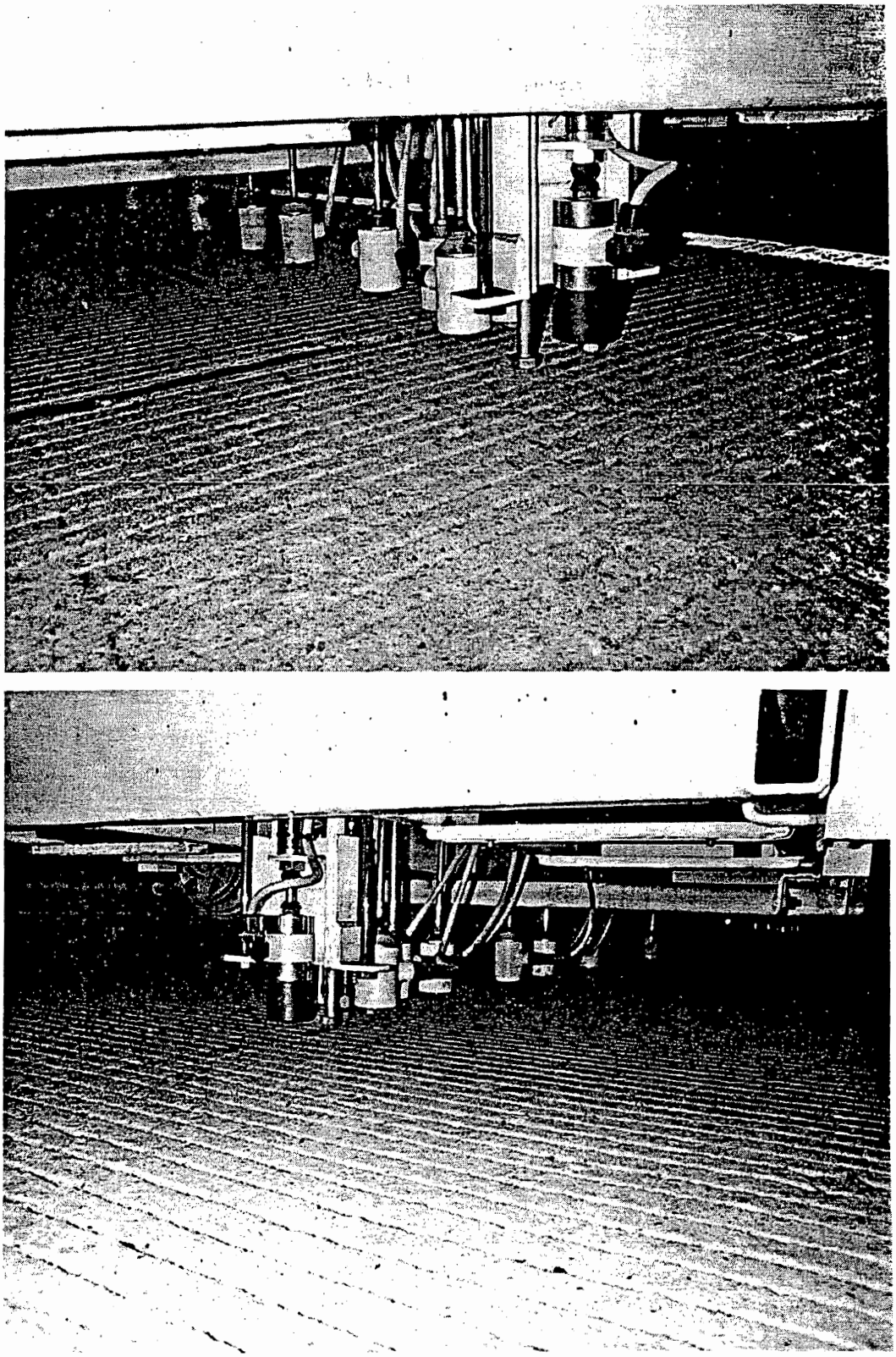

Figure 85. Testing at a joint (top) and the middle of the slab (bottom).

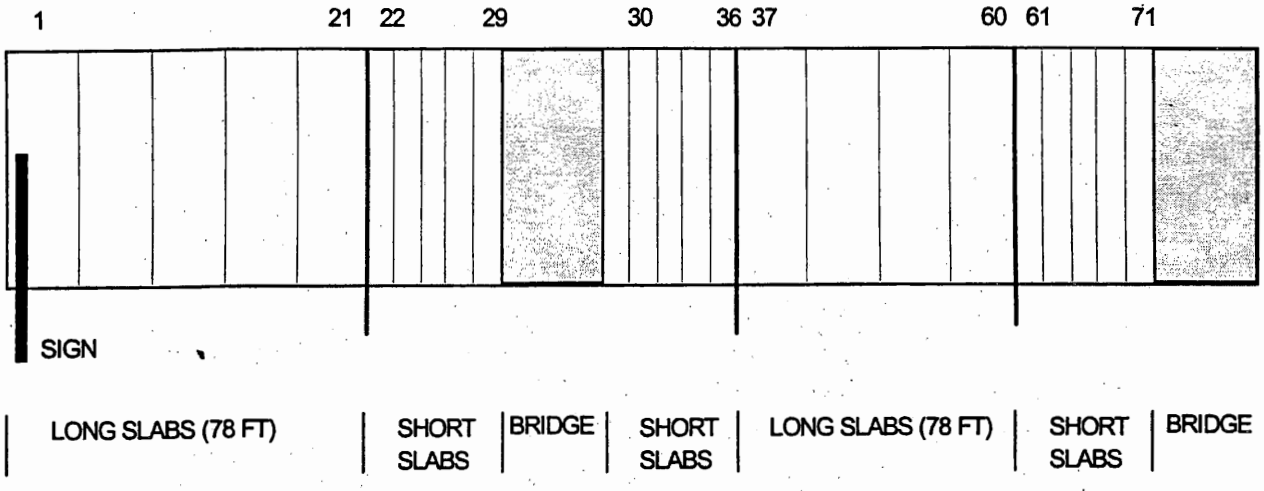


Figure 86. Schematic of the slow lane test section.

first 41 slabs, since only the first 29 slabs had been grouted.

Comparison of moduli of subgrade reaction from the before and after grouting testing at both joints is provided in Figure 87, while for testing at the middle of the slab in Figure 88. The subgrade modulus, for the first testing, for the middle of the slab was in a range from about 80 to 160 Mpa. On the other hand a number of joints had extremely low moduli values, from 5 to 40 Mpa. A significant increase in the modulus due to joint grouting can be observed for joints of slabs 3 to 27. (Only 3 to 20 are presented in the figures.) The increase is in a range from 100 to almost 3000% for joints with the lowest modulus before grouting. Except for a few joints, the subgrade modulus at joints rose to a range of 40 to 130 Mpa. The ratio of the two subgrade moduli for slab joints is summarized in Figure 89, where S stands for the starting joint and E for the end point of the slab. The subgrade modulus at slab midpoints was typically in a range of 60 to 160 Mpa. Some differences in values before and after joint grouting can be attributed to redistribution of load due to slab grouting, due to partial slab jacking under joints and a difference in the test point location. Slight differences in moduli for slabs 30 to 41 for the two series of tests, not presented herein, are attributed to slightly different test point positions. For the rest of the slabs tested, slabs 30 to 71, the modulus at joints is from less than 20 to about 40 Mpa. The damping ratio was evaluated for all testing points. However, the damping ratio did not come out as such a clear indicator of the effectiveness of grouting as the subgrade modulus.

## IR Testing of the Fast Lane Starting at MP 52

Testing of 33 slabs of the fast lane was conducted on April 30, 2001, after a certain number of slab joints was undersealed. The slabs were also tested at three points. Overall, the subgrade modulus was significantly lower than for the slow lane section. The modulus for the most points varied between 20 and 80 Mpa, as shown in Figure 90. The first ten slabs were not grouted, as can be clearly observed in the joint moduli values that ranged between 5 and 25 MPa in Figure 90. The observation is that the modulus at slab midpoints for these slabs is equal to or higher than at joints. For the most of slabs 11 to 31 the subgrade modulus at grouted joints takes significantly higher values, an increase to values,

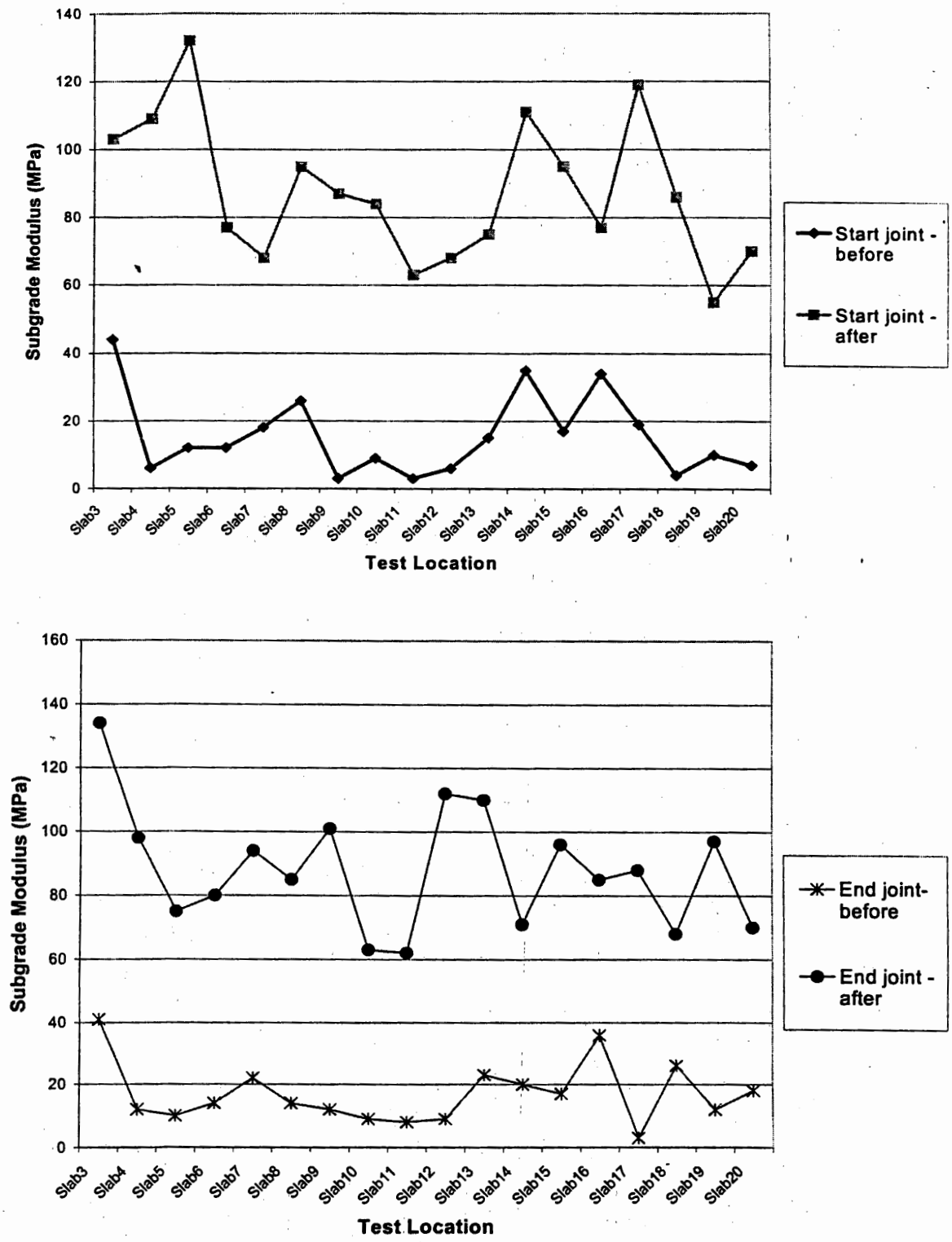


Figure 87. Subgrade modulus at the start (top) and end (bottom) joints before and after grouting -slow lane.

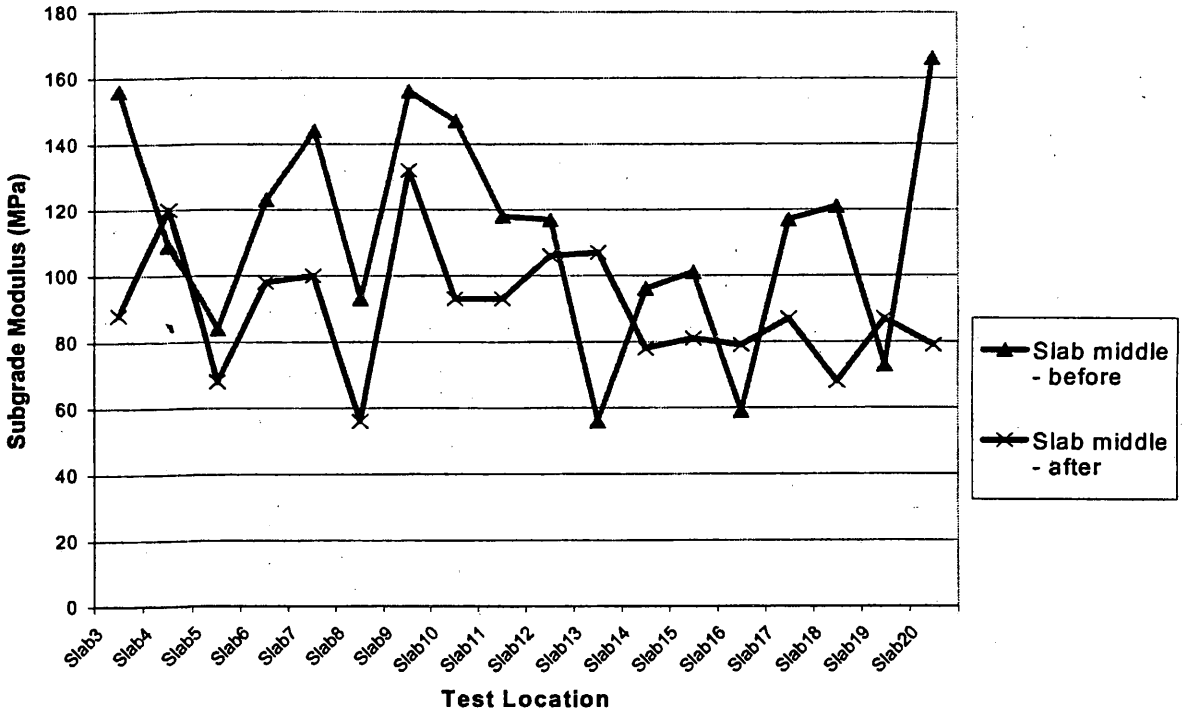


Figure 88. Subgrade modulus at slab midpoints before and after grouting - slow lane.

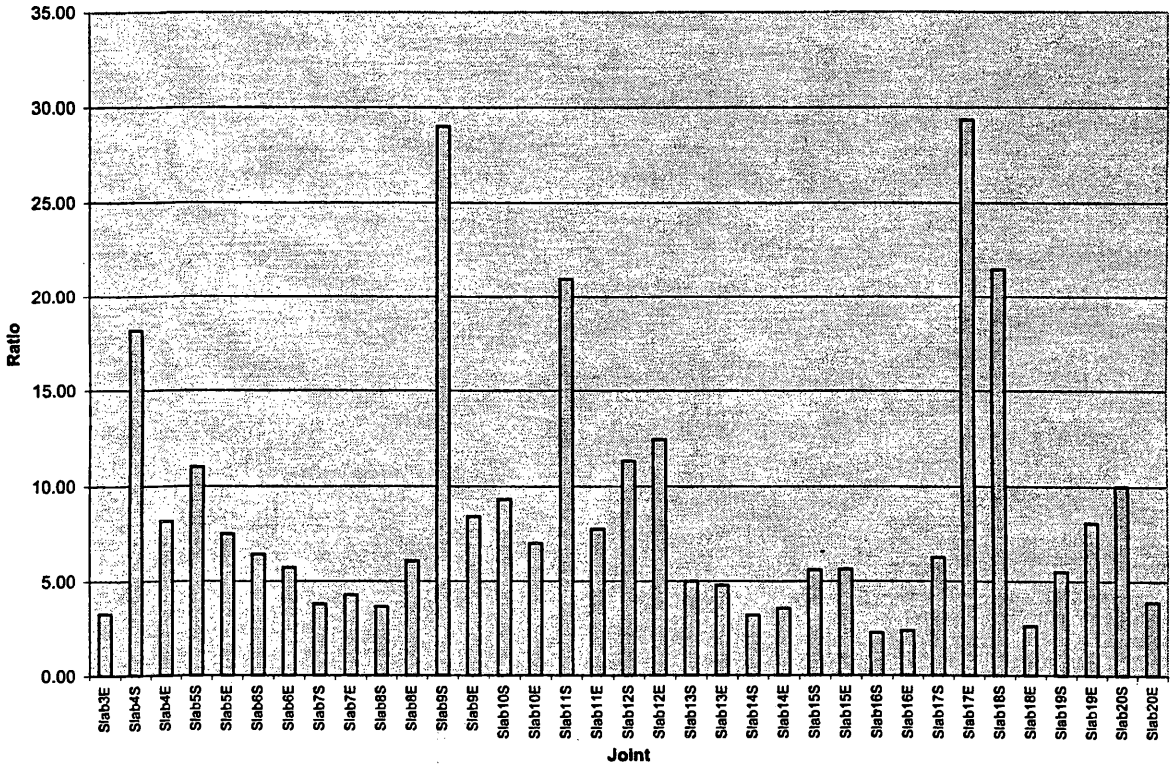


Figure 89. Ratio of subgrade moduli before and after grouting.

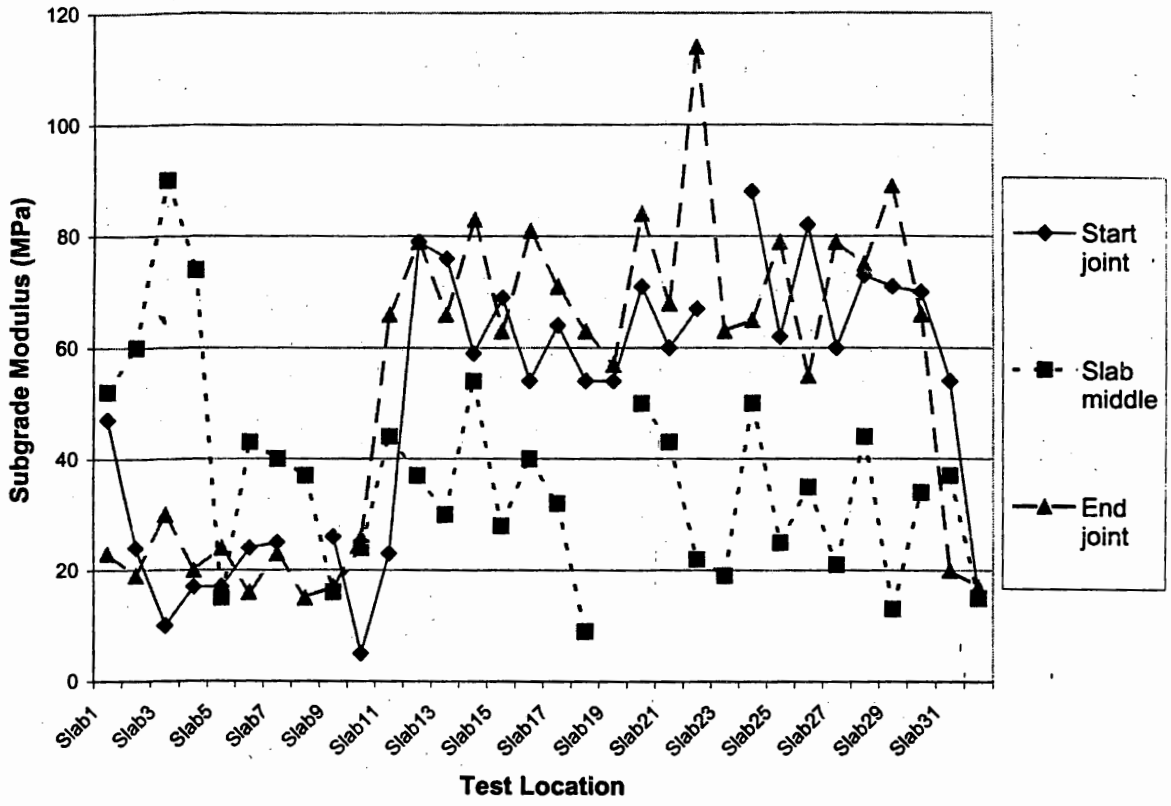


Figure 90. Subgrade modulus for the fast lane section.

in general, from 55 to 90 MPa. Interestingly, the modulus at joints took significantly higher values than the modulus at midpoints, raising a question of a possible slab jacking effect at joints due to grout injection under a too high pressure.

**Evaluation of Joint Load Transfer**

A section of Rt. 4E near Paramus, New Jersey, was tested using the SPA on September 4, 1996. The pavement was rigid (concrete) with an AC overlay. The thickness of the concrete base was estimated from the SPA results to be about 25 cm, and the thickness of the AC layer between 7.5 and 11 cm. There were two major objectives of the testing: to define the pavement profile in terms of elastic moduli, and to examine the feasibility of the SPA device in evaluation of the joint load transfer. Testing was done both next to a joint, identified from reflection cracking, and at the middle of a slab.

The process of the proposed evaluation procedure presented in Figure 91 is based on evaluation of the transfer function for the joint. The procedure can be explained by following the steps in Figure 92. During the joint load transfer evaluation accelerometers 1 and 2 are placed on the opposite sides of the joint, with a hammer on the side of accelerometer 1. The time histories for test 255 for the two accelerometers are shown in windows W1 and W2 of Figure 92. Significant differences between the two signals in both the amplitude and the shape of the signal can be observed. Below those, in windows W3 and W4, are time

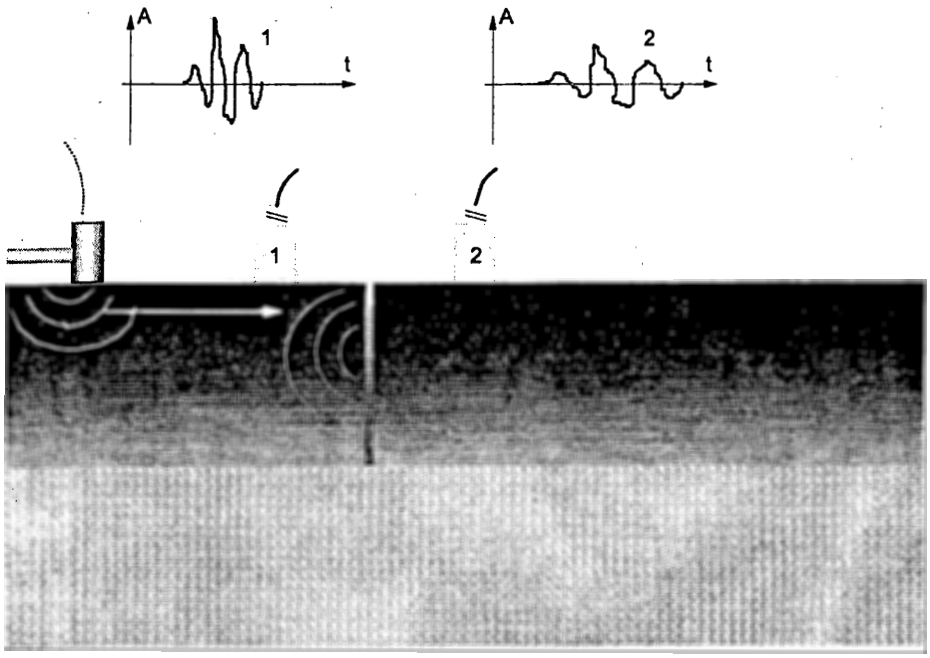


Figure 91. Joint load transfer evaluation.

histories for the same pair of accelerometers for a test 256 at the middle of the slab. While the two signals differ, the differences are less than for the joint.

The transfer function in this study is defined as the ratio of power spectral densities (auto power spectra) of the two records. The power spectral density is a measure of power of motion as a function of frequency. It is equal to the square of the spectrum of a signal divided by a half sampling rate. Windows W5 and W6 contain transfer functions for the joint and the middle of the slab, respectively, in a semi-log plot. The x-axis is frequency in Hz. Of practical interest is only the lower measurable frequency range of frequency components up to 30 kHz. It is expected that the transfer function will take lower values for the middle of the slab than for the joint, due to a poor energy transfer at the joint. This can be somewhat observed by comparing transfer function in W5 and W6. This also means that the ratio of the transfer function at the joint and the transfer function at the middle of the slab should, in general, give numbers higher than 1. This is illustrated in a linear scale in window W7, especially in a frequency range 0 to 5 kHz. It can be observed in W7 that the energy transfer at the middle of the slab is more than 10 times better than at the joint. If the ratio of these two transfer functions were 1, it would mean a perfect load transfer at the joint. The same is plotted in window W8 in a semi-log plot.

Similar trends, even though less pronounced, can be observed in the transfer functions between joint record 258 and middle of the slab records 256 and 260 in Figures 93 and 94, A very fine example of a poor joint load transfer is joint record 262. The joint transfer function for this joint was compared to middle of the slab transfer functions for records 260 and 264 in Figures 95 and 96. From a comparison of accelerograms 2 in windows W1 and W3, in both figures, it can be observed that high frequency components were filtered out in the path from accelerometer 1 to 2 across the joint. This has caused a very high transfer

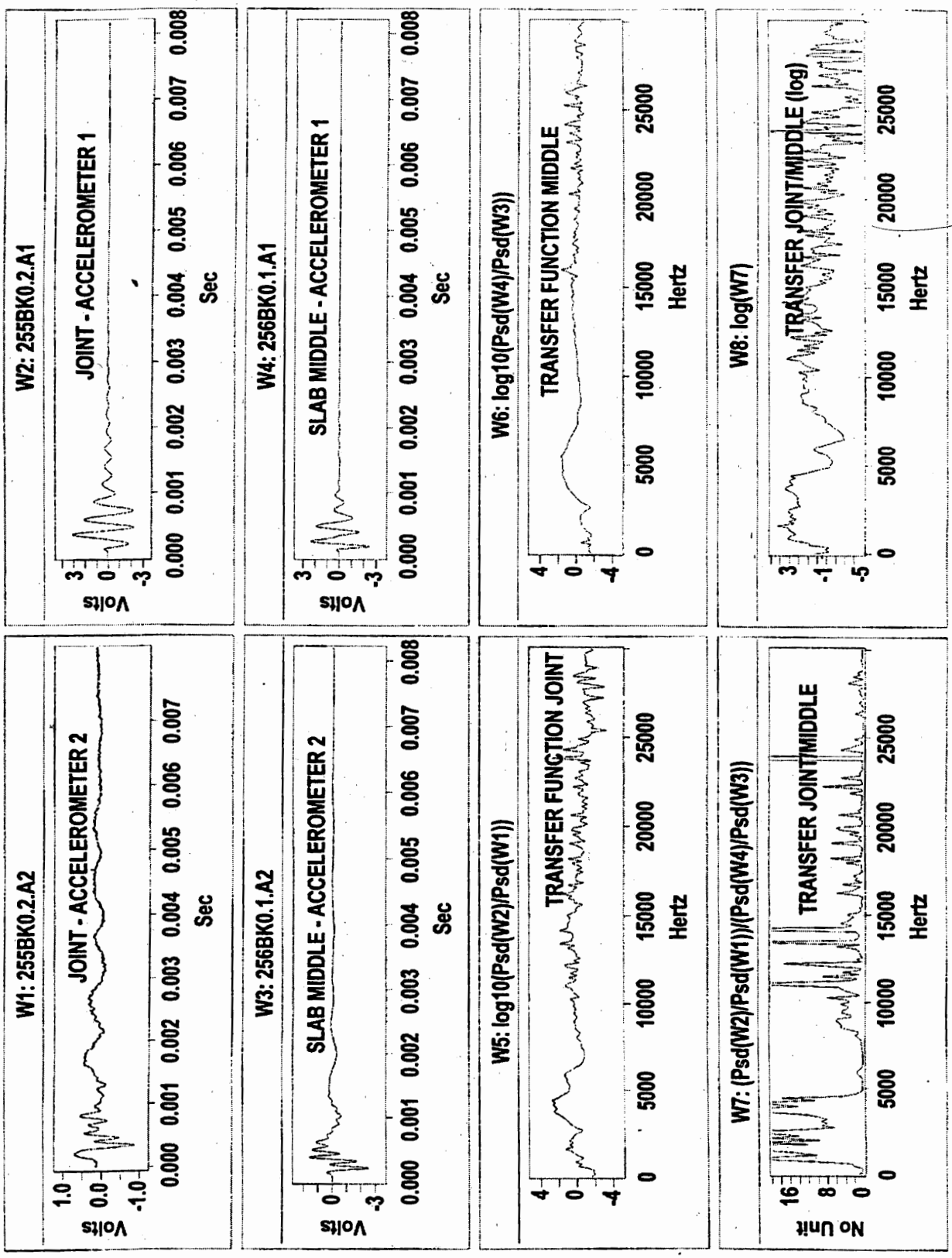


Figure 92. Evaluation of joint load transfer from joint (255) and middle of the slab (256) tests.

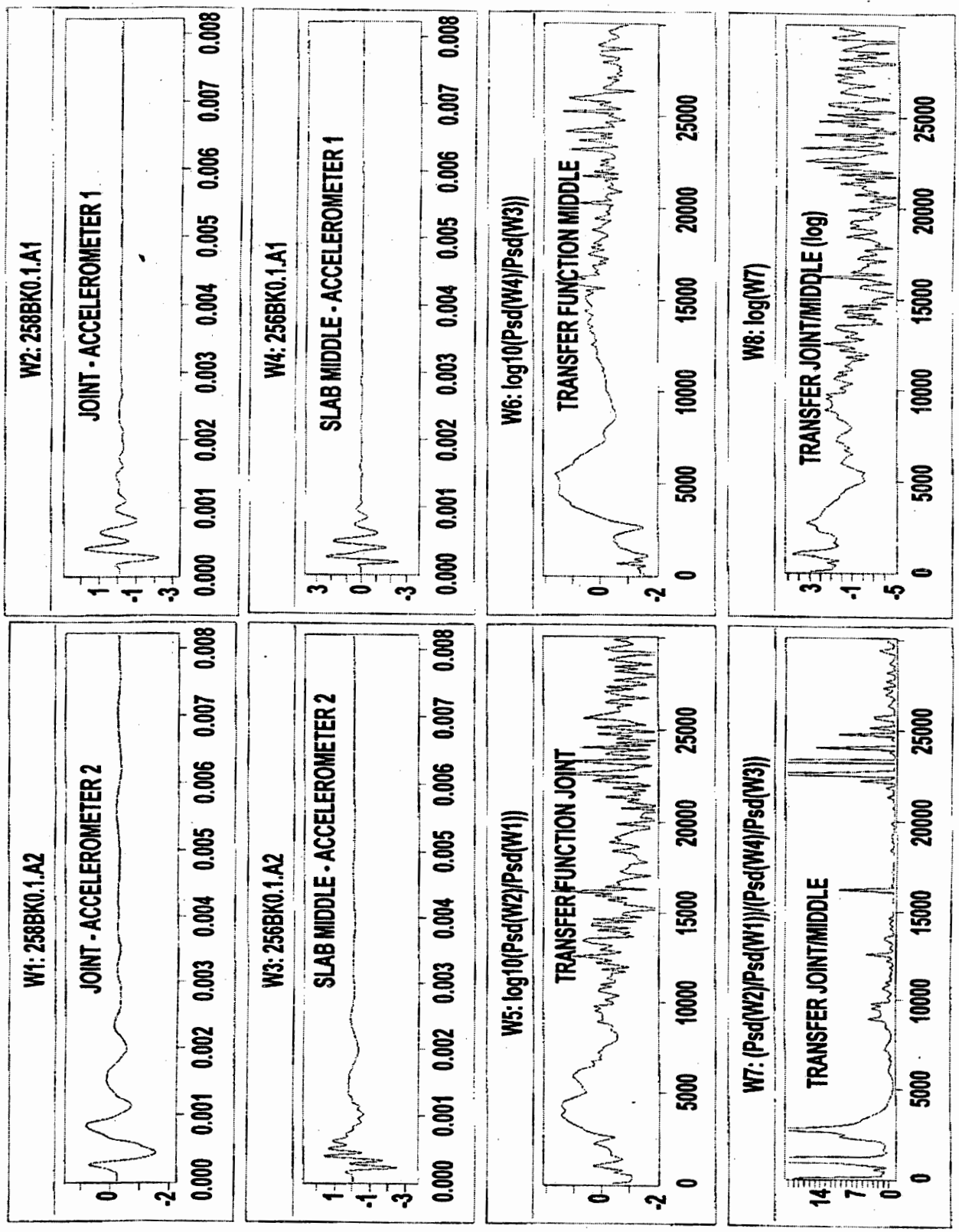


Figure 93. Evaluation of joint load transfer from joint (258) and middle of the slab (256) tests.

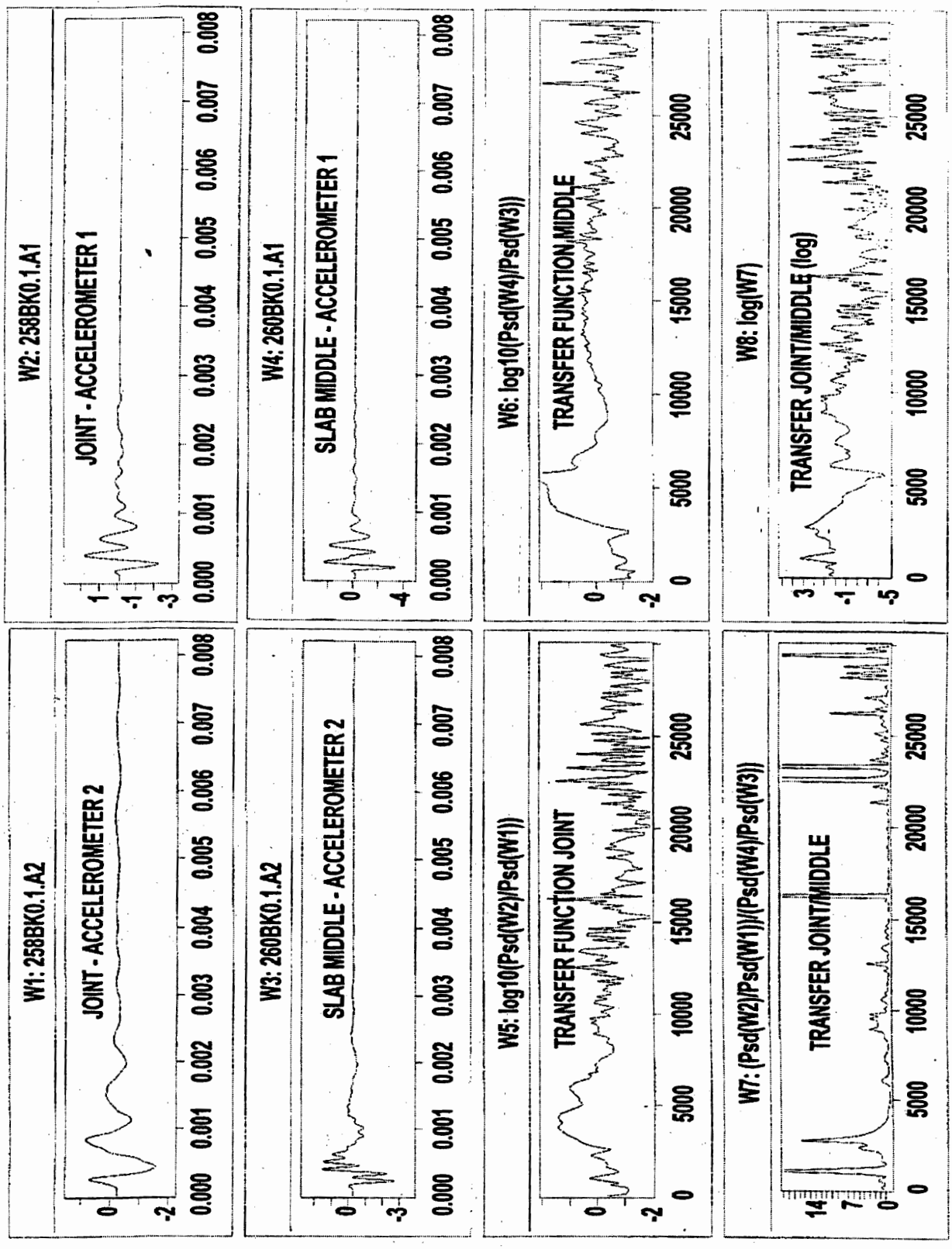


Figure 94. Evaluation of joint load transfer from joint (258) and middle of the slab (260) tests.

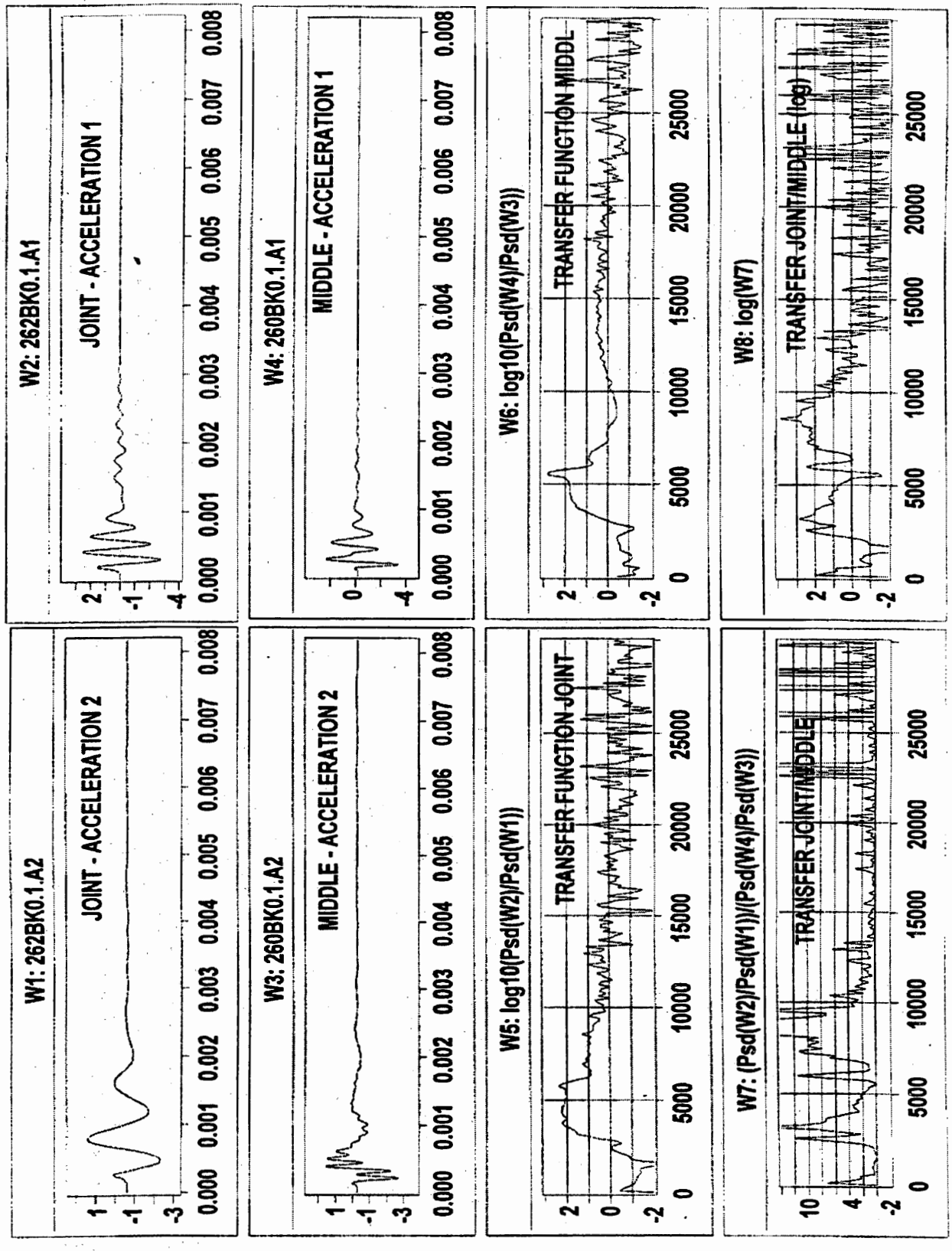


Figure 95. Evaluation of joint load transfer from joint (262) and middle of the slab (260) tests.

Figure 96. Evaluation of joint load transfer from joint (262) and middle of the slab (264) tests.

joint/middle (window W7) in a broad range of frequencies. Finally, to verify the procedure, the transfer function for two tests conducted in the middle of the slabs was evaluated. Plot W7 in Figure 97 represents the transfer function for tests 264 and 260. The transfer function varies around 1, indicating, as expected, about equal load transfer in those two cases.

The obtained results indicate a potential of the SPA and seismic methods to evaluate the joint load transfer in rigid pavements. A significant drop in the load transfer from one side of the joint to another (in comparison to an ideal contact) is a very good qualitative indicator. Transfer functions evaluated for different joints can be compared one to another and to middle of the slab transfer function. Based on those, a relative assessment of the joint condition can be made. However, additional study and measurements are suggested, if a quantitative evaluation will be needed. The first objective of the investigation would be to establish a quantitative relationship between the evaluated transfer function and the condition of the joint. The second objective of such a study would be to evaluate a potentially nonlinear relationship between the joint transfer function and the intensity of loading.

Figure 97. Transfer function for two middle of the slab tests.

## STATUS OF SEISMIC METHODS IMPLEMENTED IN THE SPA

As described in Introduction and Seismic Pavement Analyzer chapters, five seismic techniques are implemented in the SPA. Their application in evaluation of pavement layer properties and detection of defects in pavements, represents the core of the system. While the SPA hardware provides an excellent tool for data collection and data analysis, interpretation is strongly dependent on the routines implemented for the five techniques. The following sections discuss the status of the seismic methods as implemented at the moment in the SPA based on the experience so far, and in general. The discussion concentrates on the SASW and IR techniques because of their greatest potential.

### Ultrasonic Methods

The three ultrasonic methods: UBW, USW and IE have been utilized to a minor extent during this project. The primary use of the UBW and IE techniques is in measurement of the paving layer Young's modulus and thickness. Both techniques seem to work well for thick paving layers, where thick are considered those of about or more than 20 cm thick. For thin paving layers, inaccuracies in the UBW might be a result of software's inability to accurately identify P-wave arrivals. Similarly, for thin pavements the IE technique's, the SPA hammers might have difficulty generating wave components of a sufficiently high frequency. This was e.g. observed during the testing on Rt. I-295. No experience was gained during this study in the use of IE in delamination detection on either rigid or composite pavements. The USW technique has shown to be the most robust technique for measurement of the shear modulus and the thickness of the paving layer, even of paving layers thinner than seven cm, as demonstrated by Rt. I-295 results. In many situations, it a more accurate estimate of the Young's modulus can be made using the USW than UBW.

In summary, the three techniques are based on sound and simple theoretical principles. In that respect, there is no need for improvements. Success in their implementation depends primarily on the ability of the hardware to generate and detect waves of needed frequency range, and software that can precisely identify arrivals, measure velocity or identify resonant peaks. A more detailed study would be needed to identify conditions under which the ultrasonic methods provide accurate results, and what are the limitations.

### Spectral Analysis of Surface Waves (SASW)

The SASW test is the single most useful test implemented in the SPA, since the elastic modulus profile is the most sought information about the pavement. As described earlier, there are two basic steps in SASW data reduction process: evaluation of the dispersion curve and backcalculation of an elastic modulus profile from the dispersion curve.

Evaluation of the dispersion curve is in the greatest part a straight forward task and the built-in SPA software has automated the process. Details of this process are not known. The reinterpretation software Reinterp provides an operator an opportunity to intervene in the dispersion curve generation process. Based on the experience from the study, in most cases intervention is necessary. One of the elements that needs to be more closely

examined is smoothing of the dispersion curve. Reinterp, upon the generation of the dispersion curve, smooths it and describes by 30 to 40 points. There is a possibility that in certain conditions some important features of the dispersion curve, necessary for accurate and unique backcalculation, are lost.

Significant improvements can be made in the inversion or backcalculation process. Backcalculation is a complex process for several reasons: strong nonlinearity of the problem, interference of surface and body waves, "near field" effects, significant contribution of higher Rayleigh modes. The background of the SPA's built in backcalulation routine is not known. It is limited to a three layer system backcalculation, it does not allow intervention of an operator, and dispersion of results seems to be high, especially for deeper layers. The Reinterp backcalculation routine is a more robust routine, allows evaluation of four-layer pavement systems, intervention of an operator, and provides a better insight into the overall process and an estimate of the accuracy of the obtained profile. However, the process is more time consuming and it is not clear how it handles the above mentioned complexities of the process.

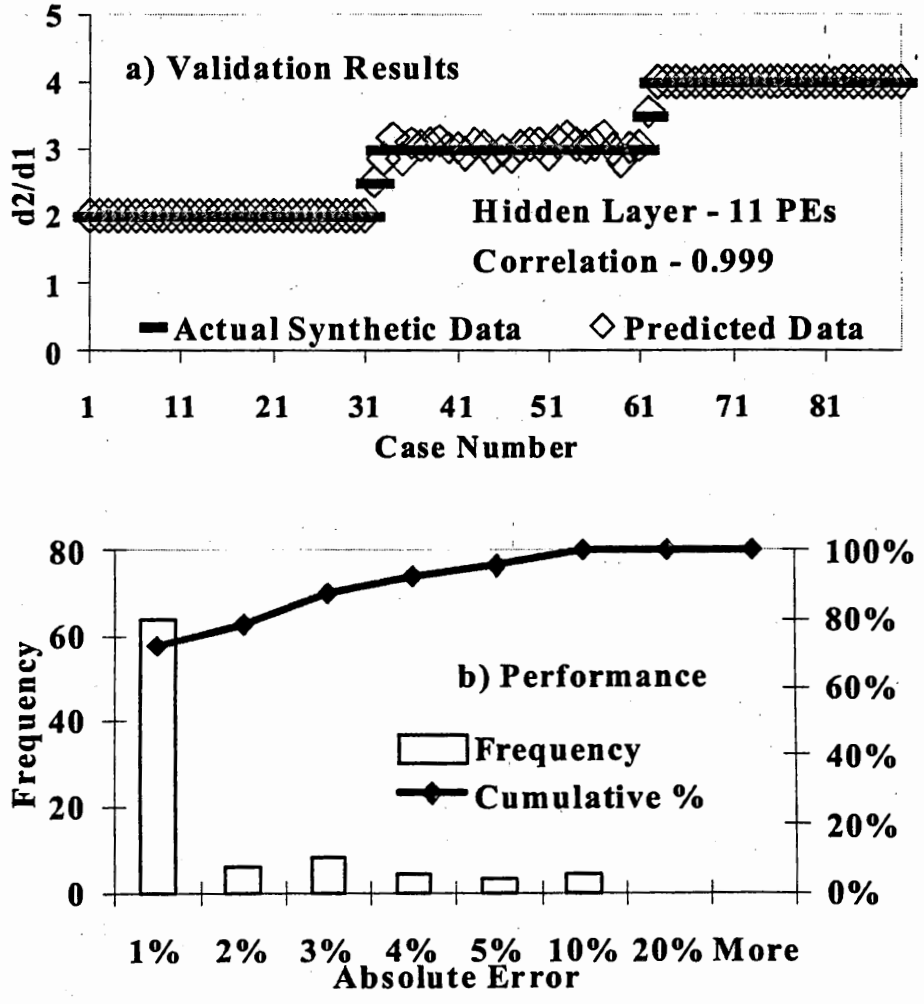


Figure 98. Comparison of Results with Actual Synthetic Data and Model's Performance for Parameter $d_2/d_1$ [43].

Recently, a new backcalculation routine based on artificial neural networks (ANNs) was developed[42] that is going to be implemented in the SPA. Previous attempts to develop ANN based backcalculation algorithms were based on simultaneous evaluation of all layer thicknesses and moduli[30]. The most important features of the newly developed network is that training and operation of the network is done for properties (thickness and elastic modulus) of each individual layer, and that the data used in training resolve issues of interference of different types of waves and multiple Rayleigh modes. Testing of the ANN backcalculation routine has shown that it is very accurate even in evaluation of properties of the base layer, typically the least accurate task. This is illustrated in Figures 98 to 101 by comparisons of true layer properties and ANN predictions for several layers. It is demonstrated by Figures 98 and 99 that the developed neural networks resolve even the previously described a difficult task of accurate definition of granular base and subbase layer thickness, especially in situations where the contrast between those layers and the subgrade is small. The parameters sought by the ANN are dimensionless thickness or

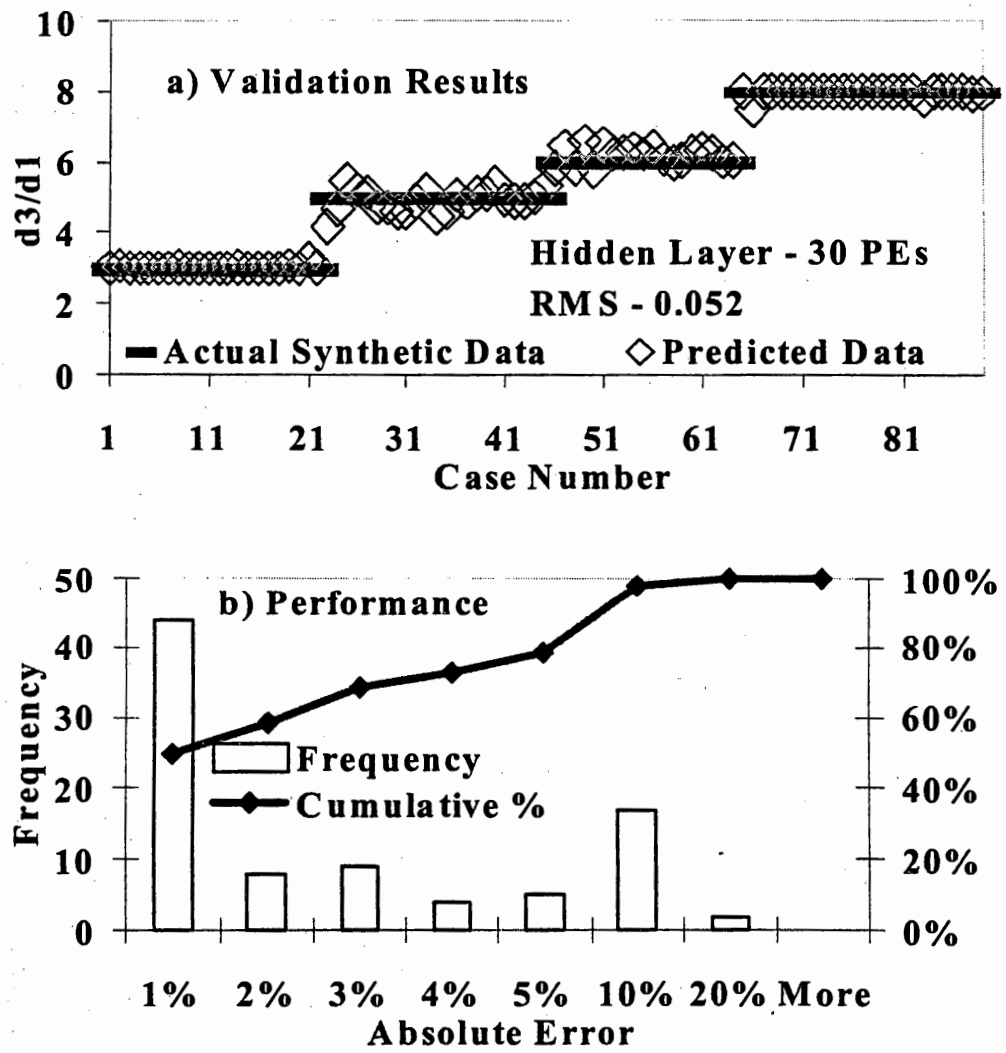


Figure 99. Comparison of Results with Actual Synthetic Data and Model's Performance for Parameter $d_3/d_1$[43].

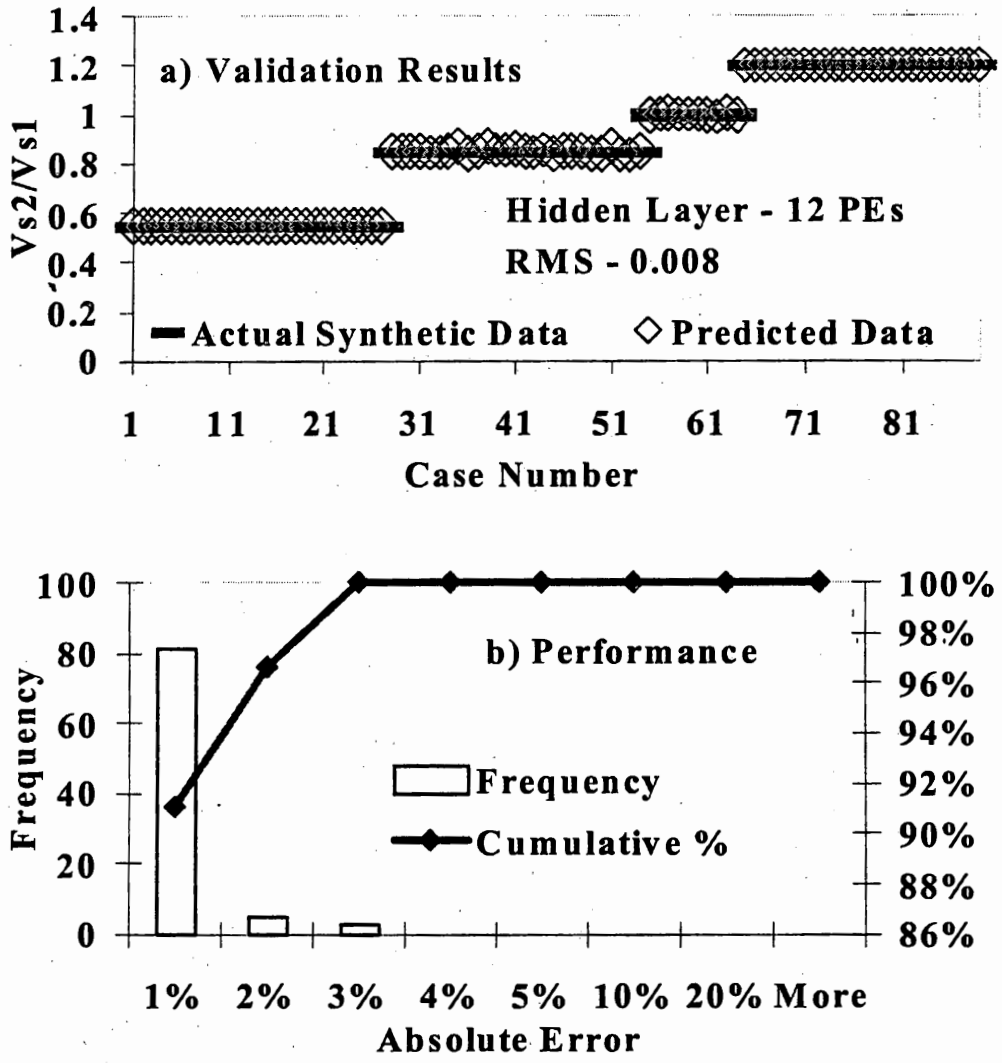


Figure 100. Comparison of Results with Actual Synthetic Data and Model's Performance for Parameter $V_{s2}/V_{s1}$[43].

velocity ratios. To reduce the number of parameters sought, the assumption of the network is that the thickness and the shear wave velocity are known, i.e. they are determined using some of the seismic tests, e.g., USW, UBW and IE. In this particular case, the second layer represents either an AC or PCC base layer, as can be also concluded from the range of velocity ratio $V_{s2}/V_{s1}$ in Fig. 100. The third layer, the subbase, is on the other hand of a granular type. It can be observed that both the thickness (Fig. 99) and the shear wave velocity (Fig. 101) are very well predicted. The ANN prediction of the subgrade shear wave velocity, not presented herein, is excellent. The ANN based backcalculation is a very promising approach. Beside the improved accuracy, a very important advantage of the ANN algorithm is significantly reduced computational time, just a fraction of a second, that will enable real time pavement profiling. Certainly, to have an accurate pavement modulus profile, the prerequisite is that the techniques utilized in measurement of the surface pavement layer properties be accurate too.

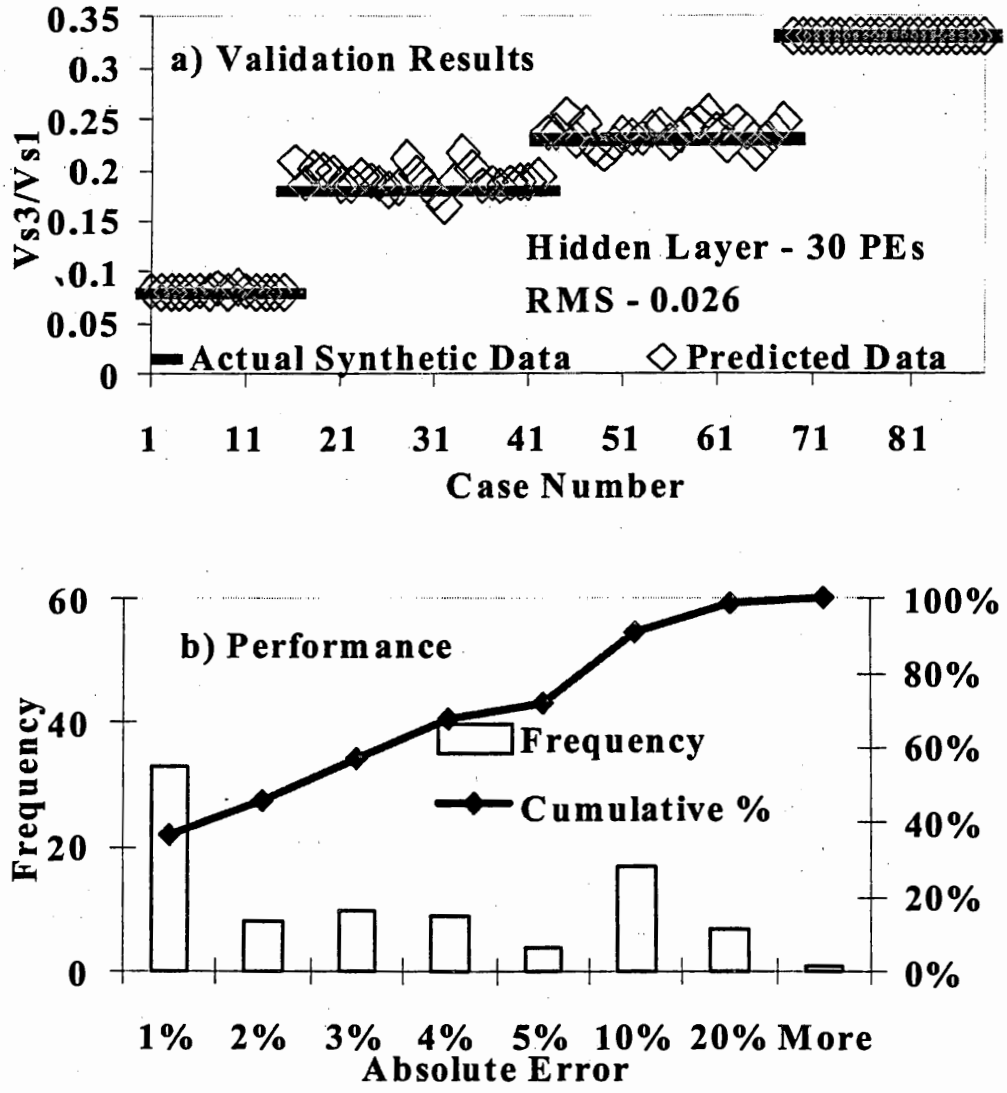


Figure 101. Comparison of Results with Actual Synthetic Data and Model's Performance for Parameter $V_{s3}/V_{s1}$[43].

Nazarian *et al.*[41] are discouraging the use of the SASW method on rigid pavements. They identify two reasons why it should be discouraged: 1) the receiver spacing is insufficient to measure accurately velocity of long wavelength surface wave components, and 2) possible presence of voids and separations between the slab and the base, and interaction of waves with joints that can lead to a complex dispersion curve that is very hard to interpret. Instead, they suggest using the USW and IE method to characterize the slab, and the IR to characterize condition of the underlying layers. Too little testing on rigid pavements was done during this study to confirm their findings. However, some other studies on effects of reflections of surface waves from pavement edges and joints[44] and on effects of anomalies and buried objects[45] suggest that conclusions of Nazarian *et al.* are correct.

## Impulse Response (IR)

The IR technique is primarily used in evaluation of the support and detection of voids under rigid pavements. As described in the chapter on seismic methods in for pavement testing, the evaluation is based on measurement of damping ratio and subgrade modulus. From the limited testing on rigid pavements, evaluation of support based on measurement of the subgrade modulus seems to be a more reliable approach. Overall, results are fairly repeatable and consistent. Based on results obtained from testing on various types of rigid and flexible pavements, Nazarian *et al.*[41] conclude that the IR and SASW provide very close subgrade modulus values when the subgrade modulus does not vary significantly with depth. Otherwise, the results may have significant differences.

The present data reduction procedure simplifies the dynamic response of the pavement-soil system to that of a single degree of freedom (SDOF) system. Curve fitting between the actual response and that of a SDOF system is done to obtain the necessary modal parameters. The assumption of a SDOF response oversimplifies the problem and, although useful for practical purposes, may introduce inconsistencies and uncertainties in data interpretation. Results from the analysis of the response of rigid foundations on layered systems (approximations of rigid pavements) are an indicator that results obtained from a SDOF simulation may not be representative of the actual response of the pavement-soil system. Variation of the stiffness and damping coefficients with frequency in those cases may be far more complex than of a SDOF system. This variation is dependent on the vibration mode, properties of the supporting soil and characteristics (geometry, rigidity) of the pavement. A study is being conducted to examine the validity of the assumption of the SDOF response and to improve IR data interpretation of the SPA[46]. Finite element simulations are being used for this purpose. In addition, alternative simple physical models[46] are considered as possible improvements of the SDOF based model. One of alternative models and its impedance matched to the impedance obtained from a finite element simulation are shown in Figs. 102 and 103.

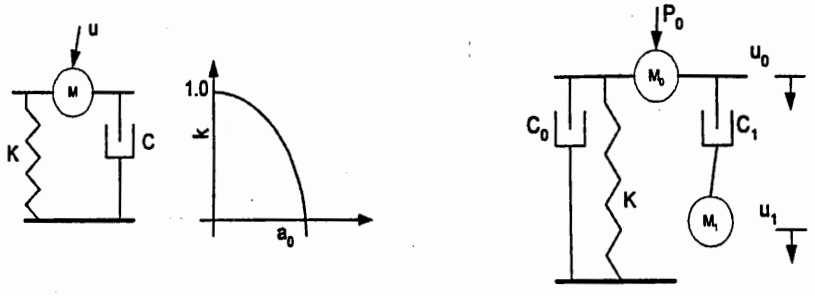


Figure 102. SDOF model (left) and a simplified lumped parameter model (right).

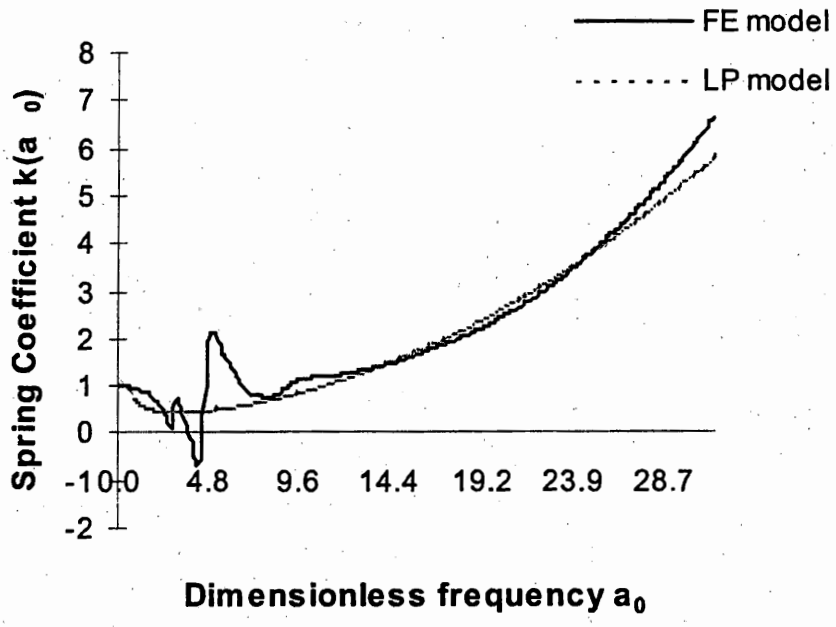


Figure 103. Spring coefficient for a finite element and simplified lumped parameter models[46].

# CONCLUSIONS

The report describes evaluation of the Seismic Pavement Analyzer (SPA) device for possible implementation in evaluation and condition monitoring of pavement in New Jersey by the New Jersey Department of Transportation. Specifically, the objectives of the study were to examine the applicability of the SPA in structural evaluation, detection of defects and distresses, and other uses relevant for pavement evaluation and condition monitoring. With respect to the equipment itself, the objectives were to examine the robustness and consistency of the SPA hardware and software, and the soundness of the seismic methods implemented in the device. The following are the conclusions of the study with respect to the stated objectives:

1. The SPA, as an automated data collection system for seismic testing of pavements, fulfills this need and objective very well. Seismic methods have been used in testing of pavements and bridge decks on the research side for almost 40 years. However, due to a lack of an automated data collection system, those did not gain attention from the transportation agencies. The development of the SPA removes this undoubtfully significant deficiency.
2. The five seismic techniques implemented in the SPA utilize sound, and in some cases very simple, physical phenomena of wave propagation in layered elastic systems. Therefore, all the current deficiencies in the data interpretation have a very good prospect of being resolved in the future.
3. The SPA hardware performed very well and consistently throughout the duration of the study. Only a couple of minor failures on the compressor circuit and a hammer assembly required a manufacturer's intervention. Regular maintenance of the SPA is simple and inexpensive.
4. The SPA built-in software performed well in the data collection aspects of the operation. However, the data analysis modules have limitations and should be improved. The limitations of the software are in a limited control of the data collection process, data analysis and presentation, and data interpretation. Some of the software limitations stem from its DOS basis. Ultrasonic and Impulse Response data analysis routines performed reasonably well. The built-in SASW module is not satisfactory for two reasons: the pavement model is limited to a three-layer system and the analysis is not sufficiently accurate. Therefore, the analysis should be repeated in the office using the reinterpretation or alternative SASW software.
5. The overall status of the seismic techniques implemented in the SPA can be described as good, with a significant space for improvement. With respect to the ultrasonic methods, the ultrasonic surface wave (USW) method is the most robust and best fitted for testing of thin paving layers. The ultrasonic body wave (UBW) occasionally encounters problems in identification of first arrivals, while the IE performance on paving layers thinner than ten cm is reduced due to insufficient energy in a high frequency range. The Impulse Response (IR) method is very robust and performs consistently in evaluation of subgrade moduli and detection of loss of support. However, the assumptions of the method should be reviewed. The SASW method is the most powerful method and at the same time has the most space for

improvement. While minor improvements are needed in accuracy and automation of the dispersion curve generation, significant improvements can be made in the backcalculation process.

6. The SPA can be successfully used for multiple purposes in evaluation and condition monitoring of pavement systems. In this study, the SPA was successfully used in pavement elastic modulus profiling, detection of voids or loss of support under rigid pavements, and to a certain extent evaluation of a joint load transfer in rigid pavements. A number of other applications, e.g. detection of delamination in rigid and composite pavements, are quite feasible considering the soundness of the wave propagation phenomena and the ability of the SPA to measure them.
7. Overall, the SPA is a well designed equipment for pavement evaluation. One of the biggest advantages of the SPA and the implemented seismic methods is that elastic properties of the paving layer are measured directly, instead of being backcalculated or correlated to some other measured property. The current deficiencies of the SPA are primarily on the software side, mostly in the data analysis and interpretation. However, those deficiencies can be viewed in a positive light, i.e., that the best features of the seismic methods have not been fully utilized yet and significant improvements are feasible.

## RECOMMENDATIONS

The presented study and obtained conclusions logically lead to a number of steps that should be implemented to maximize the benefits of the SPA. While some of the steps will require continued, fundamental research, many improvements can be achieved through a number of short analytical and experimental studies. The following are recommendations for the improvement and additional usage of the SPA:

1. The highest benefit of the SPA stems from a robust, consistent and automated data collection. Therefore, to gain a clear understanding of the potential of the SPA in long term monitoring of pavements, it is necessary to collect and preserve raw data on a continued basis. As the analysis and interpretation procedures improve, understanding of all benefits of the SPA and seismic testing will too.
2. Most of the effort should be directed towards the improvement of the analytical procedures. Some of the improvements, for example, in ultrasonic testing can be achieved through simple modifications on hardware and software sides. On the hardware side, the improvement can be achieved through an introduction of a supplemental "ultra" high-frequency source, similar to the one implemented in the Portable Seismic Property Analyzer (PSPA). Eventually, with a better source no software modifications will be needed. The SASW and IR tests require a significantly higher effort. The accuracy, stability, uniqueness, and automation of the SASW should be improved in both phases of the test, the dispersion curve determination, and the profile backcalculation. The backcalculation procedure of the IR method should be improved with respect to the assumptions of the pavement model.
3. The SPA software needs to be upgraded to Windows environment, with significant improvements on the user control side. The SPA data collection module should be separated from the analysis module, so that a user can easily implement his/her own analytical and interpretation routines. The data collection module should also allow for a complete control of the testing sequence: from the sampling rate and selection of data banks to the number of channels and samples, and impact source controls. The SPA manufacturer is planning to release the Windows based software in 2002.
4. A couple of improvements of practical nature are recommended for the SPA. The SPA should be equipped with a digital imaging system to record pavement conditions at each test point. Also, a portable system should replace the current "desktop" system, to allow a single operator usage of the SPA.
5. Other potential applications of the SPA should be examined, like: the use of SPA in detection and characterization of delaminations in rigid and composite pavements, evaluation of temperature induced modulus variations in asphalt concrete, monitoring of curing of concrete pavements, etc.

## REFERENCES


[1] AASHTO and FHWA. *Pavement Seminar for Chief Administrative Officers*. U.S. Department of Transportation, Federal Highway Administration, Washington, D.C., 1985.

[2] K.A. Zimmerman and ERES Consultants, Inc., *Pavement Management Methodologies to Select Projects and Recommend Preservation Treatments*, NCHRP Synthesis 222 Report, National Research Council, Washington, D.C., 1995.

[3] S. Nazarian, M.R. Baker & K. Crain, *Development and Testing of a Seismic Pavement Analyzer*, Report SHRP-H-375, Strategic Highway Research Program, National Research Council, Washington, D.C., 1993.

[4] B.A. Bolt. *Earthquakes*, W.H. Freeman and Company, New York, 1993.

[5] N. Gucunski and R.D. Woods. "Use of Rayleigh Modes in Interpretation of SASW Test," Proceedings of the 2nd International Conference on *Recent Advances in Geotechnical Earthquake Engineering and Soil Dynamics*, St. Louis, Missouri, March 11-15, 1991, pp. 1399-1408.

[6] M. Ewing, W. Jardesky and F. Press. *Elastic Waves in Layered Media*. Mc Graw-Hill Book Company, New York, 1957.

[7] F.E. Richart, J.R. Hall and R.D. Woods. *Vibrations of Soils and Foundations*, Prentice Hall, Englewood Hills, NJ, 1970.

[8] Aki, K., and P.G. Richards, *Quantitative Seismology: Theory and Methods*. Volumes 1 and 2. W.H. Freeman, San Francisco, CA, 1980.

[9] J.P. Wolf. *Soil-Structure Interaction*, Prentice-Hall, Englewood Hills, NJ, 1985.

[10] J.M. Roesset, D.-W. Chang, K.H. Stokoe, II, and M. Aouad. "Modulus and Thickness of the Pavement Surface Layer from SASW Tests." In *Transportation Research Record* 1260, National Research Council, Washington, D.C., 1992, pp. 53-63.

[11] R. Bonaquist and M.W. Witzak. "Plasticity Modeling Applied to the Permanent Deformation Response of Granular Materials in Flexible Pavement Systems." In *Transportation Research Record* 1540, National Research Council, Washington, D.C., 1996, pp. 7-14.

[12] P. Tian, M.M. Zaman and J.G. Laguros. "Gradation and Moisture Effects on Resilient Moduli of Aggregate Bases." In *Transportation Research Record* 1619, National Research Council, Washington, D.C., 75-84, 1998.

[13] R.F. Pezo, G. Claros, and W.R. Hudson. "An Efficient Resilient Modulus Testing Procedure for Subgrade and Subbase Material," Presented at the 71st Annual Meeting of the Transportation Research Board, Washington, D.C., 1992.

[14] B.O. Hardin and W.L. Black. "Sand Stiffness Under Various Triaxial Stresses," *Journal of the Soil Mechanics and Foundations Division*, ASCE, Vol. 92, No. SM2, 1966, pp. 27-42.

[15] B.O. Hardin and F.E. Richart, Jr. "Elastic Wave Velocities in Granular Soils," *Journal of the Soil Mechanics and Foundations Division*, ASCE, Vol. 89, No. SM1, 1963, pp. 33-65.

[16] B.O. Hardin and V.P. Drnevich. "Shear Modulus and Damping in Soils: Design Equations and Curves," *Journal of the Soil Mechanics and Foundations Division*, ASCE, Vol. 98, No. SM7, 1972, pp. 667-692.

[17] B.M. Das. *Principles of Soil Dynamics*. PWS-KENT Publishing Company, Boston, Ma, 1993.

[18] S.L. Kramer. *Geotechnical Earthquake Engineering*. Prentice Hall, Upper Saddle River, NJ, 1996.

[19] M.A. Biot. "Theory of Propagation of Elastic Waves in a Fluid-Saturated Porous Solid," *Journal of Acoustical Society of America*, Vol. 28, March, 1956, pp. 168-191.

[20] V.P. Drnevich, J.R. Hall, Jr., and F.E. Richart, Jr. "Effects fo Amplitude of Vibration on the Shear Modulus of Sand," Proceedings of International Symposium on *Wave Propagation and Dynamic Properties of Earth Materials*, Albuquerque, NM, 1967, pp. 128-140.

[21] Y.K. Huang. *Pavement Analysis and Design*. Prentice Hall, Upper Saddle River, NJ, 1993.

[22] S. Nazarian, D. Yuan and E. Weissinger. "Comprehensive Quality Control of Portland Cement Concrete with Seismic Methods." In *Transportation Research Record* 1575, National Research Council, Washington, D.C., 1997, pp. 15-26.

[23] D. Yuan, S. Nazarian, R.J. Ferrell and R. Guerra. "Laboratory and Field Evaluation in Moduli of Pavement Layers Due to Moisture and Temperature by Seismic Methods," presented at 2000 Annual Transportation Research Board Meeting, Washington, D.C., January 2000.

[24] *ACI Manual of Concrete Practice 1999*. American Concrete Institute, Farmington Hills, MI, 1999.

[25] E.G. Nawy. *Reinforced Concrete - A Fundamental Approach*. Prentice Hall, Upper Saddle River, NJ, 2000.

[26] S. Nazarian, D. Yuan and M. Baker. *Rapid Determination of Pavement Moduli with Spectral Analysis of Surface Waves Method*. Research Report 1243-1, The University of Texas at El Paso, 1995, 76 pp.

[27] S. Nazarian. *In Situ Determination of Elastic Moduli of Soil Deposits and Pavement Systems by Spectral-Analysis-of-Surface-Waves Method*. Ph.D. Dissertation, Department of Civil Engineering, The University of Texas at Austin, 1984.

[28] H.K. Stokoe, II, S.G. Wright, J.A. Bay and J.M. Roesset, "Characterization of Geotechnical Sites by SASW Method," in R.D. Woods (ed) *Geotechnical Characterization of Sites*, Oxford and IBH Publ. Comp., New Delhi, India, 1994, pp. 15-26.

[29] G.J. Rix. *Experimental Study of Factors Affecting the Spectral-Analysis-of-Surface-Waves Method*. Ph.D. Dissertation, The University of Texas at Austin, 1988.

[30] N. Gucunski, V. Krstic and M.H. Maher. "Backcalculation of Pavement Profiles From the SASW Test by Neural Networks." Chapter in *Artificial Neural Networks for Civil Engineers: Advanced Features and Applications*, Flood and Kartam Eds., ASCE, 1998, pp. 191-221.

[31] V. Ganji, N. Gucunski and S. Nazarian. "An Automated Inversion Procedure for Spectral Analysis of Surface Waves," *Journal of Geotechnical and Geoenvironmental Engineering*, ASCE, Vol. 124, No. 8, 1998, pp. 757-780.

[32] S. Reddy. *Improved Impulse Response Testing - Theoretical and Practical Validations*. M.S. Thesis, The University of Texas at El Paso, 1992.

[33] R. Dobry, and G. Gazetas. "Dynamic Response of Arbitrary Shaped Foundations," *Journal of Geotechnical Engineering*, ASCE, Vol. 112, No. 2, 1986, pp. 109-135.

[34] M. Sansalone. "Detecting Delaminations in Concrete Bridge Decks with and without Asphalt Overlays Using an Automated Impact-Echo Field System," Proceedings of the British Institute of Non-Destructive Testing International Conference *NDT in Civil Engineering*, April 14-16, 1993, Liverpool, U.K., pp. 807-820.

[35] N. Gucunski, N. Vitillo and A. Maher. "Bridge Deck Evaluation Using Integrated Seismic Devices," Proceedings of the *Structural Materials Technology IV: An NDT Conference*, Atlantic City, NJ, Feb. 28-March 3, 2000, pp. 329-334.

[36] V. Tendon and S. Nazarian. *Calibration Procedures for Seismic and Deflection-Based Devices.* Report 2984-S1, Texas Department of Transportation, 1999.

[37] S. Nazarian, M.R. Baker and K. Crain. *Development and Testing of a Seismic Pavement Analyzer - Software and Hardware*. Report SHRP-H-375, Strategic Highway Research Program, National Research Council, Washington, D.C., 1993.

[38] D. Yuan and S. Nazarian. "Automated Surface Wave Testing: Inversion Technique." *Journal of Geotechnical Engineering*, ASCE, Vol. 119, No. 7, 1993, pp. 1112-26.

[39] N. Gucunski and M.H. Maher. "Database of Dispersion Curves for Surface Wave Testing." *Advances in Site Characterization: Data Acquisition, Management and Interpretation*, Geotechnical Special Publication, No. 37, ASCE, 1993, pp. 1-12.

[40] S. Nazarian, S. Reddy and M. Baker. "Determination of Voids under Rigid Pavements Using Impulse Response Method," STP 1198, ASTM, 1994, pp. 473-87.

[41] D. Yuan and S. Nazarian. *Evaluation and Improvement of Seismic Pavement Analyzer.* Research Report 2936-1, Texas Department of Transportation, 1997.

[42] N. Gucunski, I.N. Abdallah and S. Nazarian. "Backcalculation of Pavement Profiles from the SASW Test Using Artificial Neural Networks - Individual Layer Approach." *Pavement Subgrade, Unbound Materials, and Nondestructive Testing,* Geotechnical Special Publication 98, Ed. M. Mamlouk, Geo Institute, ASCE, 2000, pp. 31-50.

[43] I.N. Abdallah, D. Yuan, H. Wu and N. Gucunski. "Use of Artificial Neural Network in Spectral-Analysis-of-Surface-Waves Method," Proceedings of *10th International Conference on Computer Methods and Advances in Geomechanics,* Tucson, Arizona during January 7-12, 2001, pp. 109-120.

[44] I. Sanchez-Salinero, J.M. Roesset, K.-Y. Shao, K.H. Stokoe, II nad G.J. Rix. "Analytical Evaluation of Variables Affecting Surface Wave Testing of Pavements." In *Transportation Research Record* 1136, 1987, pp. 86-95.

[45] N. Gucunski, V. Ganji and M.H. Maher. "Effects of Soils Nonhomogeneity on SASW Testing." *Uncertainty in the Geologic Environment: From Theory to Practice*, Geotechnical Special Publication No. 58, ASCE, 1996, pp.1083-1097.

[46] N. Gucunski and H. Jackson. "Void Detection Underneath Rigid Pavements: Numerical Simulation of the Impulse Response Method," Proceedings of the Annual Meeting of the Environmental and Engineering Geophysical Society

*SAGEEP 2001*, Denver, March 4-7, 2001, on CD.
[47] J.P. Wolf. *Foundation Vibration Analysis Using Simple Physical Models.* PTR Prentice Hall, Englewood Hills, NJ, 1994.